Aalborg University

Structural Optimization

with Topology Optimization of Complex Civil Engineering Structures

Frederik Hald

4th Semester

M.Sc. Master Thesis

Aalborg University
School of Engineering and Science
Phone: 96 35 97 31
Fax: 98 13 63 93
http://www.ses.aau.dk

Title: Structural Optimization with Topology Optimization of Complex Civil Engineering Structures

Theme: Master Thesis

Project period: Spring 2012

Frederik Hald

Supervisor: Poul Henning Kirkegaard
Lars Vabbersgaard Andersen

Print runs: 4

Numbers of pages: 105

Completed: June 8th 2012

Synopsis:

This thesis will concern topology optimization with two different commercial programs (*Absqus CAE* and *Altair Optistruct*) where SIMP optimization is used. First will the fundamental theory in the field of topology optimization be outlined and a review of the historical background is presented.

Topology optimization will be performed on three cases with increased complexity. The two commercial programs will be used and commented based on different performance parameters e.g. resulting topologies, compliance and time used. This will lead to an overview of the functionality of the programs.

Topology optimization will be performed on two civil engineering structure. First a transition piece for an offshore wind turbine. Two sizes of transition pieces in CRC concrete are optimized using SIMP optimization. A rotation constrain is used to ensure loads can be obtain from multiple directions. Second a pedestrian footbridge over a freeway optimized. The bridge in investigate through four topology optimizations. An eigenfrequency constrain is applied in a SIMP optimization task.

Preface

The present Master thesis *"Structural Optimization with Topology Optimization of Complex Civil Engineering Structures"* is prepared and compiled as a part of M. Sc. in Structural and Civil Engineering at Aalborg University. The period of which this thesis is written is from the 1st of February 2012 to the 8th of June 2012 under the supervision of Poul Henning Kirkegaard and Lars Vabbersgaard Andersen.

Reading Guide

The thesis consists of two parts; a main report and appendixes which can be found in the back of the report. In the main report there are references to the appendixes, where the extensional documentation are to be found.

For the thesis the two commercial computer programs Abaqus CAE and Altair Optistruct is used. Abaqus and Hyperworks are softwares used for creating and calculating finite element (FEM) models and preform topology optimization on a structure.

Sources are quoted by the Harvard method of bibliography with the name of the author and year of publication inserted in brackets after the text. Quoted sources from literature, papers, websites and design codes will appear e.g . (Bendsøe and Sigmund, 2003).

Figure and table numerations refers to which chapter the desired figure or table is located in. Please note that if a figure or a table is not attached to a source, they are produced by the author. The bibliography gives extensive information about each source. Since several of the sources are recurrent, the bibliography is not divided into source types. Instead, the sources are sorted alphabetically by notices, under which information about the source type, i.e.; author, title, publisher or editor, year of publication, presentation number, ISBN and URL.

Table of Contents

Chapter **1**

Introduction

In this chapter a general presentation to topology optimization and an overview of the use of topology optimization in civil engineering will be given. The historical background of topology optimization is shown and the scope of the thesis is outlined at the end of the chapter.

1.1 Topology Optimization in Civil Engineering

A large part of designing a civil engineering structure is to determine the layout of the design for a structure also called topology. When preforming structural optimization and topology optimization, the goal is to achieve a structure that with a given amount of material preform best while satisfying the necessary constrains.

Figure 1.1: *Qatar Convention Centre created by Arata Isozaki & Associates. (www.qatarconvention.com, 2012)*

Topology optimization has been used on many types of structures. From Aerospace flights, biomedical, nanotechnologies and machine design. An example of the use of topology optimization in a commercial company is Airbus' use of topology optimization in the design of the aircraft A380. Inside the wing of the aircraft was box ribs weight reused using topology optimization. This reduced the weight of the aircraft with up to 1000 kg (Krog et al., 2002).

Since the 1980's have the rapidly-growing incensement and availability of computer capacity made it possible to perform more and more complex finite element modelling. This combined with the improvements in algorithms for design optimization have moved the field of topology optimization. Optimization have mostly been an academic field of interest mainly concerned with the mathematical aspects of structural optimization. More and more engineers and architects are today experimenting with optimization techniques. Commercial finite element software packages as *Hyperworks Suite* and *Abaqus CAE* are now offering a build in module with structural optimization algorithms to preform topology and shape optimization.

The practical applications have only rarely been used on real world civil engineering structures. There is a clear gab between the many papers published concerning topology and shape optimization and the use on real life civil engineering structures. Over the resent ten years some civil engineering structures have begun to be build where topology optimization has been used in practical applications. An example is Qatar Convention Centre completed December 2011 cf. Figure 1.1. The organic design of the roof structure was original designed for Florence New Station Project in Italy. The 250 m long roof structure was initially created from a deck simply supported with legs and evolved into the final form using topology optimization. (Xie et al., 2011)

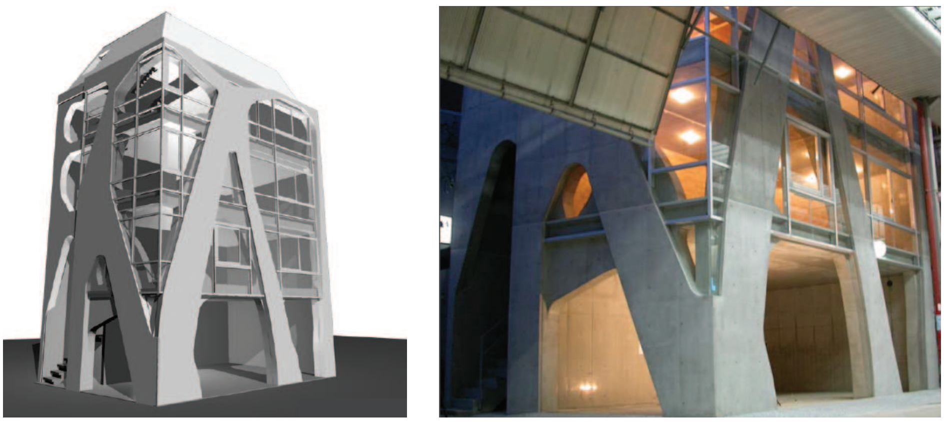

Figure 1.2: *Akutagwa River Side Project. To the left is a computer model of the structure. To the right is the finished structure. (Ohmori, 2008)*

Another example of a topology optimized building is the Akutagwa River Side Project in Japan completed in 2004 cf. Figure 1.2 . The building is approximate 10m x 6m. Optimization was applied to three of the four outer wall of the building where material in low stress regions was gradually removed and added to areas with high stress until the final optimized structure was achieved. (Huang and Xie, 2010)

The slowly growing field of topology optimization makes the design process more effective. With the new tools in the commercial programs it is easier to implement topology optimization in the design process for real civil engineering structures. The easier access to topology optimization opens for a new view of structures both for engineers and for architects where new forms will give a new design idiom.

Use of topology optimization in civil engineering has some challenges compared to the use in other field's e.g. mechanical engineering. The load patterns on a civil engineering structure are typical vary complex and different load patters can influence the structures. The use of different types of material and composite material also challenge the use of topology optimization on an civil engineering structure.

When a structure is optimized it should perform better. The material in a structure is better used and the stress distribution should be more homogeneous distributed. The final volume of the structure will also be reduces in an optimization and the final structure will therefore be lighter. These are some of the benefits an topology optimization of a structure can lead to.

This thesis will concern some of the challenges regarding topology optimization in civil engineering. Use of the commercial software packages *Hyperworks Suite* and *Abaqus CAE* to preform topology optimization will be tested and the possibilities with this new tools are investigated. Then topology optimization will be performed on two civil engineering structure. The first structure is a transition piece of an offshore wind turbine. The transition piece is the part of the wind turbine that combines the tower with the foundation (Nezhentseva et al., 2011). The second civil engineering structure to be investigated using topology optimization is a pedestrian footbridge. The bridge is based on a design for a pedestrian footbridge over a freeway (Huang and Xie, 2010).

Introduction to Transition Piece

For offshore wind turbines there are different types of foundation. A relatively new type of foundation for offshore structures is a suction bucket (caisson). A suction bucket consists of a steel bucket with approximately the same length as width attached to a centered pile. Under pressure is applied inside the bucket and the bucket pulls itself down into the soil. The suction bucket functions as a combination between gravity foundation and a monopile. Some of the advantages with a suction bucket compared to a monopile are a fair simplicity if installation, the structure is stiff compared to other foundation types and it is possible to decommissioning the structure. (Nezhentseva et al., 2010)

The connecting part between the wind turbine tower and the bucket foundation is called a transition piece. Traditional offshore structures are constructions build in steel and the bucket is designed with steel-flange-reinforced sheer panels. Another possibility may be to use a high strength concrete type called Compact Reinforced Composite (CRC) to the transition piece.

The transition piece will be designed for a 5 MW wind turbine with a rotordiameter of 126 m and a hub height of 77.5 m. The assumed water depth is 35 m. The base of the tower is assumed to be

7 m in diameter and a bucket foundation on 35 m of water is assumed to have a diameter of 18 m. (Nezhentseva et al., 2010)

Nezhentseva et al. (2011) have proposed two heights of the transition piece, 9 m and 16 m cf. green part of Figure 1.3 and has formed the transition piece as an cone like structure. The thickness of the wind turbine tower wall is assumed to be 0.04 m and the thickness of the suction bucket is assumed to be 0.03 m. Measurement for the transition piece are shown in Table 1.1.

Table 1.1: *Measurement for the transition piece.*

Height of transition piece (L)	9 m / 16 m
Radius of of suction bucket (R_1)	9 m
Radius of wind turbine tower (R_2)	3.5 m
Thickness of suction bucket (t_1)	0.03 m
Thickness of wind turbine tower (t_2)	0.04 m

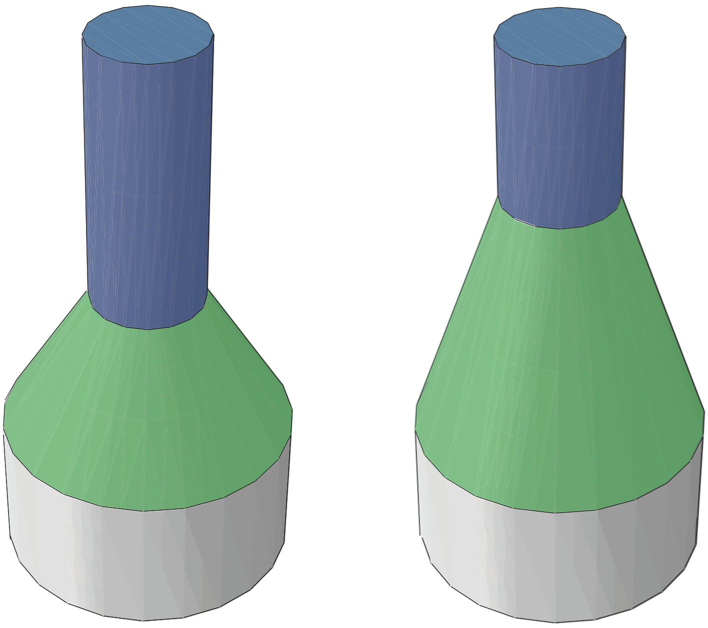

Figure 1.3: *Sketch of parts in a wind turbine foundation with two sizes of transition pieces. In the bottom is the suction bucket (gray). In the middle (green) is the transition piece. In the top (blue) is the wind turbine tower. To the left is the transition piece 16 m high and the right is the transition piece 9 m high.*

A topology optimization will be performed on the transition pieces in section 4. The optimization will be performed in steps of increasing complexity to show the development that leads to the final topology optimized design. The steps that will be performed are listed below.

- **1st Topology Optimization - Basic Solution**. An optimization will be performed on the transition Piece with a volume constrain.
- **2nd Topology Optimization - Multiple Load Directions**. A constrain is applied to ensure the structure is resistant to loads from different directions.
- **3rd Topology Optimization - Material Model and Volume.** A more advanced material modelled are applied and different choice of volume constrains are investigated.
- **Final Topology of Transition Piece.** The final topology is presented and the next steps in a design process are discussed.

Introduction to Pedestrian Footbridge

A pedestrian footbridge based on a footbridge over a major metropolitan freeway in Australia will be optimized with topology optimization. An initial sketch from BKK Architects of the project indicates the geometric constrains of the footbridge cf. Figure 1.4. The footbridge will have a free span of 72 m over the road from pier to pier. The slope of the pedestrian footbridge deck is set to maximal 1:20. The bridge will have a height over road level of 5.7 m. The footbridge is assumed to be 4 m wide. The measurements of the pedestrian footbridge is shown in Table 1.2. (Huang and Xie, 2010)

Table 1.2: *Measurements of pedestrian footbridge.*

Length	72 m
With	4 m
Free span	5.7 m
Max slope	1:20

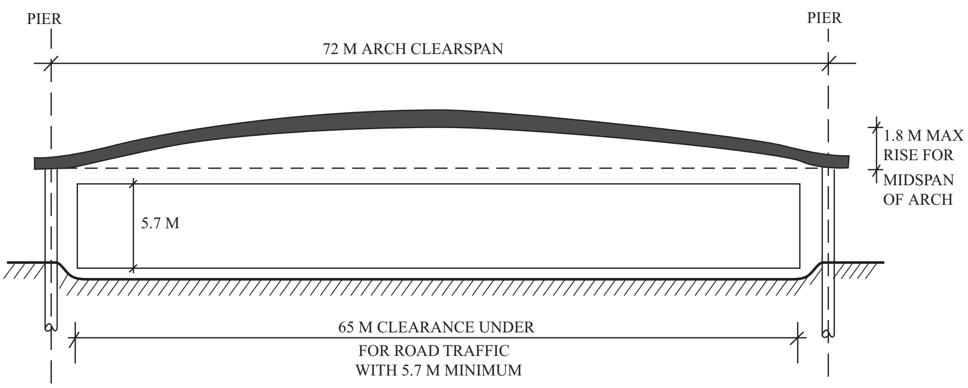

Figure 1.4: *Initial sketch from BKK Architects of pedestrian footbridge. The sketch indicating geometric constraints of the footbridge. (Huang and Xie, 2010)*

The loads on the structure for finding the optimal topology are kept simple. There are only applied a static load. The load is a pressure of 4 kPa applied to the deck of the footbridge. Other load cases will not be used to find the topology but will have to be analysed in the final design process.

The purpose of the topology optimization of the pedestrian footbridge is to find an optimal design to withstand the loads under the geometric constrains. Another imported aspect of designing a slender structure as a pedestrian footbridge is the eigenfrequency of the structure. A classic example where structures eigenfrequency have become a problem is the Millinium Bridge in London. At the opening day between 80.000 and 100.000 people cross the Millinium Bridge with a maximum density of 1.3 to 1.5 person's pr. square meter. The pedestrians created a dynamic lateral load with frequencies between 0.5 Hz and 1.0 Hz. The designers of the bridge did not take into account the load from the lateral motion caused by the pedestrians. The movements of the bridge made the pedestrian sway simultaneous from side to side adding to the moment of the bridge. The number of pedestrians allowed onto the bridge had to be reduced and the bridge was closed for pedestrian only two days after it opened. The solution for the Millinium Bridge was to install dampers on the bridge costing an extra 5 million pounds. (Dallard et al., 2001)

To avoid this problem the structures eigenfrequency is constrained in the topology optimization. A constrain will be applied so the eigenfrequency for mode shapes with lateral movement will be above 1.2 Hz and the eigenfrequency for mode shapes with vertical movement will be above 4.6 Hz. This constrain will change the topology of the structure and it will be investigated how.

A topology optimization is performed on the Pedestrian Footbridge fc. section 5. The optimization will be performed in steps leading to a final topology optimized design. The steps performed are listed below.

- **1st Topology Optimization - 2D solution.** A study of different overall designs is investigated on a 2D model of the bridge.

- **2nd Topology Optimization - 3D Solution in Steel.** The pedestrian footbridge is modelled in 3D with steel as material.

- **3rd Topology Optimization - 3D Solution in Concrete.** The pedestrian footbridge is modelled in 3D with concrete as material.

- **4th Topology Optimization - Eigenfrequency Constrains.** The pedestrian footbridge's eigenfrequencies are constrained and it is investigated how it influence the final design.

- **Final Topology of Pedestrian Footbridge** The found topologies are presented and the next steps in a design process are discussed.

1.2 History of Topology Optimization

High-speed computers have over the last three decades increased in availability. Combining the computer power with the improvements in optimization algorithms used for designing structures have moved topology optimization from a field of mostly academic interest to stage where more and more engineers and architects are experimenting with the optimization techniques. Topology optimization of structures is a relatively recent discipline in the field of structural optimization. Different method for topology optimization have been developed over the last four decades and their history are outlined here.

Bendsøe (1988) proposed the homogenization method based on studies of existence of solutions. In the homogenization method are materials with microstructure used. The material is a composite that is constructed by a unit cell consisting of one or more holes that is period repeated. The homogenization method is used to determine the material properties and optimal distribution of material can be found. The method has the drawback that the optimal microstructures and their orientations is difficult to solve or unsolvable and there are no definite length-scale associated with the microstructures resulting that the structure cannot be build. The method can still be used to understand the theoretical performance of structures. (Sigmund, 2001)

Bendsøe (1989) proposed The Solid Isotropic Material with Penalization Method. The method use isotropic material and assign each element with a relative density to the design variable. Through a power-lawed interpolation scheme is Young's modulus determined for each element. In recent years has the method been more and more popular and is now implemented in several commercial finite element programs.

Evolutionary Structural Optimization was first proposed in the early 1990's. The method is based a simple approach where inefficient material is slowly removed from the structure leaving the only necessary material. In the late 1990's an extension of the Evolutionary Structural Optimization method was made called Bi-directional Evolutionary Structural Optimization. Besides removing inefficient material the method also allowed material to be added to locations where it was most needed. The structures shown in Figure 1.1 and Figure 1.2 are optimized using Bi-directional Evolutionary Structural Optimization. (Xie et al., 2011)

1.3 Scope of the Thesis

The thesis will concern the use of topology optimization in civil engineering. There are four main parts of the thesis which will concern different aspects of topology optimization in civil engineering. The structure of the thesis is summarized in the following points.

- **Chapter 2**: General theory of topology optimization. The general concept of topology optimization and the use of different approaches for preforming topology optimization are reviewed.
- **Chapter 3**: Case study of commercial programs performance when preforming topology optimization. Possibilities and limitations when using commercial programs to preform topology optimization are discussed. Two commercial finite element and optimization programs are used.
- **Chapter 4** and **chapter 5**: Civil engineering structures. Two civil engineering structures will be analysed and optimized using topology optimization.
- **Chapter 6**: Summary of thesis conclusions and possible further work.

The first part concerns the theoretical background of topology optimization. There are many different approaches to do topology optimization and each method has different advantages and disadvantages. To give a better overall understanding on the general theory behind topology optimization is four different method reviewed: Solid Isotropic Material with Penalization Method, Homogenization method Evolutionary Structural Optimization method and Bidirectional Evolutionary Structural Optimization.

The second part of the thesis will concern a case study performed with two commercial finite element programs. To get an understanding on how topology optimization is used and how it works in commercial programs are the case study performed. The case study is performed on three cases. The first case is a so-called Mitchell type structure, which will show if the use of topology optimization gives the same optimal structure as a classical analytical solution. The second case is a 2D cantilever beam. This case will be used to compare two commercial programs topology module and investigate the difference. This will also be used to compare different aspects of the programs. The third case study is of a 3D cantilever beam. This case study is used to see how the two commercial programs will perform on a solid 3D structure. The case study will give an overview on the possibilities on using commercial finite element programs to preform topology optimization on structures.

The third part will concern the use of topology optimization on two civil engineering structures represented in section 1.1. The purpose of this part is to use topology optimization on civil engineering structures and investigate how topology optimization can be implanted as a part of the design process of a civil engineering structure.

After the three parts above will there be a conclusion of the work performed in the thesis and a discussion of possible further work.

Part I

Concept of Topology Optimization

Chapter **2**

Topology Optimization Methods

Three different types of optimization and different categories of solution methods for topology optimization are defined. Different solution methods will be defined with the main focus on the SIMP method and a solution scheme is presented.

2.1 Types of Optimizations

Topology optimization of a structure is just one way to optimize a structure substance to different variables. When optimizing the methods can be divided into three different groups: size, shape and topology optimization cf. Figure 2.1.

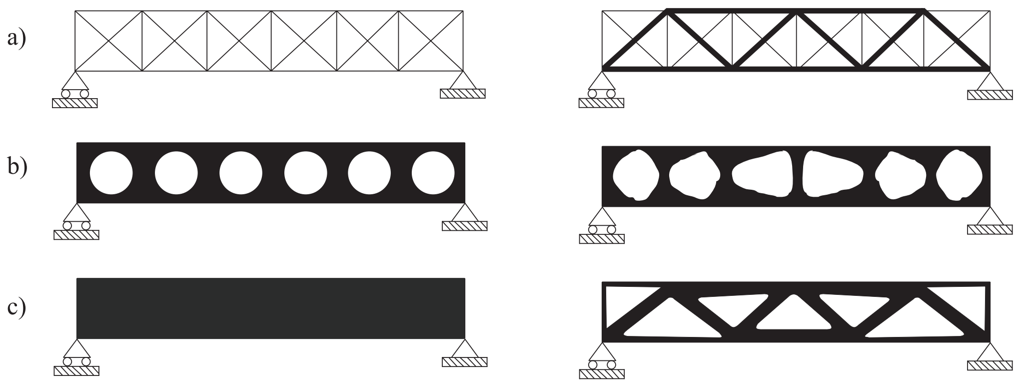

Figure 2.1: *Types and concept of optimization. To the left is the original structure and to the right is the optimized structure. a) Size optimization. Only the thickness of the truss is changed. b) Shape optimization of a beam with holes where the shape of the structure is optimized. c) Typology optimization where both the shape and topology are changed. (Bendsøe and Sigmund, 2003)*

With size optimization methods the goal can be to find the optimal cross-section of a frame or truss or optimal thickness distribution of plate. This way the optimization should maximize the performance and overall stiffness or strength of the structure or the weight of the structure. The variable will then be the thickness of a plate or the cross-section area of a truss. The design domain is known before the optimization begins and is fixed throughout the optimization process. This is illustrated on Figure 2.1 a). Only the size of the truss of the structure is changed but not the shape of the structure.

In shape optimization is the goal to find the optimal shape of a design domain which optimizes the performance of the structure. In shape optimization is the domain not fixed but a variable. The geometric boundaries of the design domain are changed throughout the optimization process but the topology of the structure is fixed cf. Figure 2.1 b) where only the shapes of the original structure changes but the topology is the same after the optimization.

In topology optimization the goal is to determine the optimal number and locations of holes within the continuum design domain. Both the structures topology and shape are design variable. This is illustrated in Figure 2.1 c). The original structure is the entire design domain. After the optimization both the shape and topology of the structure are changed. (Liang, 2005)

2.2 Types of Solutions Approaches for Optimization.

Topology optimization can be categorized in two groups: discrete and continuous approaches. In discrete approaches an element is removed by a "hard-kill" method and the element cannot reappear. Evolutionary Structural Optimization is a discrete approach. Under continues approaches are elements never completely removed and can reappear in later iterations. The density based method Solid Isotropic Material with Penalization method and the Homogenization method fall under the continuous approaches. Four solutions approaches will be reviewed. (Schmidt, 2010)

- Solid Isotropic Material with Penalization method (section 2.3)
- Homogenization method (section 2.4)
- Evolutionary Structural Optimization method (section 2.5)
- Bidirectional Evolutionary Structural Optimization method (section 2.6)

The main focus will be concentrated on the Solid Isotropic Material with Penalization method. This method will be used through the commercial programs *"Abaqus CAE"* and *" Altair Optistruct"* which is a part of *"Hyperworks Suite"* for topology optimization in this thesis. A short presentation of the Homogenization method and Evolutionary Structural Optimization methods will be given to create an overview over the different possibilities for preforming topology optimization.

2.3 Solid Isotropic Material with Penalization Method (SIMP)

Solid Isotropic Material with Penalization Method (SIMP) distributes a specific isotropic material in the design domain and finds an optimized design with the use of a penalization strategy. The objective of the density based topology optimization is to minimize the compliance. The compliance,

C, is defined in equation (2.1) and the definition of strain energy, S, is shown in equation (2.2).

$$C = \mathbf{U}^T\mathbf{F} \tag{2.1}$$

$$S = \frac{1}{2}\mathbf{U}^T\mathbf{F} \tag{2.2}$$

Where:

U	Displacement
F	Force vector

It is seen that the compliance is twice the strain energy. Therefore minimizing structures compliance is equivalent with minimizing the structures strain energy. Under the same load **F** minimizing the strain energy means minimizing the deformation, **U**, or maximizing the structures stiffness.

When Solid Isotropic Material with Penalization method is used the goal is therefore to minimize the compliance and maximizing the structures global stiffness. The optimizing problem is defined in discretized form in equation (2.3).

$$min\, C = \mathbf{U}^T\mathbf{K}\mathbf{U} \tag{2.3}$$

$$s.t. \quad \mathbf{K}\mathbf{U} = \mathbf{F}$$

The global stiffness matrix, **K**, and the local stiffness matrix, k_i, depend on the stiffness in each element, E_i, as shown in equation (2.4).

$$\mathbf{K} = \sum_{i=1}^{n} k_i(E_i) \tag{2.4}$$

The SIMP method assign an element density to each element and this is the design variable in a penalized, proportional stiffness model. This makes the topology optimization problem to a sizing problem for the size of the stiffness parameter which is the design variable. It can be shown that for isotropic material that the sizing can be seen as the size of the material. The penalized, proportional stiffness model is shown in equation (2.5).

$$\begin{aligned} E_{ijkl}(x) &= \rho(x)^p E^0_{ijkl} \\ \int_\Omega \rho(x)d\Omega \leq v; &\quad 0 \leq \rho(x) \leq 1 \end{aligned} \tag{2.5}$$

Where:

E_{ijkl}	Stiffness tensor
E^0_{ijkl}	Stiffness tensor for isotropic material
p	Penalty factor
Ω	Reference domain
ρ	Density function

The density is in fact a volume density and interpolate the material properties between 0 and E^0_{ijkl}. The desired end result is where there is a density in each element with a value of either zero or one. This corresponds to what is called a black-and-white or 1-0 design. To do this a penalty, p, in introduced. In the SIMP method the penalty is chosen to be $p > 0$ typical around 3. This make it "uneconomical" for the model to have intermediate density and the results will go to black-and-white result.

The SIMP method in a discretized based formulation is shown in equation (2.6).

$$min\, C = \mathbf{U}^T\mathbf{K}\mathbf{U} = \sum_{i=1}^{N} u_i^T k_i u_i \tag{2.6}$$

$$\begin{aligned} s.t. \quad & V = \sum_{i=1}^{N} x_i v_i \leq V_0 - V^* \\ & \mathbf{K}\mathbf{U} = \mathbf{F} \\ & k_i = (x_i)^p k_0 \\ & 0 < x_{min} \leq x_i \leq 1 \end{aligned}$$

Where:

x_i	Design variable
u_i	Local displacement
k_0	Initial local stiffness matrix
x_{min}	Minimum value of design variable
v_i	Element volume
V_0	Initial volume
V^*	Volume to be removed

There is a boundary applied for the size of the density so it does not become zero. A density value of zero may course the stiffness matrix to become singular. The volume fraction constrain determine how much of the material is removed from the structure. If the volume constrain was not applied the structure with minimum compliance and maximum stiffness will be a structure with full material and no void. The influence of the volume constrain can be seen in Figure 2.2 where a MMB-beam are optimized. A MMB beam is a classical optimization problem original from an Airbus passenger carrier where the beam is carrying the floor of the fuselage. The beam are 2400 mm x 400 mm and are loaded with a single concentrate load on the middle of the beam (Xie and Steven, 1997). When the volume fraction is low the final topology goes against a truss like structure.

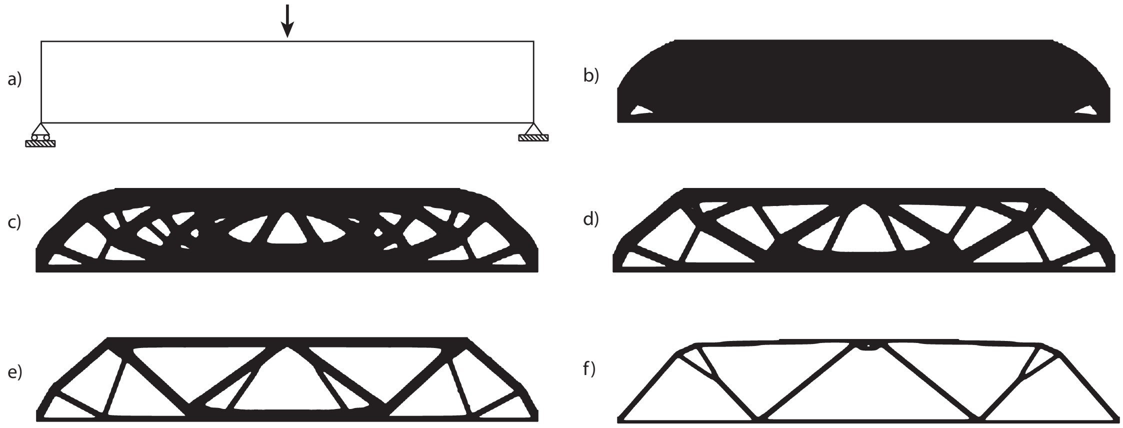

Figure 2.2: *Influence of volume fraction on SIMP topology optimization of an MMB-beam. The optimization is performed in Abaqus. The beam is meshed with 9600 quadric elements. a) Structural system of a MMB-beam. b) 90 % volume fraction. c) 70 % volume fraction. d) 50 % volume fraction. e) 30 % volume fraction. f) 10 % volume fraction.*

Approaches for Solving the Optimization Problem

For solving the optimizing problem and update the variable density can different approaches be used. This could be the Optimality Criteria method, the Sequential Linear Programming method, the Method of Moving Asymptotes or others (Sigmund, 2001). In the following section two of the methods will be reviewed: the Optimality Criteria method and the Method of Moving Asymptotes. These two methods are well suited for topology optimization problems and are therefore often used for this purpose.

Optimality Criteria method

The Optimality Criteria (OC) is a heuristic update scheme and is shown in the equation (2.3). It has been proven effective to solve structural topology optimization problems. (Bendsøe and Sigmund, 2003)

$$x_i^{new} = \begin{cases} x_i B_i^{\eta} & \text{if } \check{x}_i < x_i B_i^{\eta} < \hat{x}_i \\ \check{x}_i & \text{if } x_i B_i^{\eta} \leq \check{x}_i \\ \hat{x}_i & \text{if } x_i B_i^{\eta} \geq \hat{x}_i \end{cases}$$

Where:

$\hat{x}_i$	$max(x_{min}, x_i - m)$
$\check{x}_i$	$min(1, x_i + m)$
η	Numerical damping coefficient (typically $\eta = 1/2$)
m	Positive move limit

The optimally condition, B_i, in (2.7) can be expressed.

$$B_i = \frac{-\frac{\partial C}{\partial x_i}}{\lambda \frac{\partial V}{\partial x_i}} \tag{2.7}$$

Where:

$\frac{\partial c}{\partial x_i}$	Sensitivity of objective function
$\frac{\partial V}{\partial x_i}$	Sensitivity of the volume
λ	Lagrangian multiplier

The sensitivity of the objective function and the material volume with respect to the element densities can be find by equation (2.8) and equation (2.9).

$$\frac{\partial C}{\partial x_i} = -p(x_i)^{p-1} u_i k_0 u_i \tag{2.8}$$

$$\frac{\partial V}{\partial x_i} = 1 \tag{2.9}$$

The updating scheme in equation (2.3) adds material to the places where the strain energy is higher than the Lagrange multiplier, λ, and remove material from the places where the strain energy is lower than, λ. Therefore will the Lagrange multiplier be adjusted to satisfy the volume constraint.

The move limit m and the numerical damping coefficient η controls the rate the changes in each integrations step can happen and is chosen from experience.

Method of Moving Asymptotes

The Method of Moving Asymptotes (MMA) is a solution method well suited for programming topology optimization problems. The solution is found based on sensitivity information of the iteration point, x^0, and iteration history. A function, F, with n variable $(x_1, ..., x_n)$ is given in equation (2.10). (Bendsøe and Sigmund, 2003).

$$F(\mathbf{X}) \approx F(\mathbf{X}^0) + \sum_{i=1}^{n} \left(\frac{r_i}{U_i - x_i} + \frac{s_i}{x_i - L_i} \right) \tag{2.10}$$

r_i and s_i are numbers chosen as

$$
\begin{aligned}
&if\ \frac{\partial F}{\partial x_i}(x^0) > 0\ then\ r_i = \left(U_i - z_i^0\right)^2 \frac{\partial F}{\partial x_i}(x^0)\ and\ s_i = 0 \\
&if\ \frac{\partial F}{\partial x_i}(x^0) < 0\ then\ r_i = 0\ and\ s_i = -\left(x_i^0 - L_i\right)^2 \frac{\partial F}{\partial x_i}(x^0)
\end{aligned}
\tag{2.11}
$$

The numbers U_i and L_i give vertical asymptotes for the approximation of F (and hereby the name of the method) and gives a range for the solutions for optimization problems and are updated for each iteration based on the iteration history. The separable approximations of the design variable into sub-problems so the optimization can be solved individual for each element. This makes the method well suited for programming especially when there are only few constrains in the optimization problem.

Optimization Process in SIMP

When finding the optimized topology using SIMP method the equations in (2.1) to (2.11) are combined in an interpolation scheme. The scheme is shown in a flowchart in Figure 2.3. The goal is to find the optimal distribution of material from the density penalty based method in a clean 0-1 design. The scheme is divided into three parts: Pre-processing, Optimization and Post-Processing.

The first part is the Pre-processing. Here is a finite element model build of the structure. These involve choosing a reference domain for the model and apply load and boundary conditions. It is also necessary to define the areas of the structure that are the design domain for the optimization and areas of the structure that are frozen domains with are either only solids or void. A material need to be assigned to the structure and with the SIMP method it needs to be an isotropic material. The structure should be meshed for the design process. The same mesh will be used throughout the entire process. Beside the requirements for stress and strain converges should the mesh be fine enough to be able to describe the structure and show the final topology. If the mesh is to course the final topology may not have the right members and form cf. Figure 2.4.

The second part is the optimization process. First is a homogeneous density distribution of material chosen and a FEM analysis is calculated of the structure where stresses and strains are calculated. The compliance can be calculated for use in the OC scheme. If the MMA scheme is chosen the sensitivities with respect to the design changes is calculated as well. Both the OC scheme and the MMA scheme can be used. Bendsøe and Sigmund (2003) stated that MMA may be a bit slower at simple problems with only a single constrain where MMA has been proven to handle many constrains well.

If the compliance is only marginal improved the optimization process stops. Other stop conditions can be applied as a maximal displacement or stress in a point. If a stop condition is not met the density variable are updated using an algorithm like OC or MMA and a new iteration loop is made.

When the optimization process is finish the resulting topology can be interpreted and be a basic for further designing of a structure.

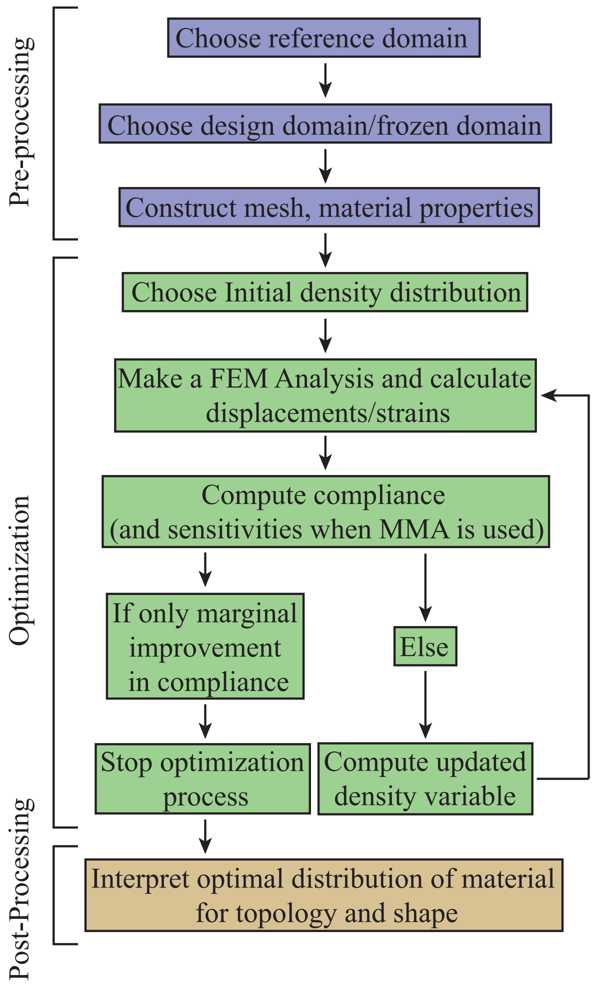

Figure 2.3: *Flow chart of topology optimization scheme based on SIMP method divided into three parts: Pre-processing, Optimization and Post-Processing.*

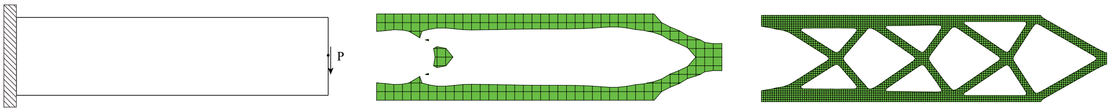

Figure 2.4: *SIMP optimization of a cantilever beam with a volume constrain of 30 % and meshed with different meshes. The topology optimization is performed in Abaqus. Left: Structural system for cantilever beam loaded with a single concentrated force. Middle: a coarse mesh where the design domain is meshed with 400 elements. Right: A finer mesh where the design domain is meshed with 6400 elements. The coarse meshed structure is not able to capture the topology of the finer meshed structure.*

Mesh Independence and Checkerboard Pattern Control

Different problems can occur under an optimization process. Two of them are mesh dependence results and checkerboard pattern solutions.

Mesh Independence

When a structure gets meshed finer it makes it possible to create more holes in the structure without changing the volume which in general will create a stiffer structure. This effect is shown in Figure 2.5 where the finer meshed structure gives more detailed topologies. Therefore it is necessary to make the solution mesh-Independent so a finer mesh only gives a more detailed model of the same topology solution. A local restriction on the variation in the density is made to make fine scale structure impossible. There are three general ways to do this:

- Applying filters in the optimization
- Adding constrains to the optimization problem
- Reducing directly the parameter space for the design

An applied filter that limits the variations of the densities is a direct way to insure mesh independence. This can be done by a filter radius for the stiffness distribution. This make the stiffness in a point depended of the density in all the nearby point. This makes the density of fine structures more "blurry" and with the penalty factor this areas will disappear in the final topology. Another possible is to filter the sensitivities which give similar results.

An indirect way to make the structure mesh-independent is a constrain that can be added as a perimeter control. By restricting the lengths/areas of all inner and outer boundaries the final form can only have restricted number of holes. Other types of restrictions can be applied.

The last method is based on the MOhnotonicity based minimum LEngth scale method (MOLE). The method makes an extra non-negative constrain that make a minimum length width of material parts and voids. The method measures the density along four equally spaced diagonals and control if they are monotonic or not. The reason for also checking the diagonals beside the horizontal and vertical way is that this also makes a filter for a checkerboard problem.

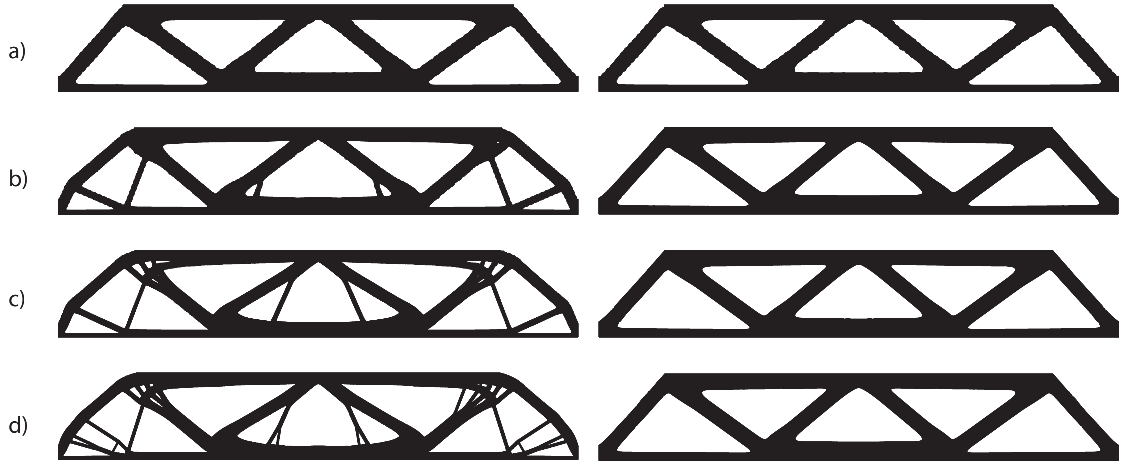

Figure 2.5: *Mesh depended and mesh independent topology optimization of MMB-beam. Optimization is performed in Abaqus. a) Meshed with 2400 elements. b) Meshed with 9600 elements. c) Meshed with 38400 elements. d) Meshed with 106400 elements. Left: No filters or constrains applied for preventing mesh dependence. Right: A minimum length constrain are applied which make the topology solutions mesh independent.*

Checkerboard Pattern Control

Under a topology optimization checkerboard patterns can be observed. The phenomena show where the material is varied between solid and void in a periodic matter like a checkerboard pattern. The reason for the checkerboard pattern is the finite element analyses that overestimate the numerical stiffness of a checkerboard pattern. This produces a solution that is not practical possible. A way to prevent the checkerboard pattern is to implement one of the three solutions mentioned for mesh independence above.

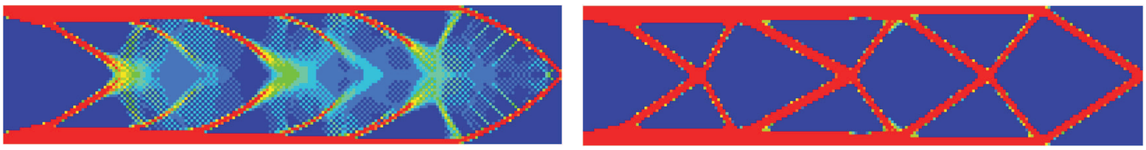

Figure 2.6: *SIMP optimization of a cantilever beam with a volume constrain of 30 %. The optimization is made in Optistruct. Left: No checkerboard pattern control. There is distinct checkerboard pattern in the final solution. Right: Checkerboard pattern control is applied to the model and the checkerboard pattern has been removed.*

The method used in this thesis will be the third solution which is implementing a minimum member size in as a geometric constrain. This will prevent both checkerboard pattern and make the solution mesh Independent. The result of implementation the MOLE method is shown i Figure 2.5 and 2.6.

2.4 Homogenization Method

The homogenization method is used to model a composite material. When a structure is finer and finer meshed and optimized using the SIMP method it is showed that the final structure will contain a fine grit of solid and void. The general concept of the homogenization method are to create a composite material by using a isotropic material defined by E^0_{ijkl} and void. A base material is then created and the design variable is the density of the base material. A density is introduced where $\rho = 1$ is material and $\rho = 0$ is void. Values between zero and one is composite material with void on a microstructure level.

The composite material consist of many infinitely small sells that are repeated periodically through the material cf. Figure 2.7. The stiffness tensor and the material density can then be described as in equations (2.12). (Bendsøe and Sigmund, 2003)

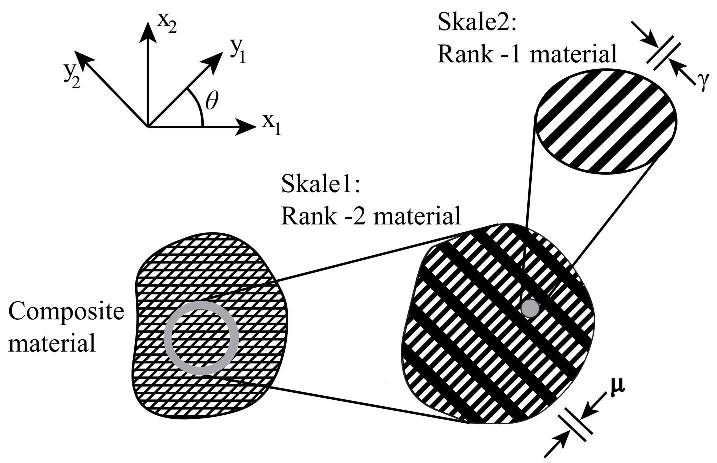

Figure 2.7: *Layered material for two dimensional cases. The material is built of a second rank layered material and can be rotated. (Bendsøe and Sigmund, 2003)*

$$\begin{aligned}
\text{Geometric variables } \ \mu, \gamma, \ldots \in L^{\infty}(\Omega),\ \text{angle } \theta \in L^{\infty}(\Omega) \\
E_{ijkl}(x) = \tilde{E}_{ijkl}(\mu(x), \gamma(x), \ldots, \theta(x)) \\
\text{density of material } \ \rho(x) = \rho(\mu(x), \gamma(x), \ldots) \\
\int_{\Omega} \rho(x) d\Omega \leq v; \quad 0 \leq \rho(x) \leq 1\ ,\ x \in \Omega
\end{aligned} \tag{2.12}$$

Where:

E_{ijkl}	Effective material parameters for the composite

The composite material can be an anisotropic material and the rotation angle of the micro structure is a design variable. Both the effective material parameters for the composite and the density is a function of a number of variables. These variables are then the design parameters that will have to be

optimized.
The homogenization method can be used to minimize the compliance of a structure and hereby find an optimal topology. Generally will the resulting topology consist of "gray" areas where the material use is optimized but not a "black-white" solution. This can be used to understand how the use of composite material influences the effectiveness of a structure.

2.5 Evolutionary Structural Optimization (ESO)

Another approach for structural optimization is the Evolutionary Structural Optimization Method (ESO). The method is based on a simple idea. By slowly remove inefficient material from a structure the residual structure will reach an optimum where the residual material is used more effective.

Material is placed over the design area, meshed into element and the stresses in the each element are determined by a FEM calculation. The stress in each element is found as an average over the stresses in the integration points. A rejection criterion based on local stresses in an element is made. The Von Mises yield criterion can be used for isotopic materials as steel. The element stresses are compared with the maximal stresses in the structure. The rejection criterion is then given by:

$$\frac{\sigma_e^{vm}}{\sigma_{max}^{vm}} < RR_i \tag{2.13}$$

Where:

σ_e^{vm}	Von Mises stress in element
σ_{max}^{vm}	Maximum Von Mises stress in model
RR_i	Current Rejection Ratio

Elements that fulfil the rejection criteria in (2.13) are being deleted from the model and the FEM analysis of the model is run aging. This cycle continues until no more elements are being deleted at the end of the iteration. An evolution rate is then added to the Rejection Ratio as shown in equation (2.14) and an new iterations cycle is run.

$$RR_{i+1} = RR_i + ER, \qquad i = 0, 1, 2, 3... \tag{2.14}$$

Where:

ER	Evolutionary Rate

With the ESO method the final structure is stressed more equity and there should not be any unnecessary material. The evolutionary rate and rejection ratio is chosen from experience and the iterative optimization process can stop after the end of each iteration for a given Rejection Ratio. A flow chart of the ESO method is shown in Figure 2.8. The pre-processing and post-processing are identical to the SIMP method cf. Figure 2.3.

The ESO method can also be formulated to maximize the stiffness of the structures by minimizing the compliance. This is done by determine how much the stiffness of the structure will change when removing the i'th element. A sensitivity number is calculated for each element and the elements with the lowest number can be removed.

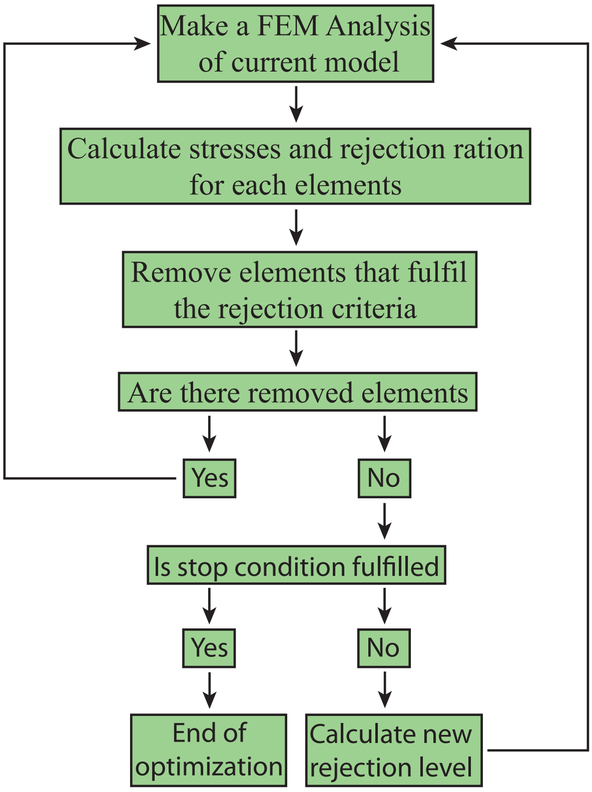

Figure 2.8: *Flow chart of topology optimization scheme based on ESO method. Only the optimization part of the scheme is shown.*

2.6 Bidirectional Evolutionary Structural Optimization (BESO)

The Bidirectional Evolutionary Structural Optimization (BESO) is an extension to the ESO method. The ESO method is a hard-kill method meaning that when an element is removed it cannot return in later iterations. The BESO method is a soft-kill method. Elements are allowed to be added again at places where they are most demanded. Elements displacement fields are estimated with FEM analyses also of void elements through a linear extrapolation. The elements with the lowest sensitivity number can then be removed and void elements with the highest sensitivity numbers can be changed back into elements. The BESO method shown below is based on optimizing the stiffness of the structure. The optimization statement with a volume constrain is then formulated in equation (2.15)

$$min\, C = \mathbf{U}^T \mathbf{K} \mathbf{U} \tag{2.15}$$

$$s.t. \quad V = \sum_{i=1}^{N} x_i v_i \leq V_0 - V^*$$
$$x_i = \; 0 \;\; or \;\; 1$$

The stiffness change by removing each element is shown in equation (2.16) and the sensitivity number for the mean compliance, α_i^e, is defined in equation (2.17). The sensitivity number for void elements is set to zero. The BESO method have the same challenges with checkerboard patterns and mesh-independence as the SIMP method cf. section 2.3. A filter scheme will have to be added to prevent ill solutions. The filters will not be explained, but can be found in Huang and Xie (2010).

$$\Delta \mathbf{K} = \mathbf{K}^* - \mathbf{K} = -k_i \tag{2.16}$$

$$\alpha_i^e = \Delta C_i = \frac{1}{2} u_i^T k_i u_i \tag{2.17}$$

Where:

$\mathbf{K}$	Global stiffness matrix.
$\mathbf{K}^*$	Stiffness matrix of the resulting structure after the element is removed
k_i	Stiffness matrix of the i'th element

Criterion for Adding and Removing Elements

The volume constrain in equation (2.15) have to be respected. The volume for a iteration step are expressed in equation (2.18).

$$V_{k+1} = V_k(1 + ER) \quad (k = 1, 2, 3...) \tag{2.18}$$

Where:

ER	Evolutionary volume ratio
$Vk+1$	Target volume for the next iteration

The sensitivity number is calculated for each element and void element and threshold sensitivity numbers for adding of removing elements are calculated. The adding criterion where void elements should be added are shown in equation (2.19) and the removed criterion where elements should be removed are shown in equation (2.20).

$$\alpha_i^e \leq \alpha_{del}^{th} \tag{2.19}$$

$$\alpha_i^e > \alpha_{add}^{th} \tag{2.20}$$

Where:

α_{del}^{th}	Threshold sensitivity numbers for removing element
α_{add}^{th}	Threshold sensitivity numbers for adding element

To determine the right volume fraction the thresholds can be found by sitting $\alpha_{del}^{th} = \alpha_{del}^{th} = \alpha^{th}$. When knowing $Vk+1$ can α^{th} easily be determined by sorting the sensitivity numbers in the structure and set threshold sensitivity equal to the value of the sensitivity numbers with the desired volume fraction. If the volume is not constrained after this operation can the thresholds be adjusted.

When the desired volume fraction is reached a convergence criterion can be formulated to see if the compliance is converted. If the convergence criterion is not fulfilled a new finite element calculation will be made and a new iteration process begins. A flowchart of the optimization process using BESO are shown in Figure 2.9.

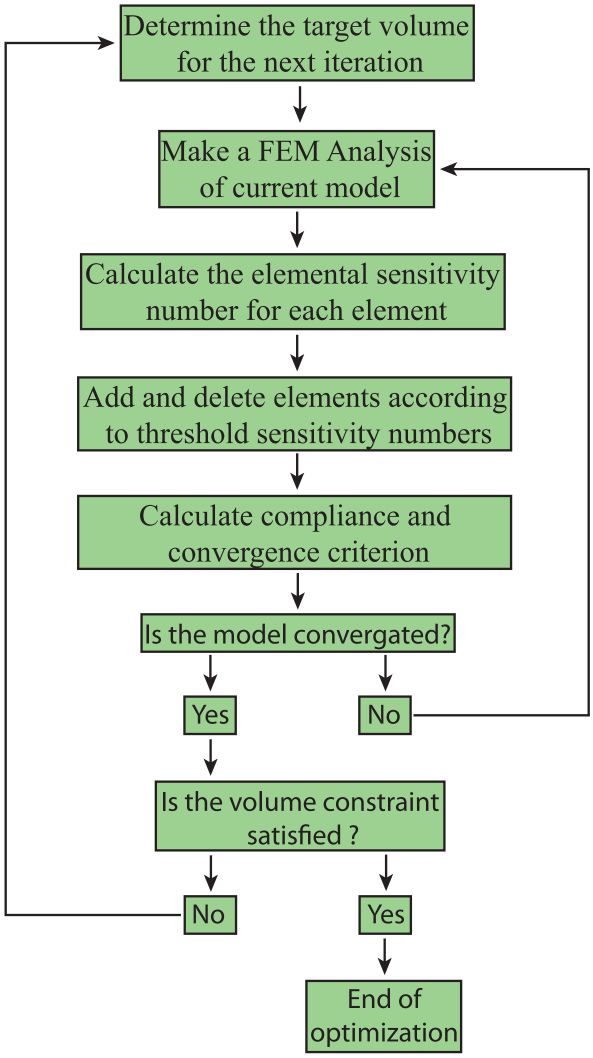

Figure 2.9: *Flow chart of topology optimization scheme based on BESO method. Only the optimization part of the scheme is shown.*

Part II

Case Study

Chapter 3

Case Study

In the following section three case studies are performed: two 2D problems (a Michell type structure and a cantilever beam) and a 3D problem. The cases will be compared for two analytical finite element and optimization programs and a conclusion on the programs functionality is shown.

Tools for Optimization and Tasks

Two commercial finite element programs will be compared for the optimization: Abaqus CAE and Altair Optistruct. Abaqus is a finite element program to solve a large number of numerical problems. Altair Optistruct is a part of the finite element program suite Hyperworks. The two programs does essential follow the flow charts in Figure 3.1. This means that the process of finding the optimal topology is divided into two parts: A pre-process part and a optimization parts. These parts are similar to the parts shown in Figure 2.3 for a SIMP optimization.

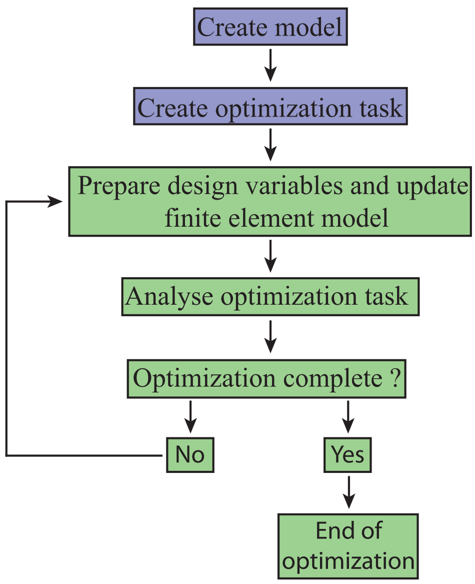

Figure 3.1: *Flow chart of topology optimization scheme in commercial optimization programs. After Abaqus (2012).*

In the pre-process part (blue on Figure 3.1) is the model created. This means build and mesh the FEM model, material properties are chosen and load and boundary conditions is defined. In the pre-process part is the optimizing task is also created. The optimizing task includes creating the design responses, create objective functions and constrains and submitting the optimization process for analysis.

Where all steps in the pre-process part are controlled by the user is the steps in the optimization parts actions (green on Figure 3.1) automated in the commercial programs. An iterative optimization process will continue until the results converged or a stop condition is met. A final step is the post processing part where the final topology is visualized and relevant data can be extracted.
There will be made three models in each program and the models will be made with the same materials, boundary conditions, object function, constrains etc. so the results can be compared.

3.1 Case 1: Michell Type Structure

A Michell type structure is a classical analytical solution for finding a structure with minimum weight. To find a Michell type structure it has to have a framework that satisfy two conditions, one for the forces and one for the stains in the structure.

- The stresses in all members are equal to $\pm\,\sigma$, where σ is the allowable stress for tension and compression.
- There exists a virtual deformation of the region Ω, with displacement vanishing on the surfaces of support and with strains along the members of the structure equal to $\pm\,\varepsilon$, where the sign agrees with that of the end load carried by the particular member, and such that no linear strain in R exceeds ε, which is a small positive number, in absolute value. (Chan, 1960)

The Michell Theorem states that a Michell type structure gives a framework where the volume is equal or less than any other framework that satisfy the equilibrium conditions for a given force. (Chan, 1960).

Design and Optimization Task

The structural system with the design domain and load can be seen on Figure 3.2 and the theoretical solution for the Michell type structure can be seen on Figure 3.3.

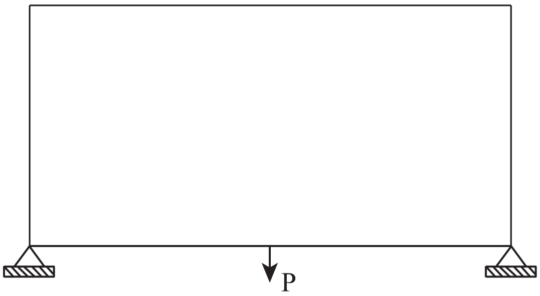

Figure 3.2: *Structural system for case 1. The design domain is simple supported in corners with single concentrated force acting in bottom of design domain.*

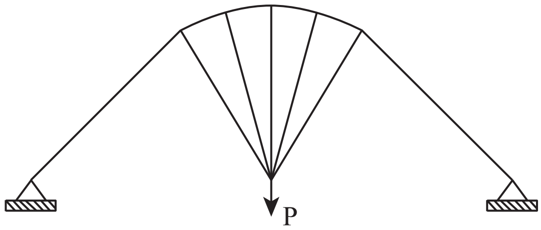

Figure 3.3: *Michell type structure. The Michell structure has the solution with minimum of volume for design problem in Figure 3.2. (Xie and Steven, 1997)*

The objective of the optimization is to minimize the compliance of the structure. The design variables will be the density of each element in the design domain. The material of the structure is modelled as an isotropic material and has the properties of steel. Elements used are a 4-node bilinear plane stress quadrilateral with reduced integration (CPS4R). Information about the finite element model and the optimization task is given in Table 3.1 and 3.2.

Table 3.1: *Model information.*

Material	Isotropic linear elastic
Young's modolus	E = 210000 MPa
Possion's ratio	$\upsilon = 0.3$
Elements Optistruct	10153 elements
Elements Abaqus	10082 elements

Table 3.2: *Optimization task information.*

Optimization type	Topology
Method used	SIMP
Opject	Minimize compliance
Constrains	Volume fraction = 20 %
	Min member size =

Results

The final design from topology optimization in the two programs can be seen in Figure 3.4 and 3.5. Results from topology optimization of the Michell type structure are shown in Table 3.3.

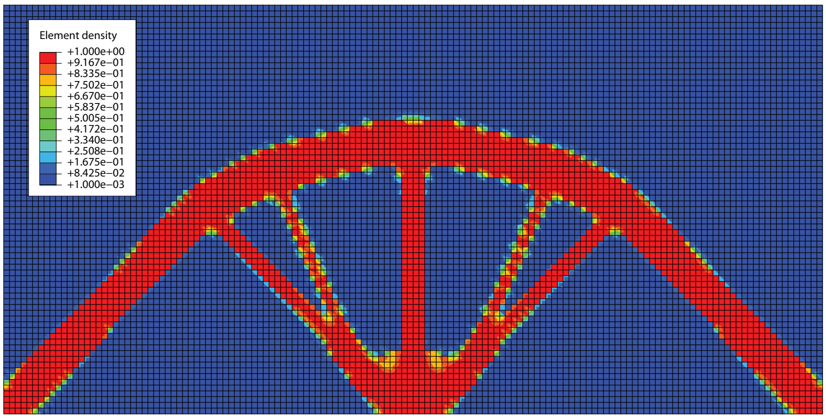

Figure 3.4: *Topology optimization of Michell type structure with Abaqus. The material density is plotted with colours.*

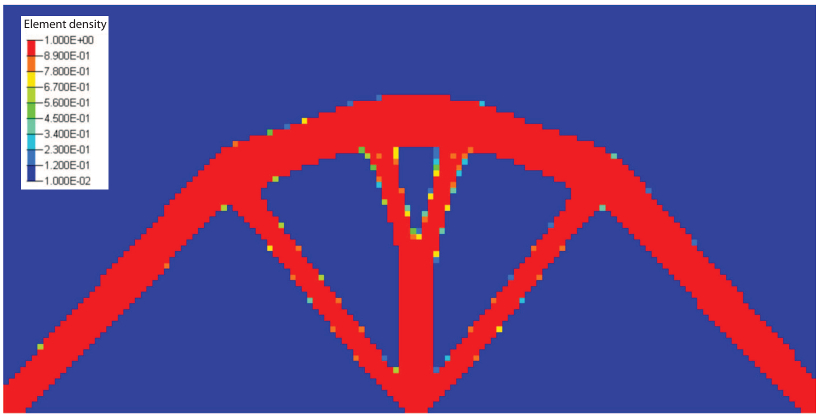

Figure 3.5: *Topology optimization of Michell type structure with Optistruct. The material density is plotted with colours.*

Table 3.3: *Results of optimization with Abaqus and Optistruct.*

	Abaqus	Optistruct
Final Compliance	59.62	49.96
Final volume fraction	20.0 %	20.0 %
Number of iterations	34	42
Wall clock time used	20 min	3 min

As seen in Figure 3.4 and 3.5 does the topology optimizations reach a final design. It can also be seen that both programs reach a clear 0-1 distribution of density. Only few elements have a density in the middle interval. Both programs reach a topology similar to the theoretical Michell type structure shown in Figure 3.2. Both with an arc form with trust like structure to the point where the force attacks. Abaqus and Optistruct do not obtain exactly same solution for the topology of the structure. The Abaqus solution has five horizontal trusts where the Optistruct solution only has four. To compare the two solutions the compliance is plotted for the two models cf. Figure 3.6.

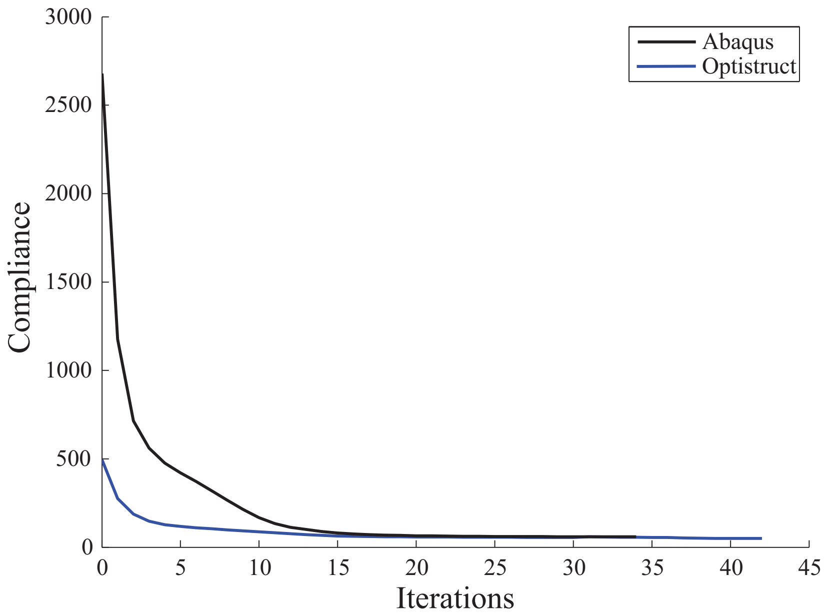

Figure 3.6: *Plot of compliance for topology optimization of Michell type structure with Abaqus and Optistruct.*

The compliance converged for the solutions in both Abaqus and Optistruct. There are a difference in the final value of compliance in the two programs but compared to the initial values is the difference relative small cf. Table 3.3. Both solution may therefore be seen a feasible solutions to the optimization problem of the Michell structure.

Another parameter for the optimization process is how much time the process use. There is a noticeable difference in the use of time. Abaqus solver uses approximately seven times as much time to solve the optimization problem. The same general trend is observed with other optimizations tasks.

3.2 Case 2: 2D Cantilever Beam

Design and Optimization Task

The second case study is of a 2D cantilever beam. The beam is pinned in one end and loaded with a single concentrated load, *P* in the other end. The structural system is shown in Figure 3.7.

Figure 3.7: *Second case. Structural system of cantilever beam.*

The beam is pinned for all translations and rotations in one end. The optimized structure does not need to be pinned along the entire side. Therefore is the boundary conditions not defined as a frozen area. The volume fraction i chosen to be only 20 % which should give a trust like structure. The objective is to minimize the compliance and the method used is SIMP. To make the optimization independent a minimum member size control is applied. Information of the finite element model and optimization task is given in Table 3.4 and 3.5.

Table 3.4: *Model information.*

Material	Isotropic linear elastic
Young's modulus	E = 210000 MPa
Poisson's ratio	υ = 0.3
Element type Optistruct	10000 elements
Element type Abaqus	10000 elements

Table 3.5: *Optimization task information.*

Optimization type	Topology
Method used	SIMP
Opject	Minimize volume
Constrains	Volume fraction = 20 %
	Min member size

Results

The result of the optimization are shown in Figure 3.8 and 3.9. The final optimized material distribution obtained with Abaqus and Optistruct are almost identical. This is also seen from the graph shown in Figure 3.10 where the compliance is plotted. Though the two programs use a different number of iterations is the final compliance close to each other cf. Table 3.6.

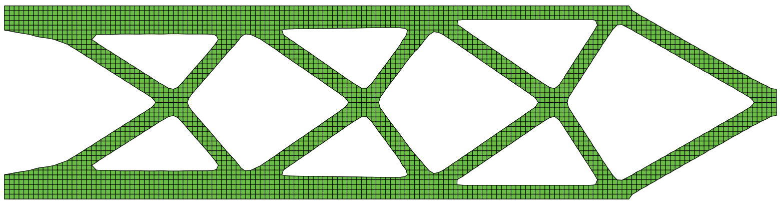

Figure 3.8: *Topology optimization of Cantilever Beam with Abaqus. Optimized material distribution is showed.*

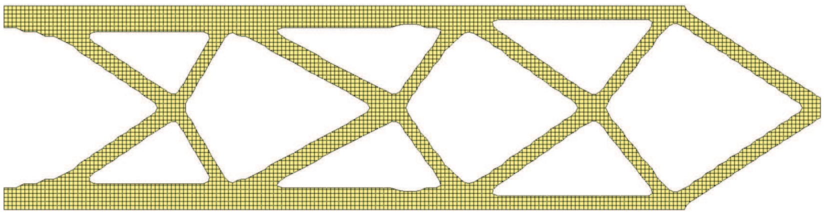

Figure 3.9: *Topology optimization of Cantilever Beam with Optistruct. Optimized material distribution is showed.*

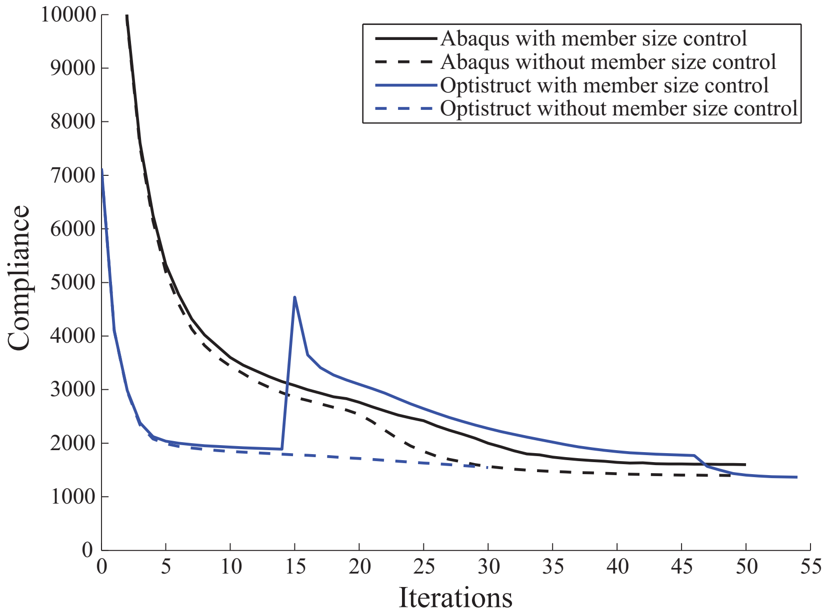

Figure 3.10: *Plot of compliance for topology optimization of 2D cantilever beam with Abaqus and Optistruct.*

Table 3.6: Results of optimization with Abaqus ATOM and Optistruct.

	Abaqus	Optistruct
Final Compliance	1601.4	1365.0
Final volume fraction	20 %	20 %
Number of iterations	51	54
Wall clock time used	37 min	2 min

Influence of Checkerboard Control

The build in checkerboard control in the both programs is investigated. To be able to do this the optimization process is run without the minimum member size control. This will show if the programs will be able to remove checkerboard patterns from the final topology. It is expected that the final result will differ from the results shown in Figure 3.8, Figure 3.9 and Table 3.6. The new topology can be seen in Figure 3.11 and Figure 3.12.

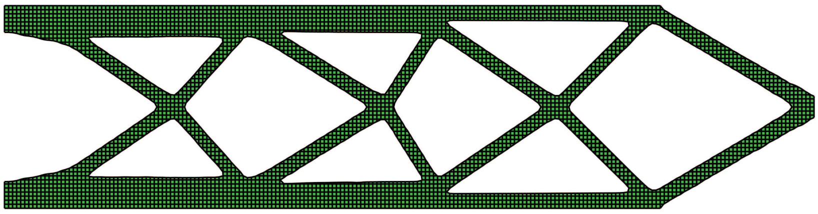

Figure 3.11: *Topology optimization of cantilever beam is Abaqus with no member size control. Optimized material distribution is showed.*

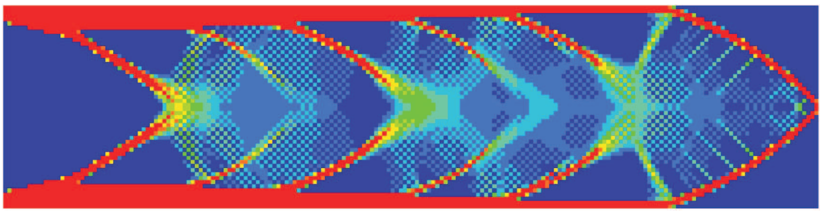

Figure 3.12: *Topology optimization of cantilever beam in Optistruct with no member size control. Optimized material distribution is showed.*

The topology changes in Abaqus when the minimum member size is removed. This show that the model has become mesh depended and some of the trust members have become smaller than the minimum size. The removed constrain also shows in the final compliance fc. Figure 3.10. The compliance is minimized more and the final structure is hereby stiffer. After the minimum size constrain is removed the final topology does not show any checkerboard pattern. Abaqus have a build in filter function where a filter radius and a filter diameter are chosen automatic to prevent checkerboard pattern. This filter is automatically applied to all topology optimization tasks in Abaqus.

The changes in the final topology are larger in Optistruct then in Abaqus. When the minimum size control is removed are there not applied another filter automatic and a checkerboard pattern appear in the final topology. As stated in section 2.3 should a checkerboard pattern increase the stiffness of the structure and the compliance should be lower. This is not what is shown in Figure 3.10 where the compliance from the model without minimum member size is not lower than the model with minimum member size. The design with checkerboard pattern is not a feasible result and cannot be used.

The optimization without checkerboard control has shown the necessity of a user defined checkerboard control in the programs special if using Optistruct. Without will the resulting topology be misguiding.

3.3 Case 3: 3D Cantilever Beam

Design and Optimization Task

The third case study is a three dimensional solid structure. The study will show if the two finite element programs Abaqus and Optistruct are able to perform topology optimization on a three dimensional solid structure with multiple loads. The structural system of the beam to be optimized is shown in Figure 3.13.

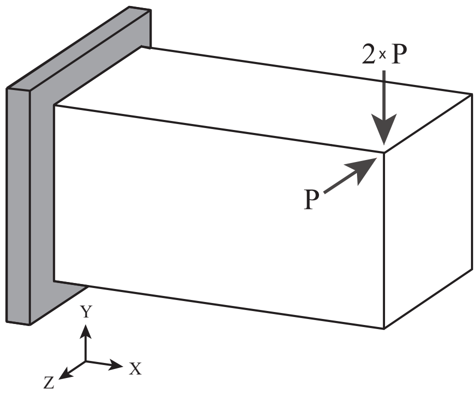

Figure 3.13: *Structural system of three dimensional cantilever beam.*

All translations and rotations degrees of freedom are fixed at one end of beam. In the opposite corner of the beam is two forces acting, one half the size of the other. This gives a three dimensional problem. The only frozen area of the structure is the point where the forces attach. The volume fraction is chosen to be 10 %. Information of the finite element model and optimization task is given in Table 3.7 and 3.8. The objective is to minimize the compliance and the method used is SIMP. Minimum member size control is applied.

***Table 3.7:** Model information.*

Material	Isotropic linear elastic
Young's modulus	E = 210000 MPa
Poisson's ratio	υ = 0.3
Element type Optistruct	16000 linear elements
Element type Abaqus	16000 linear elements

***Table 3.8:** Optimization task information.*

Optimization type	Topology
Method used	SIMP
Opject	Minimize compliance
Constrains	Volume fraction = 10 %
	Min member size

Results

The result of the optimization are shown in Figure 3.14 and 3.15.

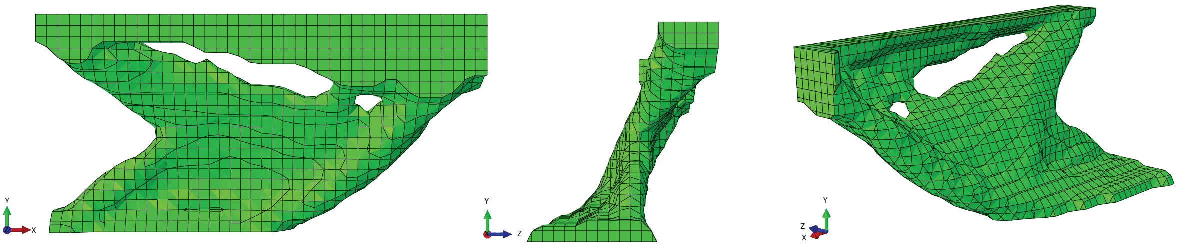

***Figure 3.14:** Topology optimization of 3D cantilever beam in Abaqus. Optimization material distribution is showed.*

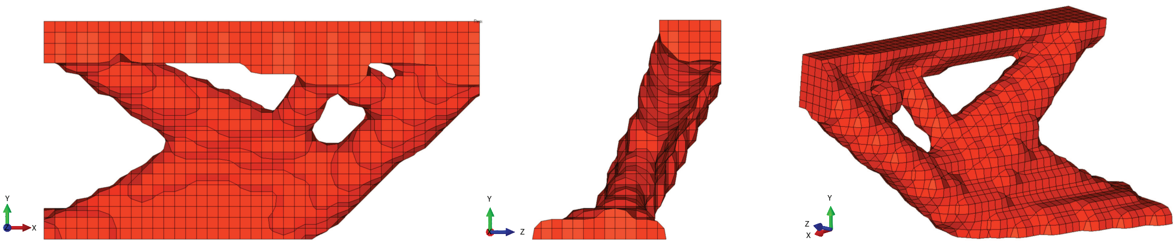

***Figure 3.15:** Topology optimization of 3D cantilever beam in Optistruct. Optimization material distribution is showed.*

As seen on the figures above does the optimization task in Abaqus and Optistruct ends out with similar topologies. The compliance obtained from the optimization can be seen i Figure 3.16 and the general results can be seen i Table 3.9. The final structures from both programs have similar end compliances. It is also observed that the difference in time used for the optimization process is smaller for the three dimensional problem then in the previous cases.

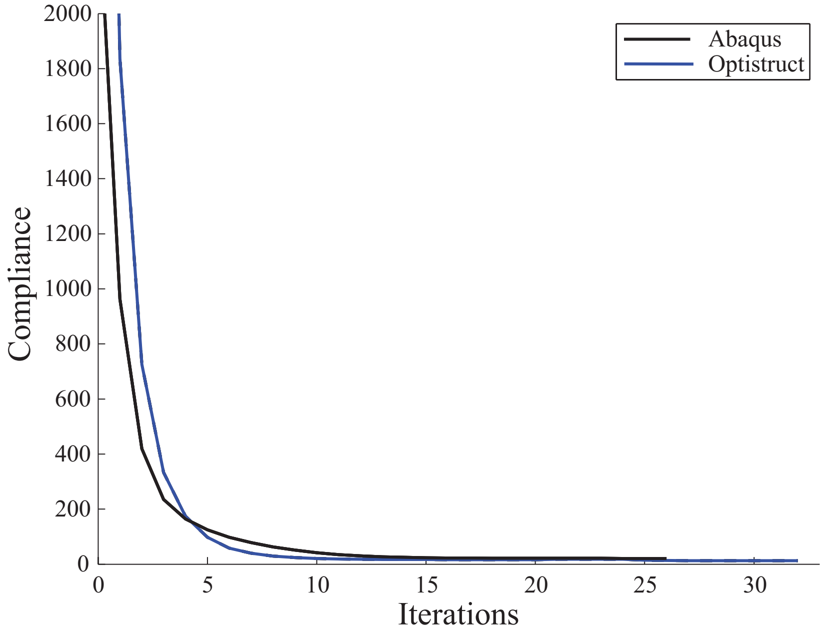

Figure 3.16: *Plot of compliance for topology optimization of cantilever beam with Abaqus and Optistruct.*

Table 3.9: *Results of optimization with Abaqus and Optistruct.*

	Abaqus	Optistruct
Final Compliance	17.07	12.56
Final volume fraction	10 %	10 %
Number of iterations	22	32
Wall clock time used	22 min	7 min

3.4 Abaqus vs. Optistruct

The commercial topology optimizations programs Abaqus and Optistruct have been evaluated though three case studies in section 3.1, 3.2 and 3.3. Some of the observed results and comments on how the programs preformed are listed below.

In the case studies a classical SIMP optimization has been performed with compliance as the object and with a volume fraction as a constrain. Other object and constrains are possible in both programs. Some of the possible object functions beside compliance are volume, weight, displacement and rotation. Possible constrains are strain energy, volume, weight, displacement, rotation, eigenfrequency and more. This gives a large number of opportunities for an optimization tasks. Both programs also give the possibility to apply a geometric constrain beside the minimum member size constrain used in the case studies. This makes it possible to apply a constrain that demand symmetric around a plain or rotations symmetric around an axis.

Both programs have proven suitable to preform topology optimization. Both on a two dimensional shell structure and on a three dimension solid structure. The two programs have in all case studies found similar final topology and compliance. In the 2D case studies does Optistruct in general converge faster against the final compliance where Abaqus and Optistruct converge the same rate in the 3D case. It is possible to select a more aggressive algorithm as an update strategy for the density in the setup of the optimization task in Abagus. This may make Abaqus converge faster. Both programs are also able to reach a 1-0 density distribution. It has been observed that in 3D cases are there more elements with a density in middle interval. This makes it necessary to determine a lower boundary for element densities to accept in the final topology.

The overall time spend on an optimization task for all three studies are listed in Table 3.10. The time spent in Abaqus for an topology optimization is generally longer. This is both due to the time spent on the optimization but also the time spent on FEM calculations and other tasks. An investigation of the log files from the Abaqus optimization shows that only approximately 20-25% of the time is spend on the optimization. 75%-80% of the time is spend on FEM analysis and under 1% of the time on preparing the job and others tasks.

Table 3.10: *Wall clock time used for optimization in Abaqus and Optistruct.*

	Abaqus	Optistruct
Case 1	20 min	3 min
Case 2	37 min	2 min
Case 3	22 min	7 min

It is observed that with a manual applied checkerboard control do both programs obtain a checkerboard free solution. When the manual checkerboard control was not applied did the build in checkerboard filter able Abaqus to reach a checkerboard free solution. There is no automatic checkerboard filter in Optistruct and a checkerboard control method has to be applied manual.

Abaqus will be used for modelling two civil engineering structures in chapter 4 and 5. This is chosen based on the result of the three case studies and the knowledge on modelling complex structures in Abaqus. It is the experience that Abaqus is able to solve larges complex non-linear FEM problems, is able to model different material properties and the user interface for building a model, meshing and applying elements and Post-Processing works very well.

Part III

Civil Engineering Structures

Chapter 4

Transition Piece for Offshore Wind Turbine

Topology optimization is performed on a civil engineering structure. The structure is a transition piece of an offshore wind turbine. With the use of topology optimization an optimal design is found while satisfying the necessary constrains.

4.1 Introduction

Topology optimization is used to design a transition piece of an offshore wind turbine fc. section 1.1. The transition piece will be designed for a 5 MW wind turbine with a rotordiameter of 126 m and a hub height of 77.5 m. The assumed water depth is 35 m. Two sizes of the transition piece will be investigated. A sketch of the transition pieces is showed in Figure 4.1. The optimization is divided in three steps to investigate different aspects of the design and a final optimized structure is presented.

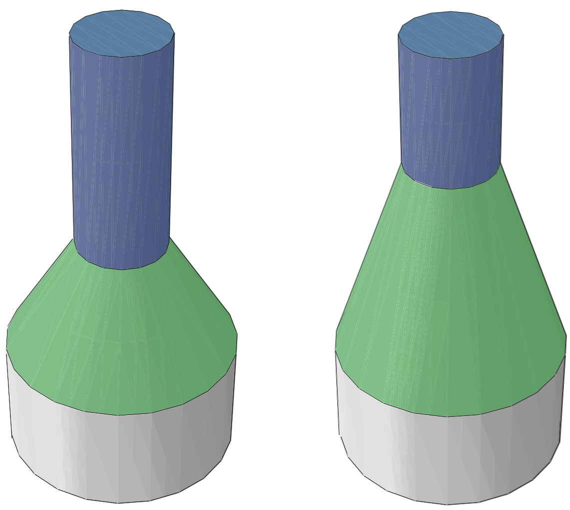

Figure 4.1: *Sketch of parts in a wind turbine foundation with two sizes of transition pieces. In the bottom is the suction bucket (gray). In the middle (green) is the transition piece. In the top (blue) is the wind turbine tower. To the left is the transition piece 16 m high and the right is the transition piece 9 meters high.*

4.2 Loads and Material

The material used for the transition piece is a high performance concrete called CRC. The concrete is mixed with steel fibre (typically 2-12%). CRC concrete has a number of advantages compared to conventional concrete. It has a higher compressive and tensile strengths and increased durability. Due to the dense micro-structure in CRC concrete there is also a stronger anchorage of the reinforcement. There is only needed a cover layer of 5-15 mm which is small compared to approximately 50 mm for conventional concrete.

The transition piece will be designed after the Ultimate Limit State (ULS) and the force will be applied as an equivalent quasi-static force. Other limit states as Fatigue Limit state will not be considered. The extreme wind load is assumed to be 2 MN. The load is acting 91 m above sea level. The load is moved to the top of the transition piece and generate a bending moment on 220 MNm on the high transition piece and 234 MNm on the short transition piece. The vertical load is 7.5 MNm. (Nezhentseva et al., 2010)

Table 4.1: *Loads applied to top of transition piece form wind load.*

Horizontal Load (H)	2 MN
Vertical load (V)	7.5 MN
Moment (high TP) (M_h)	220 MNm
Moment (short TP) (M_s)	235 MNm

Beside wind load does a wave load also act on the structure. Nezhentseva et al. (2011) state that the wind load contribute with the main stress development in the structure. The wave load acting on the transition piece is very dependent on the shape and size of the structure. In an optimization process where the shape is changing for every iteration is it hard to apply the wave load. If the load had been constant and independent of the shape applying the load inside the design domain would still have been difficult. The SIMP method is a soft-kill method and all elements are present throw-out the optimization process. Applying the load on the surface of the design domain will give a incorrect picture of the stress distribution in the structure. It is possible to make the attack point where the loads act as a frozen zone. To do this for the transition piece will cause that the surface of the design will be frozen and this will give a incorrect result. The load from wave action is simplified to a force and moment acting on the top of the transition piece together with the wind load.

The material used for the transition piece is CRC concrete. In the material are there added 2-12 % steel fibre to the concrete. The tensile properties are improved by including high-strength steel reinforcement bars. The steel bars also improve the ductility of the composite material. The fine fibred CRC concrete only need a cover layer and layer between bars of 5-15 mm compared to 50 mm for conventional concrete. This allows five to ten times more steel reinforcement in the concrete. The material properties are shown in Table 4.2.

Table 4.2: *Material properties for CRC concrete. (Nezhentseva et al., 2010)*

	Conventional concrete	CRC	CRC with rebar
Compressive strength [MPa]	80	160–400	160–400
Tensile strength [MPa]	6-15	10–30	100–300
Young's Modulus [GPa]	50	60–100	60–110

4.3 General Design and Optimization Task

The task is to optimize the transition piece using SIMP topology optimization. The design domain is defined as a cylinder formed around the space where the transition piece will be. The design domain will have the same radius as the suction bucket which is 9 m in radius. The height will be 9 m for the short transition piece and 16 m for the high transition piece cf. Figure 4.2.

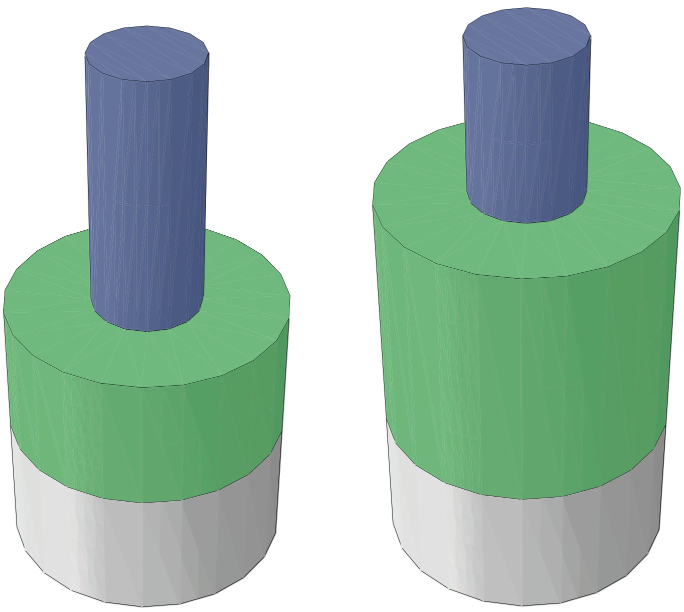

Figure 4.2: *Design domain for short and high transition piece. The design domain is showed with green. Below the design domain is the suction bucket and above the design domain is the bottom of the wind turbine tower.*

Only the design domain is modelled. The loads is applied on a ring on the surface of the design are. The ring will have the same measurements as the bottom of the wind turbine tower which is a radius of 3.5 m and a thickness of 0.04 m.

Boundary conditions are applied where the top of the suction bucket touches the design domain. A 0.03 m wide circle with an outer radius of 9 m is constrained by the boundary condition. On the circle are all translations and rotations constrained. The boundary conditions and loads for the short transition piece are shown on Figure 4.3.

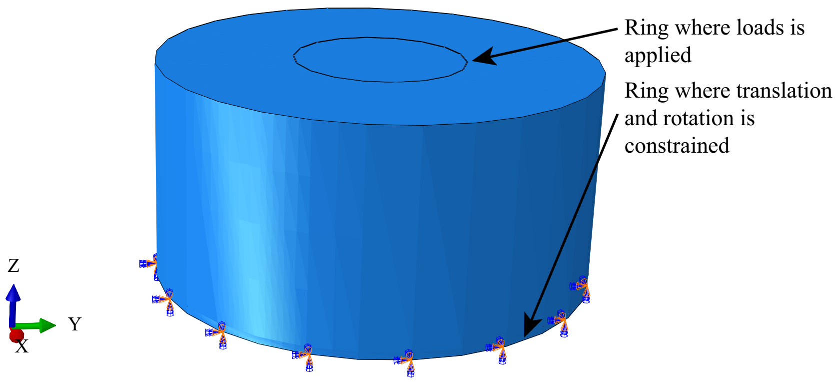

Figure 4.3: *Design domain for short transition piece. Loads are applied on top of the domain where the wind turbine tower interacts with the design domain. In the bottom is the design domain constrained against all translations and rotations. Loads and boundary conditions are applied similar to the high transition piece.*

The design domain is modelled as a solid. The element type used is a Ten-node tetrahedral element (C3D10). The element has quadratic shape functions and uses four integration points. The area around the boundary conditions and where the load is applied are meshed with a finer mesh than the rest of the model. This is done to be able to model these areas more detailed. The high transition piece is meshed with 100901 elements and the short transition piece is meshed with 98573 elements.

4.4 1st Topology Optimization - Basic Solution

Design and Optimization Task

The first topology optimization of transition piece is a classical density based SIMP optimization with compliance as the object. There is applied a single constrain namely 10 % volume fraction. This volume constrain is the same for both the short and the high transition piece. This optimization is only to investigate how the optimized topology will be formed if only a single volume constrain is applied. The stress distribution is therefore not interesting at these stages. The material is modelled as a linear elastic material and there is no plasticity. A small deflection theory is applied which mean there will not be any geometric non-linearity. The finite element model information and optimization task information is shown in Table 4.3 and 4.4.

Table 4.3: *Model information.*

Material	Isotropic Linear elastic
Young's modulus	E = 90000 MPa
Poisson's ratio	υ = 0.25
Element type	Ten-node tetrahedral element
Element Short TP	100901 elements
Element High TP	98573 linear elements

Table 4.4: *Optimization task information.*

Optimization type	Topology
Method used	SIMP
Object	Minimize compliance
Constrains	Volume fraction = 10 % Min member size = 0.1 m
Checkerboard filter	On
Task	Standard general analysis No geometric non-linearity

Results

Figure 4.4 shows the final topology for the short transition piece and Figure 4.5 shows the final topology for the high transition piece. The topology shows two members formed in the direction of the forces. Between them is a truss structures formed. It can be seen that the overall design are the same for both the short and the high transition piece.

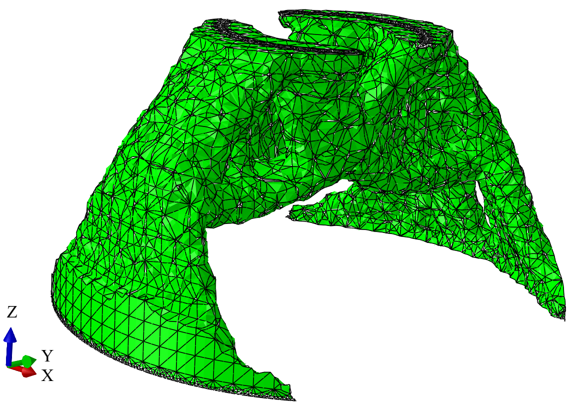

Figure 4.4: *Topology optimized short transition piece.*

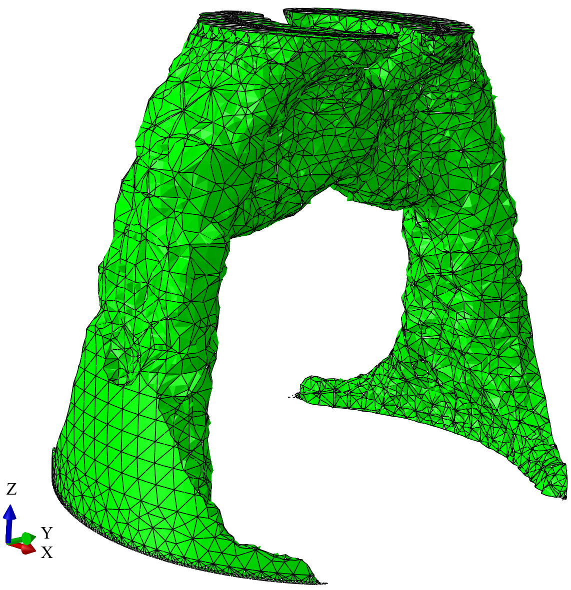

Figure 4.5: *Topology optimized high transition piece.*

It is obvious that this design will not be suitable for a transition piece. The structure may be able to transfer the loads in the one direction that is investigated. But an offshore wind turbine can be influence of loads in many directions. One load case may be dominating on some structures, but in others may there be multiple equal sized load cases acting in different direction. It is therefore necessary to add an extra constrain to the topology optimization task.

4.5 2nd Topology Optimization - Multiple Load Directions

Design and Optimization Task

A rotation constrain is added to the topology setup from the 1 Topology Optimization of Transition Piece. The constrain is a geometric constrain. This type of constrain influence how the geometric is formed.

The constrain used is a rotation constrain. It demands that the structure should be repeated after a number of degrees of rotation around the middle axis of the structure. The use of four rotation constrains are investigated namely 120°, 90°, 60° and 45° which is equal to three, four, six and eight repetitions around the middle axis. Information about the finite element model is shown in Table 4.5 and information about the optimization task is shown in Table 4.6.

Table 4.5: *Model information.*

Material	Isotropic
	Linear elastic
Young's modulus	E = 90000 MPa
Poisson's ratio	υ = 0.25
Element type	Ten-node tetrahedral element
Element Short TP	100901 elements
Element High TP	98573 elements

Table 4.6: *Optimization task information.*

Optimization type	Topology
Method used	SIMP
Object	Minimize compliance
Constrains	Volume fraction = 10 %
	Min member size = 0.1 m
	Rotation constrain (45° - 120°)
Checkerboard filter	On
Task	Standard general
	No geometric non-linearity

Results

Figures of all the resulting topologies with rotation constrain are shown in appendix A1. The resulting topology for a 60°and 90° rotation constrain for the short and high transition piece are shown in Figure 4.6 to 4.9. The compliance for each rotation constrains are shown in Table 4.7 and are plotted on Figure 4.10 and Figure 4.11.

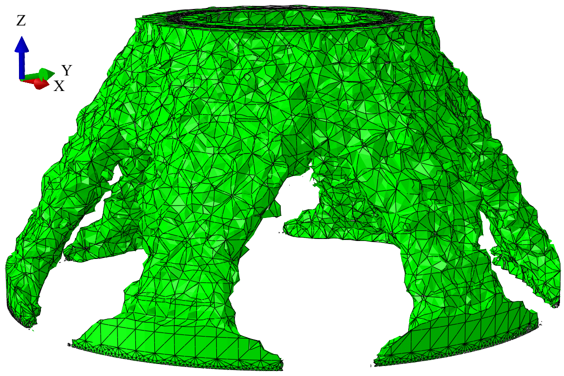

Figure 4.6: *Topology optimized short transition piece with a 60° rotation constrain. There are formed six legs from the top to the bucket foundation.*

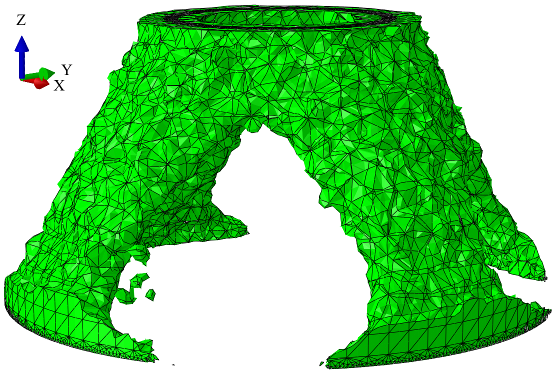

Figure 4.7: *Topology optimized short transition piece with a 90° rotation constrain. There are formed four legs from the top to the bucket foundation.*

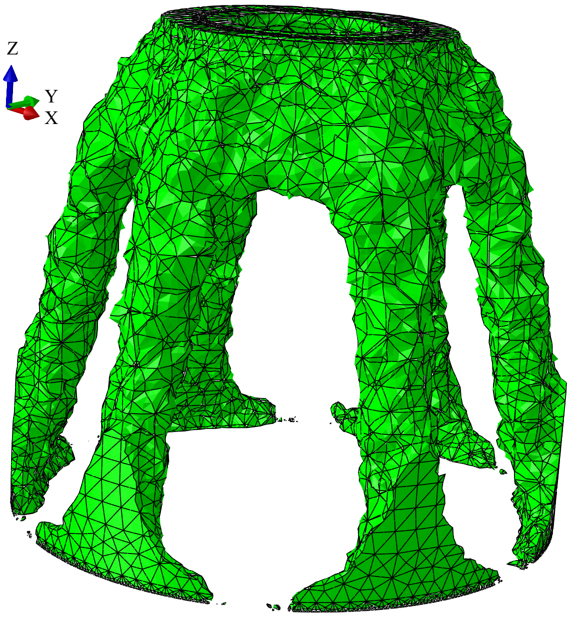

Figure 4.8: *Topology optimized high transition piece with a 60° rotation constrain. There are formed six legs from the top to the bucket foundation.*

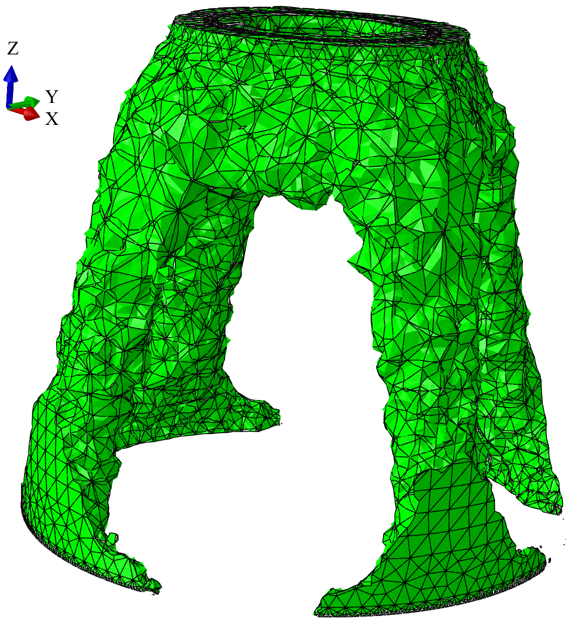

Figure 4.9: *Topology optimized high transition piece with a 90° rotation constrain. There are formed four legs from the top to the bucket foundation.*

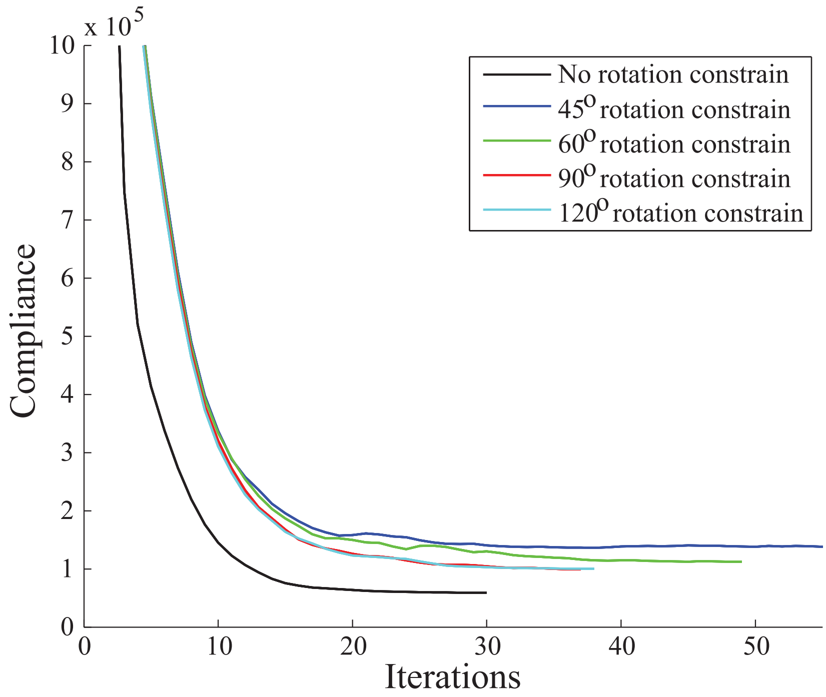

Figure 4.10: *Compliance for short transition piece.*

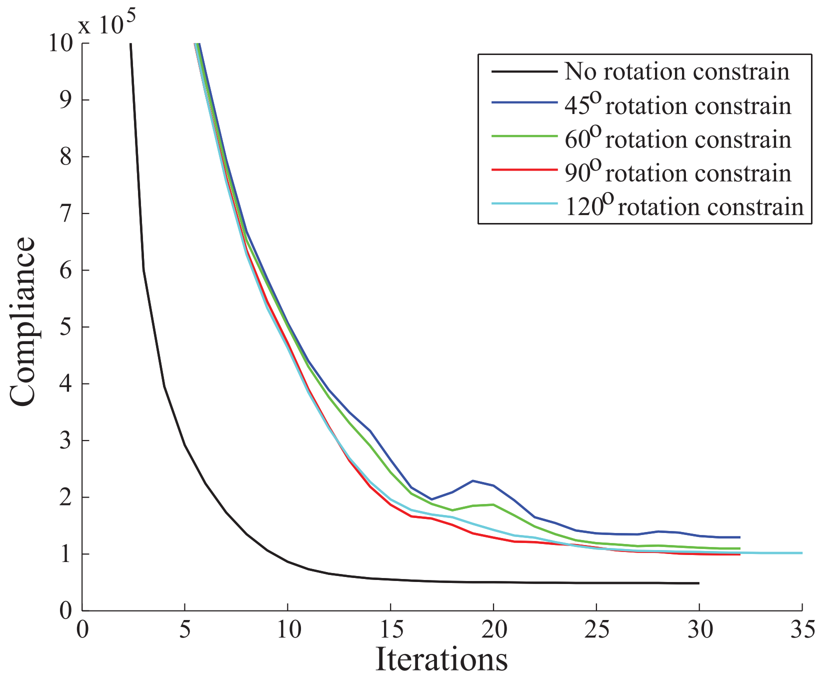

Figure 4.11: *Compliance for high transition piece.*

Table 4.7: *Number of iterations and final compliance for the short and high transition piece.*

	Short transition piece		High transition piece	
	Iterations	Compliance	Iterations	Compliance
No rotation constrain	30	58898	30	48436
45° rotation constrain	33	137660	32	129120
60° rotation constrain	49	112380	32	109650
90° rotation constrain	37	99408	32	99220
120° rotation constrain	38	100330	37	101350

The final compliance is lowest for the optimization without rotation constrain. When the rotations constrain is added the material is forced away from the optimal placing to obtain the loads. Therefore will the structure become less stiff and the final compliance will become higher. A rotation constrain on 45° gives the highest compliance and the compliance becomes lower when less circular repetitions is required.

The resulting compliance does not give a good estimate on which rotation constrain there is more optimal for the transition piece. The 90° rotation constrain does have the lowest final compliance but only haves four legs cf. Figure 4.7 and 4.9. It is therefore necessary to choose a rotation constrain based on other parameters. It is chosen to use the 60° rotation constrain for the transition piece. This will give six legs around the structure which is assumed will give the necessary stiffness against loads in multiple directions.

4.6 3rd Topology Optimization - Material Model and Volume

The material has been modelled as an isotropic linear elastic material with no plasticity for the first two topology optimization of the transition piece. The real material is a composite of CRC concrete and steel reinforcement cf. Figure 4.12 where a possible cross sections of a structure in CRC concrete is showed.

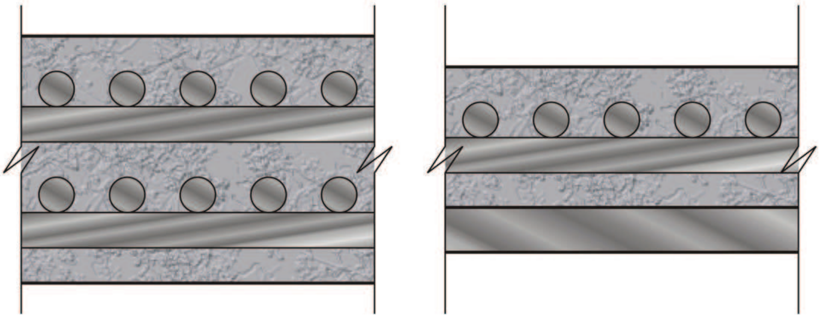

Figure 4.12: *Two possible cross sections of CRC-steel composite. Only 5-15 mm of cover layer is necessary and there can therefore be 5-10 times more reinforcement in the CRC concrete then in conventional concrete. In the cross sections to the left a 5-10 mm thick steel sheet is combined with CRC concrete. (Nezhentseva et al., 2010)*

Material Model for reinforced CRC concrete

The CRC concrete in itself is also a composite material which consists of steel fibre and concrete. The orientation of the steel fibres in the CRC concrete and the placement of the reinforcement steel in the concrete are not taken into account in the material model. Instead an isotropic material response is assumed. The compressive strength, tensile strength and Young's modulus of CRC concrete with rebar is shown in Table 4.2.

The exact material is not known and values in the middle interval is therefore chosen. The isotropic material model is assumed to have the strength parameters shown in Table 4.8. In the elastic domain is the material modelled linear elastic.

Table 4.8: *Strength parameters for isotropic material model for CRC concrete with reinforcement steel.*

Compressive strength	200 GPa
Tensile strength	200 GPa
Young's modulus	92 GPa

It is assumed the material has a ductile behaviour after the compressive strength and strength is reach. It is known from Nezhentseva et al. (2010) that CRC concrete has a plastic softening after the yield limit in compression is reached. It is assumed that the reinforcement in the concrete can give the concrete the necessary strength to obtain the same behaviour in tensile as in compression. A plastic response is therefore modelled as shown in Figure 4.13. There are plastic softening in the material after the compressive or tensile strength have been reached.

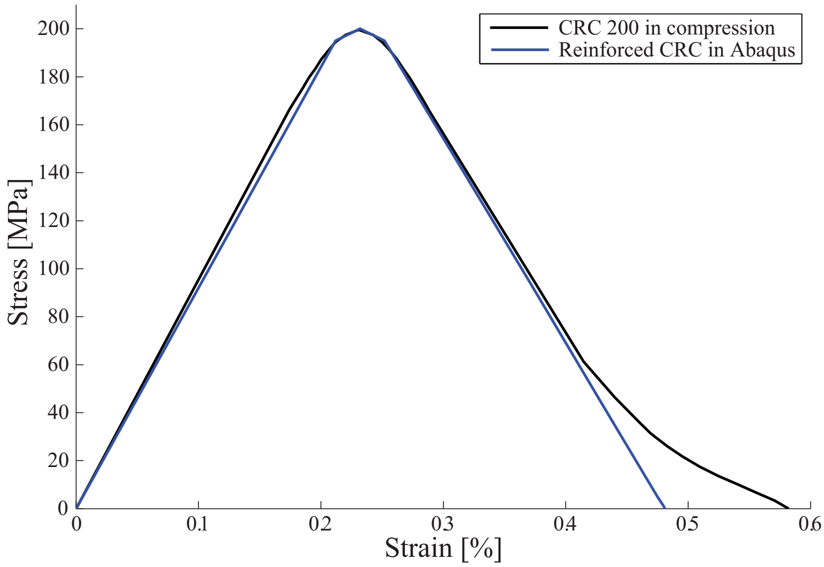

Figure 4.13: *Stress strain curve for CRC concrete. The black line is compressive behaviour for CRC concrete based on Nezhentseva et al. (2011). The blue line is how the CRC concrete is modelled for the transition piece in Abaqus for both tensile and compressive behaviour.*

Design and Optimization Task

In the 1st and 2nd topology optimization of the transition piece it is assumed that the volume fraction is 10 % of the initial volume. To investigate the optimal volume is different topology optimizations made with varying volume constrains. The object is chosen to be the compliance. A 60° rotation constrain are made to ensure the structures ability to obtain loads in multiply directions.

One of the design criteria's for a wind turbine is the rotation of the tower. An often used design criteria is 0.25° of rotation of the tower around a vertical axis after the installation. Most of this rotation is due to settlement in the soil. The demand to the transition piece will therefore be set to a smaller value. A design criteria for the transition piece is chosen to be 0.05° of rotation. Information about the finite element model is showed in Table 4.9 and information on the optimization task is showed in Table 4.10.

Table 4.9: *Model information*

Material	Isotropic material model
	Reinforced CRC concrete
Young's modulus	E = 43000 MPa
Poisson's ratio	$\upsilon = 0.25$
Element type	Ten-node tetrahedral element
Element Short TP	100901 elements
Element High TP	98573 elements

Table 4.10: *Optimization task information*

Optimization type	Topology
Method used	SIMP
Object	Minimize Compliance
Constrains	Volume fraction = 10 % - 20 %
	Min member size = 0.1 m
	60° rotation constrain
Checkerboard filter	On
Task	Standard general
	Geometric non-linearity

Results

Different volume constrains have been investigated. Maximal rotation of the wind turbine tower and final compliance for each volume constrain is showed in Table 4.11 for the short transition piece and in Table 4.12 for the high transition piece.

Table 4.11: *Rotation of wind turbine tower and final compliance for short transition piece for different volume constrains.*

Volume constrain	Rotation	Compliance
5 %	0.088°	179540
10 %	0.055°	112380
11 %	0.049°	103740
15 %	0.023°	47110
20 %	0.017°	35640
100 %	0.008°	17868

Table 4.12: *Rotation of wind turbine tower and final compliance for high transition piece for different volume constrains.*

Volume constrain	Rotation	Compliance
10 %	0.056°	109650
11 %	0.047°	94871
12 %	0.041°	83521
13 %	0.037°	75881
15 %	0.023°	60612
100 %	0.008°	17898

As shown in Table 4.11 and Table 4.11 the overall stiffness depends on the volume fraction constrain.The volume necessary to ensure less than 0.05° of rotation is 11 % for the short transition piece and 11 % for the high transition piece. This is equal to a volume of 252 m^3 for the short transition piece and 448 m^3 for the high transition piece.

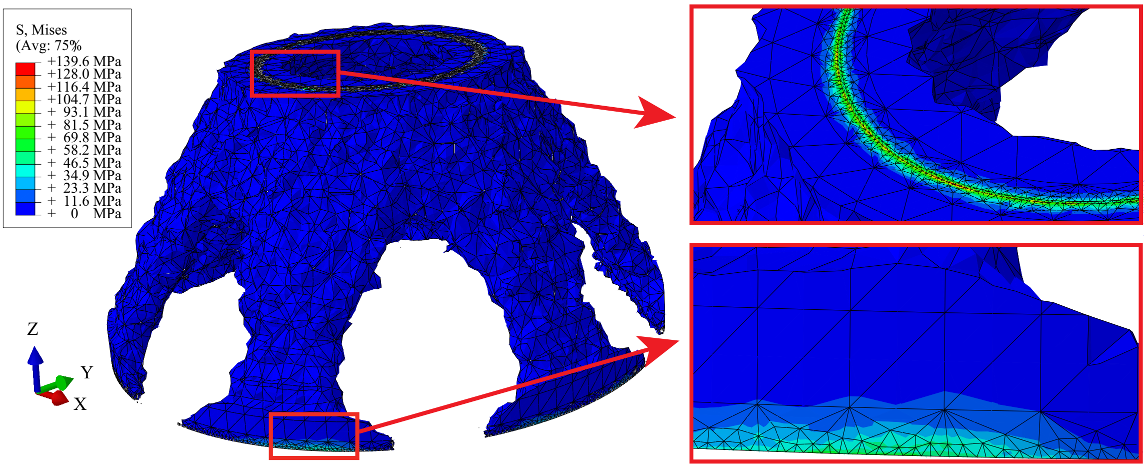

Figure 4.14: *Distribution of Von Mises stresses in the short transition piece*

It is assumed for the optimization purpose the CRC material has ductile isotropic properties and the Von Mises yield criterion is therefore used to analyses the stresses in the transition piece. For further investigation and designing of the transition piece where the steel reinforcement and concrete are modelled separately should another yield criterion be used. The Von Mises stress distributions for the short transition piece are shown in Figure 4.14. A similar stress distribution for the high transition piece are shown in appendix A2. The stress in most of the structures is between 0 MPa and 23 MPa which is in the elastic area of the material. The maximal stresses are concentrated around the top of the structure where the loads are applied. There are also stress concentrations around the foots of the six legs where the loads are transferred to the suction bucket. The maximum stress in the high transition piece is 126.4 MPa and the maximum stress in the short transition piece is 139.6 MPa. This means that the maximum stresses does not exceed the materials compression strength or tensile strength of the CRC concrete.

4.7 Final Topology of Transition Piece

After three topology optimizations of the transition piece is a final topology found. The final topology for the short and high transition piece are shown on Figure 4.15 and 4.16. From the 2$^{\text{nd}}$ topology optimization it is found that rotation constrain is set to 60° so the transition piece have six legs. Both the short and the high transition piece have the same overall topology and shape.

In the 3$^{\text{rd}}$ topology optimization the material of the transition piece is modelled as CRC concrete. It is investigated from a design criteria what the necessary volume of the transition piece is and it is found to be 11 % of the original volume for both sizes of the transition piece. The stress distribution in both sizes of transition piece is below the compressive strength and tensile strength. The final result of the topology optimization should not be seen as a final design for the transition piece. Below are listed a number of issues needed to be concerned in the final design.

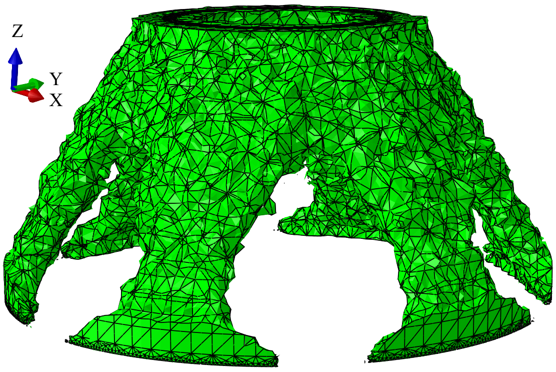

Figure 4.15: *Topology optimized short transition piece.*

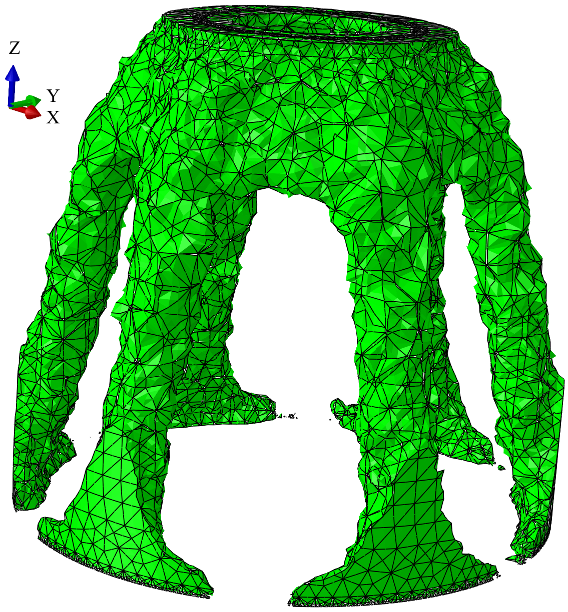

Figure 4.16: *Topology optimized high transition piece.*

The material is modelled as an isotropic material but as stated in section 4.6. This is not correct. A finite element model of the structure needs to be created where the anisotropic behaviour of the CRC concrete and the reinforcement is modelled together. It is possible to take the final topology and use the geometric as a basic for a new finite element model. This makes it possible to perform a more detailed finite element investigation of the structure.

There is only investigated one simplified load combination on the transition piece. More load combinations needs to be investigated. The wave load is simplified to a moment and vertical force acting in the top of the transition piece. The real load has to be determined and they are acting on the legs of the transition piece. The six legs make the wave load calculation complex and experimental data may be necessary to determine the load.

The six legs may also create more turbulence in the water than a solid shell structure. More turbulence may lead to scour around the bucket foundation which leads to less bearing capacity. The shape of the transition piece has to be investigated for the influence on scour around the structure.

As seen of Figure 4.15 and 4.16 does the topology for the transition piece have six slender legs. The stress does not reach the compressive strength or tensile strength in the legs and the ULS limit state is not exceeded. Another limit state is the limit state of buckling where a structure suddenly loses stability and large deformations happen. Buckling is a specific type of instability, where the structure will deform from the original shape. The structure will under a loading go from the existing state of equilibrium and find a new form of equilibrium state. This structure could be a slender beam, a cylindrical shell structure etc.

This form for instability can be included in an optimization process. After the topology optimization is finished can the geometry found be used for a shape optimization. The wave load acting vertical on a legs can be vary imported to find the critical buckling load. The load on the side of the legs of the transition piece was not possible to apply in the topology optimization because the shape and placement of the legs changes throughout the optimization process. In a shape optimization of the transition pieces can the legs be loaded with the wave load and the optimal shape to withstand buckling can be applied as a constrain. The critical bucking load is found by a linear perturbations analysis where the eigenvalue is determined by a eigenvalue problem. The optimization with a buckling constrain are formulated in equation (4.1). The object function could be compliance but also stress or other object functions can be used.

$$
\begin{aligned}
& min\ f(x) \\
& s.t.\quad p_{crit} \geq \delta_i, \quad i = 1, ..., N_{dof} \\
& \qquad\quad p_{crit} = \lambda_i Q_i \\
& \qquad\quad (\mathbf{K}_0^{\mathrm{M\ N}} + \lambda_i \mathbf{K}_\Delta^{\mathrm{M\ N}}) \upsilon_i^{\mathrm{M}} = 0 \quad i = 1, ..., N_{dof} \\
& \qquad\quad V = \sum_{i=1}^{N} x^i v^i \leq V_0 - V^* \\
& \qquad\quad \mathbf{KU} = \mathbf{F} \\
& \qquad\quad k^i = (x^i)^p k_0 \\
& \qquad\quad 0 < x_{min} \leq x^i \leq 1
\end{aligned}
\tag{4.1}
$$

Where:

$f(x)$	Object function
δ_i	Constrained lower value for i'th eigenvalue
λ_i	i'th eigenvalue
Q_i	Perturbation load pattern
Φ_i	i'th eigenvalue eigenvector
$\mathbf{K}_0^{\mathrm{M\ N}}$	Stiffness matrix corresponding to the initial state. Includes effects of the preloads
$\mathbf{K}_\Delta^{\mathrm{M\ N}}$	Differential initial stress and load stiffness matrix due to incremental loading
υ_i^{M}	i^{th} mode shape

With the use of shape optimization can the shape of the structure be optimized with other types of constrains e.g minimization of stress concentrations. The surface nodes will in a shape optimization be the design variables and can be modified in an optimization step. This way only the shape chances but the topology of the structure stays the same. A shape optimization can be used to refine the shape and topology found in a topology optimization and optimize the structure to perform better e.g. reduce stress concentrations or risk of buckling.

As shown above are the topology optimization only the first step in a design process. Topology optimization can be used to investigate possible configuration for the structure and can provide a potential good design chose for further investigations and designing.

Chapter 5

Pedestrian Footbridge

Topology optimization is performed a pedestrian footbridge over a freeway. An optimal design is investigated with the use of topology optimization which satisfying the necessary constrains.

5.1 Introduction

The second civil engineering structure designed using topology optimization is a pedestrian footbridge based on a footbridge over a major metropolitan freeway in Australia. A general introduction to the structure is given in section 1.1. An initial design sketch is presented in Figure 1.4 where the geometric constrains for the bridge is shown.

Topology optimization will be performed in three steps. First is a 2D solution of the bridge investigated. This will give an estimate on the overall topology of the bridges and the importance of supports of the bridge and slope of the pedestrian deck. The second and third topology optimization will be performed on a 3D model of the bridge. Here will the load and different geometric constrains be applied. This will lead to a topology optimized bridges for the static load. Last an optimization will be performed with constrains for the eigenfrequency. This will lead to a topology design that is optimized for the static loads and where the risk for resonance in the bridges is minimized.

5.2 Loads and Material

The material used for designing the bridge is steel. It is assumed to have isotropic properties and will be modelled as a linear elastic perfect plastic material. The used type of steel is assumed to have the same tensile and compressive strength properties and is modelled with a Young's Modulus of 210 GPa. Material properties are shown in Table 5.1. The load on the structure for finding the optimal topology is one static load. The load is a vertical pressure of the 4 kPa applied to the deck of the footbridge.

Table 5.1: *Material properties for steel used in optimization of pedestrian footbridge.*

Compressive strength	325 MPa
Tensile strength	325 MPa
Young's Modulus	210 GPa
Poisson's ratio	0.3

5.3 1st Topology Optimization - 2D Solution

Design and Optimization Task

Based on the sketch of the pedestrian footbridge cf. Figure 1.4 are design domains of the bridges determined. The height of the design domain is set to $H_2 = 3.5$m. It is assumed that the baring structure is placed under the pedestrian deck. In each side of the bridge are the a area of re $L_2 = 3.5$m width where the structure can be supported without interfering with the clearance under the bridges. This area is included in the design domain. The dimensions of the design domain are shown on Figure 5.1 and in Table 5.2.

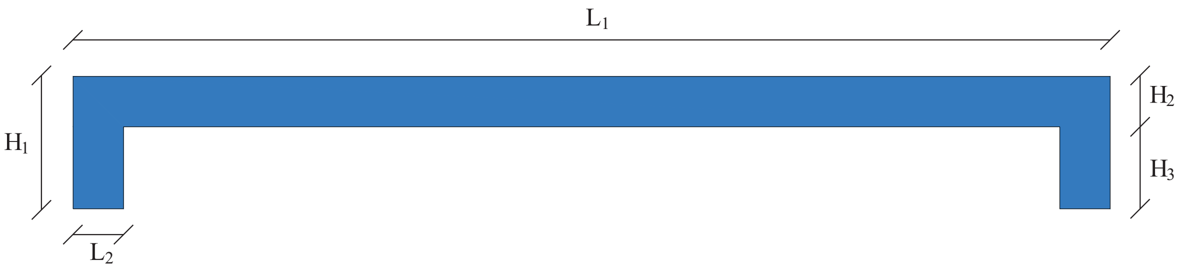

Figure 5.1: *Dimensions of design domain illustrated.*

Table 5.2: *Dimensions of design domain.*

Total length (L_1)	72 m
Length of support (L_2)	3.5 m
Total Height (H_1)	9.2 m
Bridge height (H_2)	3.5 m
Free span height (H_3)	5.7 m

The maximal ramp slope is set to be 1:20. For the 2D solution are three possible forms of the deck slope investigated cf. Figure 5.2. A model with a ramp slope of 1:20 where the middle 20 m is modelled as an arc with the radius of 200.4 m, a model where the entire ramp is modelled with an arc with a radius of 721.5 m, and a model without any ramp slope.

The load is applied on the design domain where the pedestrian deck is assumed to be. The load zone is set to be a frozen zone. The frozen zone is showed with red on Figure 5.2. It is assumed the width of the deck is 4 m cf. section 1.1 . The applied load in the 2D case is set to 16 kN/m.

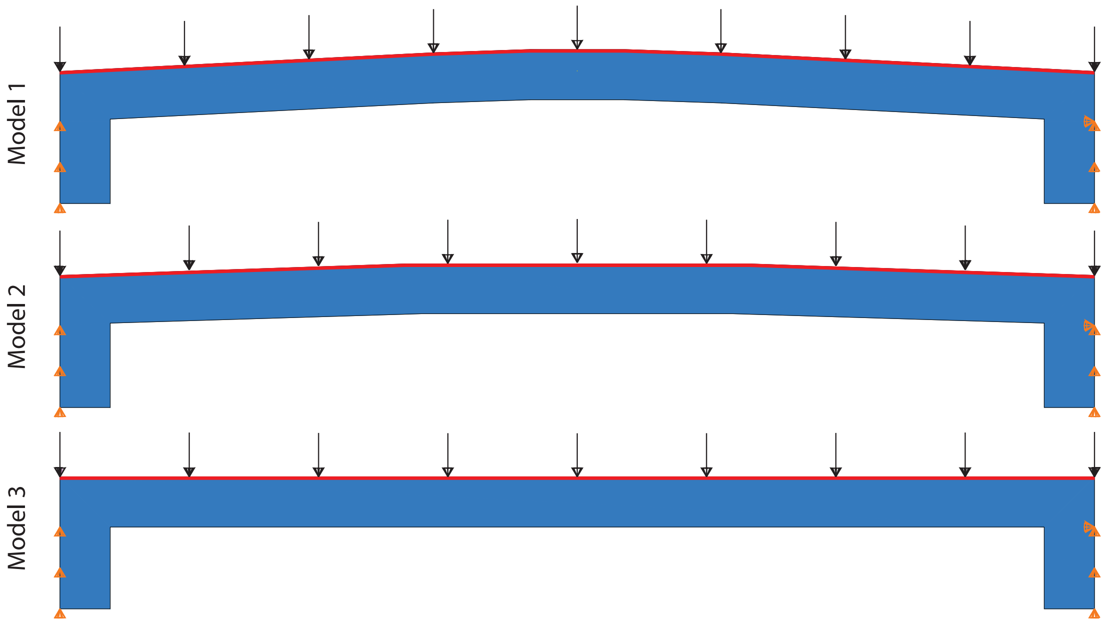

Figure 5.2: *Design domains for pedestrian footbridge modelled in 2D. Model 1: Pedestrian deck with a slope of 1:20 and an arc in the middle. Model 2: Pedestrian deck formed as an arc with a beginning slope of 1:20. Model 3: Pedestrian deck with no slope. Boundary condition are showed as pinned for translation i vertical direction in the left side and pinned for translation in vertical and horizontal direction in the right side. The frozen zone is showed with red.*

Each model of the pedestrian footbridge is modelled with two sets of boundary conditions. In the first set is both sides of the footbridge double pinned in vertical and horizontal direction. For the second set of boundary condition are both sides only single pinned i vertical direction. A single point is also pinned in horizontal direction. The boundary conditions showed on Figure 5.2 are the single pinned.

The pedestrian footbridge is meshed with an 8-node biquadratic plane stress quadrilateral elements with reduced integration (CPS8R). Model 1 is meshed with 8638 elements, model 2 is meshed with 8516 elements and model 3 is meshed with 8763 elements. The finite element analyses is a static general analysis and there will be no geometric non-linearity.

The objective of the optimization is to minimize the structures compliance. The design variables are the density of each element in the design domain. A volume constrain is applied to the three models. The total volume of the model varies coursed the different design domains form. The volume constrain is therefore set to 25 % of the original volume of model 3. This will give the same final volume and the results are therefore comparable. To avoid small truss and to make the model mesh independent are a member size constrain of 0.40 m is applied. It is desired that the bridges is symmetric around the middle of the bridges. There are therefore applied a planer symmetric constrain where the final topology have to be symmetric around a planner through the middle of the bridge.

To make the model symmetric Abaqus is finding nodes that are approximately symmetric and adding them into a symmetry group and determines the master node of the symmetry group. Then can the design displacements be calculates for the master and client nodes so they move symmetrically to the symmetry plane.(Abaqus, 2012)

Information about the finite element model and the optimization task is given in Table 5.3 and 5.4.

Table 5.3: *Model information.*

Material	Isotropic
	Linear elastic perfect plastic
Young's modulus	E = 210000 MPa
Poisson's ratio	υ = 0.3
Element type	8-node quadrilateral elements
Element Model 1	8638 elements
Element Model 2	8516 elements
Element Model 3	8763 elements

Table 5.4: *Optimization task information.*

Optimization type	Topology
Method used	SIMP
Object	Minimize compliance
Constrains	Volume fraction = 25 % (of model 3)
	Min member size = 0.4 m
	Planner symmetric constrain
Checkerboard filter	On
Task	Standard general analysis
	No geometric non-linearity

Results

The final topology of the pedestrian footbridge in 2D is shown in Figure 5.3 for model 1. All three models topologies are shown in appendix A3. The compliance from topology optimization are shown in Figure 5.4 and 5.5 and final compliance from the six topology optimization are shown in Table 5.5.

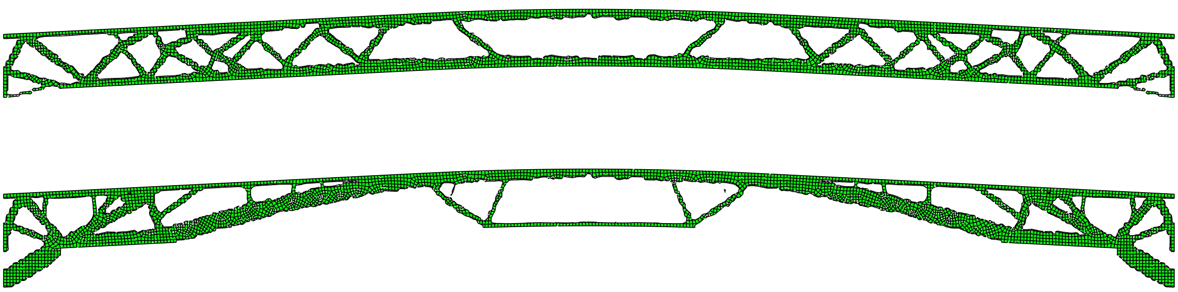

Figure 5.3: *Topology of model 1 pedestrian footbridge. Top: Bridge is single pinned in both sides. Bottom: Bridge is double pinned in both sides.*

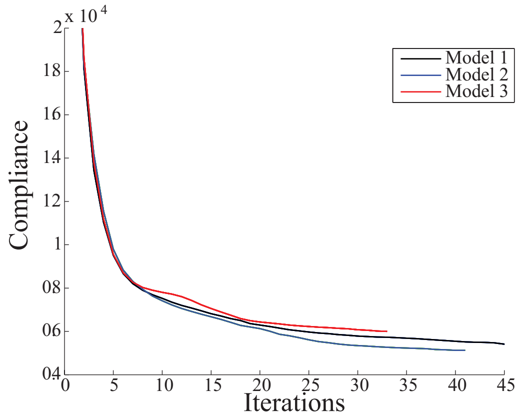

Figure 5.4: *Compliance for pedestrian footbridge with single pinned boundary conditions.*

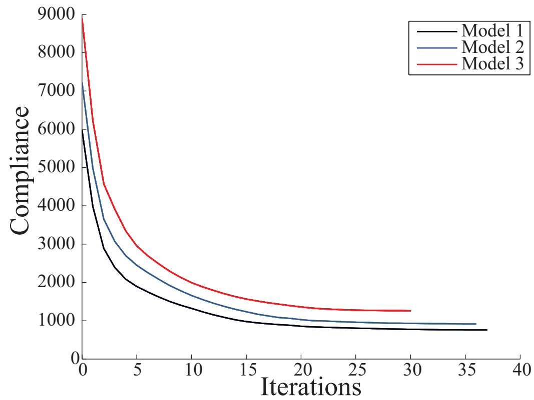

Figure 5.5: *Compliance for pedestrian footbridge with double pinned boundary conditions.*

Table 5.5: *Final compliance of pedestrian footbridge in 2D.*

	Single pinned	Double pinned
Model 1	758	5278
Model 2	916	5123
Model 3	1260	6001

The final topology of the single pinned bridges are similar for all three models and the final topology of the double pinned bridge for all three models are also similar to each other cf appendix A3. The single pinned structures form two planes with a trust like system in between. The double pinned structures form arc structure under the pedestrian deck. As expected the double pinned structure is stiffer which is shown in the final compliances in Table 5.5.

Model 3 has the highest compliance for both sets of boundary conditions. Both model 1 and model 2 have the advances of a general arc form which gives a higher stiffness against a vertical load and hereby a lower compliance. Model 3 are therefore not a good design choice.

Model 1's design domain is higher than the design domain of model 2. This makes it possible to make a larger arc structure under the pedestrian deck and hereby form a structure with higher stiffness. Therefore is model 1's compliance lower than models 2's compliance for the double pinned boundary conditions.

For further topology optimization of the structure in three dimensions and with a frequency constrains is the design domain of model 1 with double pinned boundary conditions used.

5.4 2nd Topology Optimization - 3D Solution in Steel

Design and Optimization Task

Based on the sketch on Figure 1.4 and results from section 5.3 a 3D model of the pedestrian footbridge is created. It was chosen to use the profile of model 1 with a slope of 1:20 of the pedestrian deck and connected in the middle 20 m with an arc. The width of the bridge is 4 m and the design domain will therefore be 4 m wide. The design domain are showed in Figure 5.6.

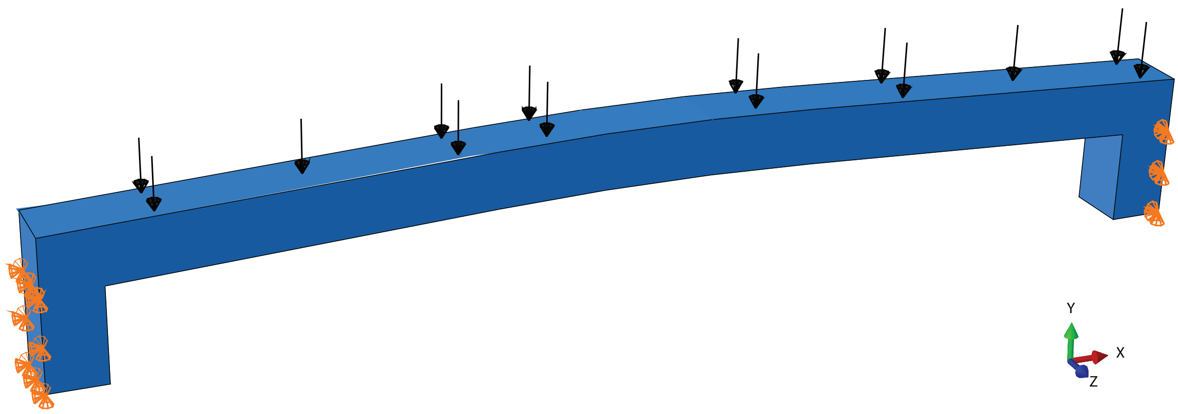

Figure 5.6: *Design domains for pedestrian footbridge modelled in 3D. The bridges are pinned against translation in all three directions in each side. The vertical load is applied on the pedestrian deck.*

The design domain i loaded with the vertical pressure on 4 kPa. The load zone is set to be a frozen zone and the load is applied on the top of the design domain. The boundary conditions are, based on section 5.3 set to be pinned in all three directions in both sides of the bridge.

The pedestrian footbridge is meshed with a 20-node quadratic brick element with reduced integration and quadratic shape functions (C3D20R). There are used 10664 elements to mesh the model and the sides of each element are approximately 0.5 m. This is the same size as the minimum member size desired and it is therefore assumed the model will be able to form the desired topology. A finite element analyses will be run as a static general analysis and there will be no geometric non-linearity.

The objective of the optimization is to minimize the structure compliance and a volume constrain is applied between 20 % - 50 %. A member size constrain of 0.50 m applied to avoid small trusts and ensure mesh independents.

To ensure symmetry in the bridge a planer symmetric constrain is added. As in section 5.3 it is desired that the structure is symmetric around the middle in the length direction of the bridge. This symmetry plane are added to the 3D model as well and are shown on Figure 5.7. Information about the finite element model and the optimization task is given in Table 5.6 and 5.7.

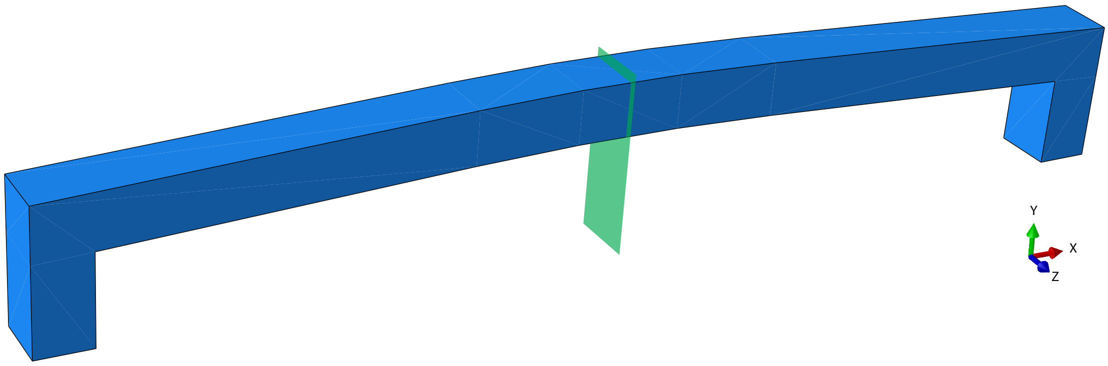

Figure 5.7: *Symmetry plane used to create symmetric constrain on pedestrian footbridge.*

Table 5.6: *Model information.*

Material	Isotropic
	Linear elastic perfect plastic
Young's modulus	E =210000 MPa
Poisson's ratio	υ = 0.3
Element type	20-node quadratic -
	brick element
Elements	10664

Table 5.7: *Optimization task information*

Optimization type	Topology
Method used	SIMP
Object	Minimize compliance
Constrains	Volume fraction = 20% - 50%
	Min member size = 0.5 m
	Planner symmetry
Checkerboard filter	On
Task	Standard general analysis
	No geometric non-linearity

Results

A volume fraction varying between 20 % to 50% is investigated. The final topology of the pedestrian footbridge with a volume fraction of 50 % is shown on Figure 5.8 and with a volume fraction of 20 % on Figure 5.9. The topology optimizing of the pedestrian footbridge with the remaining volume fractions is shown in appendix A4.

The supporting truss structure uner the middle of the bridge in the 2D solutions for the footbridge cf. Figure 5.3 are disappeared in the 3D solution and only the arc structure is left. This trend is common to all the investigated volume fractions. In each end of the footbridges is a hollow box structure formed for the higher volume fractions. As the volume fraction is reduced is a truss like structure emerging. With a volume fraction of 20 % are an arc truss structure formed in each side of the bridge with horizontal and vertical supporting truss. A larges truss from the bridge deck to the pinned support are also formed in each side of the bridge.

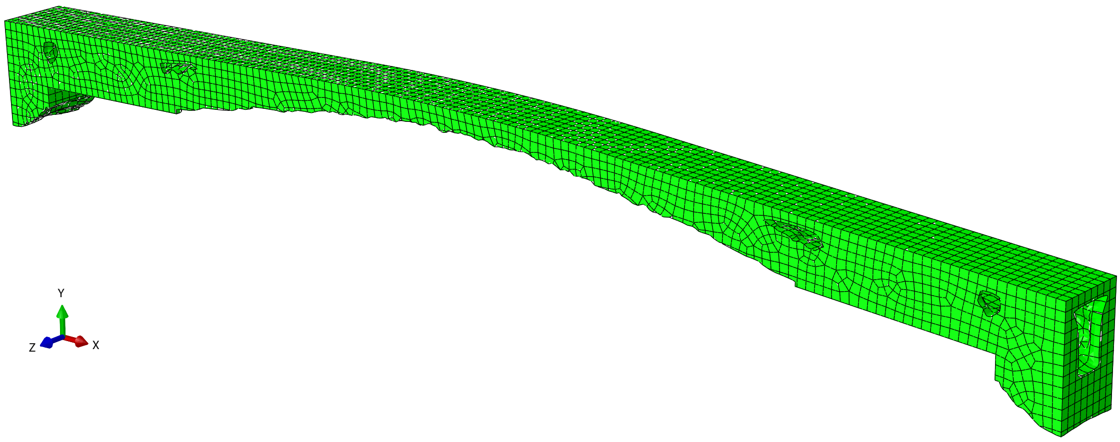

Figure 5.8: *Topology optimized footbridge with a volume fraction of 50 %.*

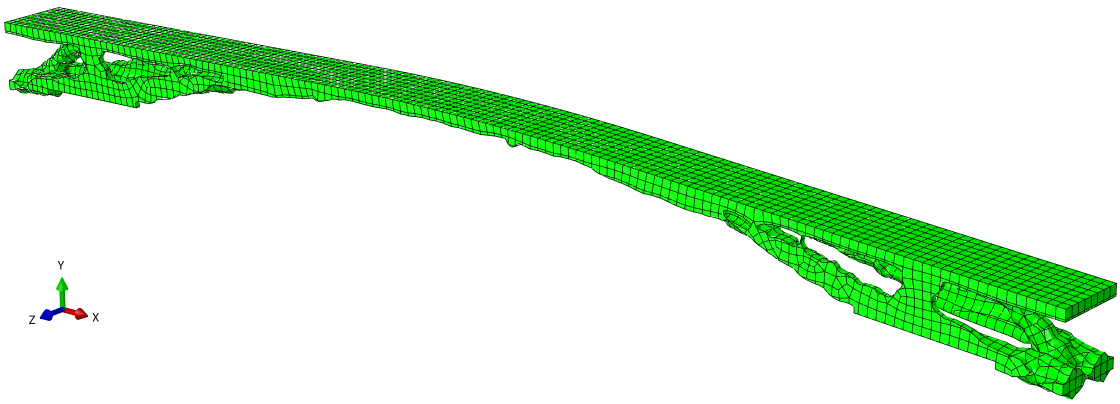

Figure 5.9: *Topology optimized footbridge with a volume fraction of 20 %.*

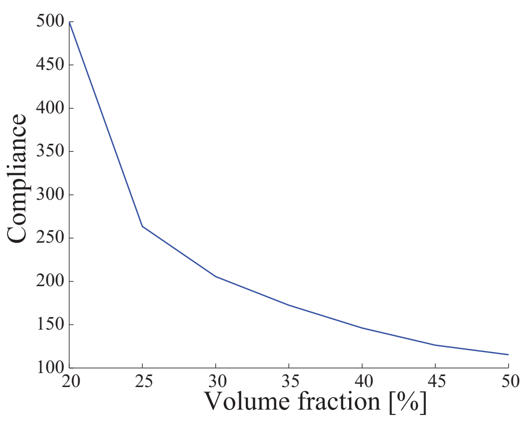

Figure 5.10: *Compliance for pedestrian footbridge plotted for different volume constrains.*

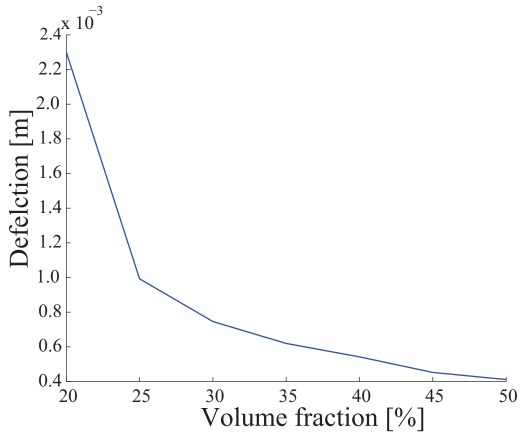

Figure 5.11: *Maximum deflection of pedestrian deck plotted for different volume constrains.*

The maximal deflection occurs in the middle of the bridge. The compliance and deflection are plotted on Figure 5.10 and 5.11. The deflection of the footbridges with a volume fraction of 20 % is 2.3 mm. The Von Mises stresses reach only 4.6 MPa cf. Figure A4.5 in appendix A4. The stresses is within the reach of conventional concrete cf. Table 4.2. A designed of the pedestrian footbridges in concrete will therefore be investigated.

5.5 3rd Topology Optimization - 3D Solution in Concrete

Design and Optimization Task

The material used for the 3rd optimization of the pedestrian footbridge is a conventional concrete. Material properties for the conventional concrete are listed in Table 4.2. For the optimization process is the material modelled isotropic linear elastic. Concrete material behaves non-linear but is assumed approximately linear as long the stresses does not exceed compressive strength.

The design domain, loads and optimization task is the same as in section 5.4. Based on the resulting topologies of section 5.4 is a volume constrain of 20 % used. The pedestrian footbridge is meshed with a 20-node quadratic brick element with reduced integration and quadratic shape functions (C3D20R). The structure is meshed in the same way as the pedestrian footbridge optimized in steel with 10664 elements with an element side length of approximately 0.5 m. A static general finite element analysis will be used with both geometric non-linearity and no geometric non-linearity.

Information about the finite element model and the optimization task are given in Table 5.8 and 5.9.

Table 5.8: *Model information.*

Material	Isotropic Linear elastic
Young's modulus	E = 50000 MPa
Poisson's ratio	υ = 0.25
Element type	20-node quadratic - brick element
Elements	10664

Table 5.9: *Optimization task information*

Optimization type	Topology
Method used	SIMP
Object	Minimize compliance
Constrains	Volume fraction = 20% Min member size = 0.5 m Planner symmetry
Checkerboard filter	On
Task	Standard general analysis With/No geometric non-linearity

Results

The final topology of the pedestrian footbridge has change after the material has been changed from steel to concrete cf. Figure 5.12. The larges change is the supporting structure in the middle of the bridge that has reappeared in the optimization.

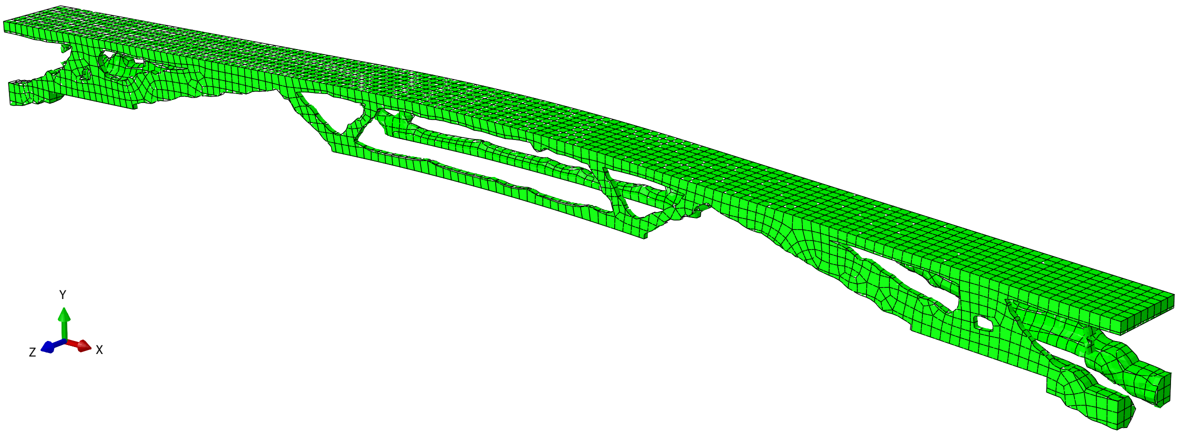

Figure 5.12: *Topology optimized footbridge with concrete as the material and a volume fraction of 20 %. Geometrical non-linearity is taken into account in the finite element analysis.*

The bridge has been modelled with and without geometric non-linearity cf. Figure A5.2. There are no larges visual differences in the topologies with and without geometric non-linearity. Compliance and total deflection of the bridge are plotted on Figure 5.13 and 5.14 for the two models.

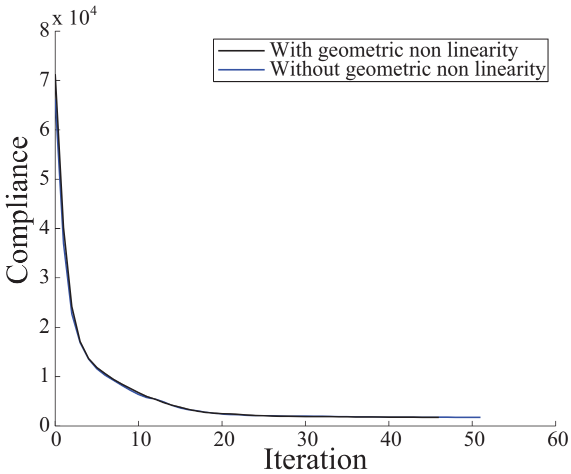

Figure 5.13: *Compliance for pedestrian footbridge with and without non-linear geometric effects.*

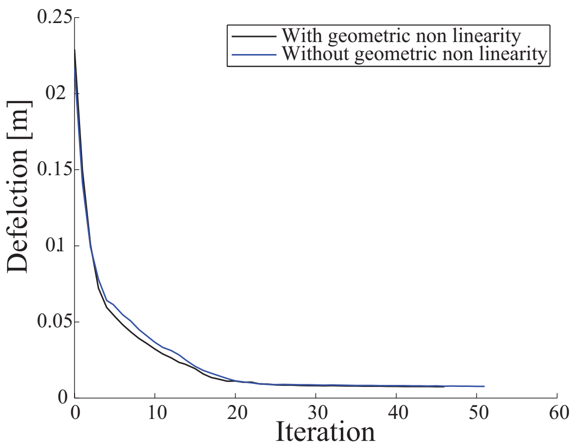

Figure 5.14: *Maximum deflection of pedestrian footbridge deck with and without non-linear geometric effects.*

There are no larges difference between the compliance and the deflection for the pedestrian bridge with and without non-linear geometric effects. The small deflection of the bridge makes the non-linear geometric effects negligible. The deflection of the footbridges with non-linear geometric effects and a volume fraction of 20 % is 7.4 mm. The concrete material is approximated as isotropic material and the stresses are approximated with Von Misses stresses. The Von Mises stresses reach 4.42 MPa. It is therefore assumed the design shown on Figure 5.12 can be used for the pedestrian footbridge based on a load case with a static load. The simple load applied on the structure is not enough for a final design. More load combination need to be investigated to find the final design. Another important load case is dynamic loads on the structure. This area will be investigated in the next section.

5.6 4th Topology Optimization - Eigenfrequency Constrains

A structure like a pedestrian footbridge is subject to dynamic loads. This load may be a dynamic wind load or the dynamic load from pedestrians waking over the bridge. If the loads frequencies are close to the structures eigenfrequency may the load course oscillations of the bridges movement. It is therefore necessary not only to design the footbridge by a static load but also design by the structures dynamic behaviour. It is desirable to keep a structures eigenfrequency away from the frequencies of the dynamic loading from the pedestrians. A structure with a high fundamental eigenfrequency also tent to be reasonable stiff for a static load and may therefore be a good design choice (Bendsøe and Sigmund, 2003).

A formulation of the SIMP method with a eigenfrequency constrain is given in equation (5.1). This eigenfrequency constrain is added to the general formulation of the SIMP method with a volume constrain given in equation (2.6).

$$min\, C = \mathbf{U}^T \mathbf{K} \mathbf{U} = \sum_{i=1}^{N} u^i k^i u^i \tag{5.1}$$

$$\begin{aligned} s.t.\quad & \lambda_i \geq \beta_i, \quad i = 1, \ldots, N_{dof} \\ & (\mathbf{K} - \lambda_i \mathbf{M}) \Phi_i = 0, \quad i = 1, \ldots, N_{dof} \\ & \\ & V = \sum_{i=1}^{N} x^i v^i \leq V_0 - V^* \\ & \mathbf{K}\mathbf{U} = \mathbf{F} \\ & k^i = (x^i)^p k_0 \\ & 0 < x_{min} \leq x^i \leq 1 \end{aligned}$$

Where:

β_i	Constrained lower value for i,th eigenvalue
λ_i	i'th eigenvalue
Φ_i	i'th eigenvalue eigenvector
$\mathbf{M}$	Structures mass matrix

An modal dynamic analysis of the design domain are made to be able to evaluate how many eigenfrequency are necessary to include in the optimization process cf. appendix A6. The frequencies are found with a linear perturbation procedure. It is found that the first nine eigenfrequencies will be used in the optimization task.

Design and Optimization Task

The material used for the 4^{th} optimization of the pedestrian footbridge is conventional concrete and the material properties are modelled isotropic linear elastic as in section 5.5. There are assigned a density to the design domain so the mass matrix can be created and used in the calculation of the eigenfrequencies. The density assigned to the domain are 2400 kg/m^3 which are the density for conventional concrete (Jensen, 2008).

There will be performed two analyses of the pedestrian footbridge in each iteration cycle, a standard general analysis with geometric non-linearity and a modal analysis of eigenfrequencies. The first analysis is used to calculate stress and strains in the structure and hereby compliance. The second analysis is used to determine the eigenfrequencies for the mode shapes. The design domain, loads, mesh and optimization task are modelled as in section 5.5.

For a footbridge with pedestrian excitation are the critical ranges of natural frequencies, f_i, given below. These criteria will be applied as constrains two the optimization task as a lower bound for the eigenfrequencies. There will be made two constrains. One constrain for lateral vibrations and one constrain for vertical and longitudinal vibrations. (Heinemeyer et al., 2009)

The demand for frequencies ranges for vertical and longitudinal vibrations is given in equation (5.2) :

$$1.25 \text{ Hz} \leq f_i \leq 2,3 \text{ Hz} \tag{5.2}$$

There is a possibility for a resonance by the 2^{nd} harmonic frequencies for the vertical and longitudinal vibrations and the demand is therefore changes to the double interval of frequencies cf. equation (5.3).

$$1.25 \text{ Hz} \leq f_i \leq 4,6 \text{ Hz} \tag{5.3}$$

For lateral vibrations the critical ranges is shown in equation (5.4) and the lateral vibrations are not affected by the 2nd harmonic frequencies.

$$0.5\text{ Hz} \leq f_i \leq 1.2\text{ Hz} \tag{5.4}$$

Beside the eigenfrequency constrains are the pedestrian footbridge modelled with a volume fraction constrain on 20 %, 25 %, 30 %, 40%, and 50%. Information about the finite element model and the optimization task is given in Table 5.10 and 5.11.

Table 5.10: *Model information.*

Material	Isotropic
	Linear elastic
Young's modulus	E = 50000 MPa
Poisson's ratio	υ = 0.25
Element type	20-node quadratic
	brick element
Elements	10664

Table 5.11: *Optimization task information.*

Optimization type	Topology
Method used	SIMP
Object	Minimize compliance
Constrains	Volume fraction = 20% - 80%
	Lateral eigenfrequency > 1.2 Hz
	Vertical eigenfrequency > 4.6 Hz
	Min member size = 0.5 m
	Planner symmetric constrains
Checkerboard filter	On
Task	Standard general analysis
	Modal frequency analysis

Results

The first nine mode shapes have been constrained in the optimization process. The most critical mode shapes are for all volume constrain is found to be the first and second mode shape with one half waves in vertical or lateral direction cf. Figure A6.1 and A6.2 in appendix. The models investigated obtains a final topology that fulfils the lateral eigenfrequency constrain for all volume fractions investigated. Only the investigated structures with a volume constrain over 30 % fulfil the vertical eigenfrequency constrain. Results from the optimization task with eigenfrequensy constrains is shown in Table 5.12.

Table 5.12: Results from topology optimization of pedestrian footbridge with eigenfrequency constrain.

Volume constrain	Compliance	Lowest vertical eigenfrequency [Hz]	Lowest lateral eigenfrequency [Hz]
20 %	5083.0	2.05	3.41
25 %	2735.0	2.64	4.38
30 %	1152.0	3.96	4.60
40 %	591.8	3.65	4.60
50 %	484.0	3.54	4.63

The compliance for the optimization process with a volume fraction of 30 % are shown in Figure 5.15 and the lowest lateral and vertical eigenfrequency are shown in Figure 5.16. Eigenfrequencies and compliances are potted for all investigated volume constrains in appendix A6. It is seen that the optimization fulfil the constrains and minimise the compliance. When the eigenfrequency constrain is fulfilled for a given optimization step is the frequency constrains almost fulfilled throughout the rest of the optimization. There are iteration steps where the constrains is not fulfilled due to the minimization of the compliance but over the next iteration steps is the eigenfrequency elevated to the constrained level.

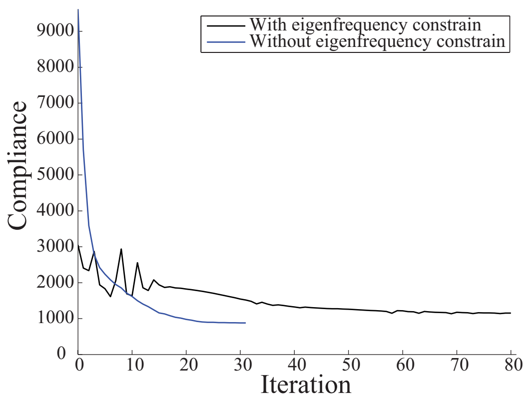

Figure 5.15: Compliance plotted for footbridge with and without frequency constrain and 30 % volume fraction constrain.

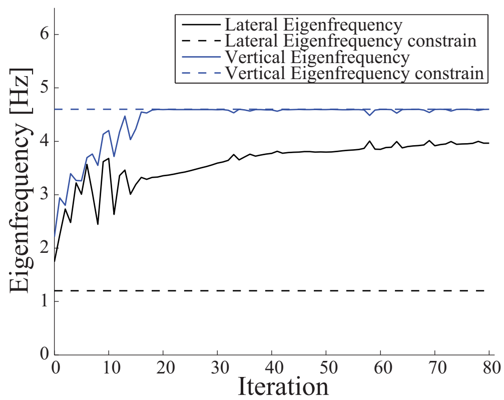

Figure 5.16: Lowest lateral and vertical eigenfrequency and eigenfrequency constrains with a 30 % volume fraction constrain.

The final topologies with a volume constrain of 25 % and 50 % are shown in Figure 5.17 and 5.18. Remaining topologies are shown in appendix A6.

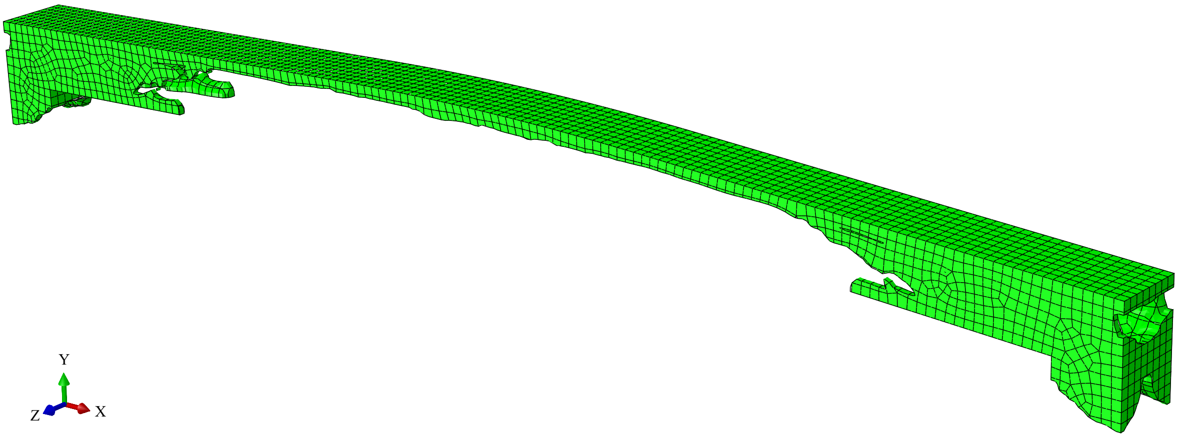

Figure 5.17: *Topology optimized pedestrian footbridge with eigenfrequency constrain and 25 % volume constrain.*

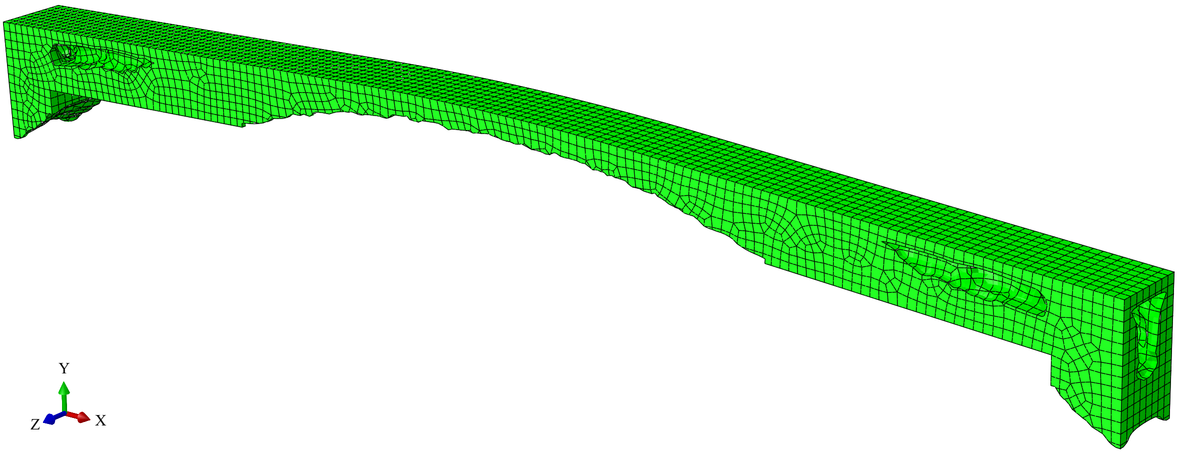

Figure 5.18: *Topology optimized pedestrian footbridge with eigenfrequency constrain and 50 % volume constrain.*

The implementation of the eigenfrequency constrains has changes the topology of the pedestrian footbridge. Material is moved from the middle of the bridge to each side. This works as a fixation of the bridge side and makes each side of the bridge mode resistance against bending. Hereby the eigenfrequency is raises to the constrained level. The forced relocation of material makes the final topology less stiff and the compliance of the structure is therefore higher. This effect is shown on Figure 5.15 for a volume constrain on 30 % and for remaining volume constrains in appendix A6.

5.7 Final Topology of Pedestrian Footbridge

Topology optimization has been used to investigate possible designs of a pedestrian footbridge.

I section 5.3 the bridge is investigated in a 2D model. The boundary conditions are chosen to be double pinned. This solution gives the lowest compliance and the highest total stiffness. Other influences on the selection of the pedestrian footbridges boundary condition have to be considered. When the bridge is fixed for translation in the vertical direction in both sides there is no possibilities for the bridge to expand and increased stresses may occur. A possible reason for expansion is heat. When a structure is exposure to heat different will the structure expand or shrink.

In section 5.4 and 5.5 the topology design of a 3D model of the bridge with steel and concrete as the material is investigated. The bearing construction under the pedestrian deck is formed as an arc. It is chosen to use concrete as a material.

It has to be considered how to construct the bridge. If the bridge is built in concrete it has to be considered if it is possible to cast the bridges elements or if the design has to be adapted. If the bridge was chosen to be built in steel it may be desired not to have to large members. A solution may be to make a topology optimization where the maximal size of members is also constrained.
The bridge has only been topology optimized for a vertical load. It is assumed this are the dominating load of the bridge. To verify the design of the bridge other loads have to be considered in the final design process.

In section 5.6 it is investigated how an eigenfrequency constrain influences the final design. It is possible to constrain the bridge to have a higher eigenfrequency than the constrained level but will require a higher volume. In section 5.4 and 5.5 it is found that a volume fraction of 20 % is enough to obtain a satisfying design. With an eigenfrequency constrain at least 30 % volume is necessary to satisfy the constrains. The final compliance is larger with a eigenfrequency constrain. It may therefore be a possibility to install dampers to the bridge instead. This way it would be possible to maintain the design of the bridge found in section 5.5.

The investigation of the pedestrian footbridge does not end with a finished design of the pedestrian footbridge. Instead the topology optimization provides a good initial design for a further design process. With the use of topology optimization it is possible to investigate the influence of different parameters and make a well-founded chose of the topology of the structure.

Part IV

Conclusions

Chapter 6

Conclusions

In this thesis topology optimization in civil engineering is investigated. In this chapter are investigations of the thesis outlined and the main conclusions are summarized.

6.1 Summary of the Thesis

Chapter 1 A general presentation to topology optimization is given and the use in civil engineering is reviewed. Presentations of the civil engineering structures that are analysed using topology optimization are given. In the end of the chapter is the history of topology optimization reviewed and the scope of the thesis outlined.

Chapter 2 The theoretical background for topology optimization are reviewed. Four different solution schemes for topology optimization are defined: the SIMP method, the Homogenization Method, ESO method and BESO method. The method used to preformed topology optimization in the thesis is the SIMP method and the main focus is therefore on this method. Possible problems that can occur under a topology optimization are discussed and possible solution methods for solving checkerboard pattern problems and mesh independents problems are shown.

Chapter 3 A Case study is performed in a SIMP optimization with compliance as the object and with a volume fraction as a constrain. Three cases are investigated: A Michell type structure, a 2D cantilever beam and a 3D cantilever beam. The case study is performed with two commercial finite element and optimization programs: Abaqus CAE and Altair Optistruct.

From the case study of a Michell type structure it is found that with both Abaqus and Optistruct it is possible to find a feasible solution for the topology optimization task. Both solutions found with Abaqus and Optistruct are similar to the analytical solution of the Michell type structure.

In the second case a 2D cantilever beam is topology optimized. Both programs give similar topology solutions when a manual checkerboard pattern control is applied. The automatic checkerboard pattern control is investigated for both programs. Abaqus have an automatic checkerboard control and is able to find a feasible solution to the optimization task without a manual applied checkerboard control. Optistruct do not have an automatic checkerboard control and the solution is only feasible when a checkerboard control is applied manual.

A case study of the 3D cantilever beam is performed. It shows that both programs are able to perform topology optimization on a 3D structure with solid elements.

It is found that both Abaqus and Optistruct are suitable to preform topology optimization on 2D shell structures and on 3D solid structures. The two programs have both in all case studies found similar final topology and compliance. In the 2D case studies Optistruct in general converges faster against the final compliance than Abaqus. In the 3D casee Abaqus and Optistruct converge in almost the rate. Both programs are also able to reach a 1-0 density distribution. It has been observed in 3D cases there are more elements with a density in middle interval. This makes it necessary to determine a lower boundary for element densities to accept in the final topology. The time spent in Abaqus for an optimization task is generally longer then in Optistruct. This is both due to the time spent on the optimization but also the time spent on FEM calculations and other tasks.

Chapter 4 A transition piece for an offshore wind turbine is optimized. The transition piece is optimized for two sizes. The topology is investigated in three optimization tasks. First is a topology optimization made with no additional constrains to the classical SIMP formulation. Then the optimization is expanded to include a rotation constrain. The rotation constrain of 60° makes it possible to find a structure that is optimized to obtain loads from multiply directions.

In the third optimization the material is modelled as CRC concrete. The optimization is also performed with geometric non-linearity. It is investigated what the volume constrain should be to satisfy a design criteria. The found optimized topologies of the transition pieces are shown in Figure 6.1 and 6.2. The stresses in the structure are investigated and it is found to be below the tensile and compressive strength of CRC concrete.

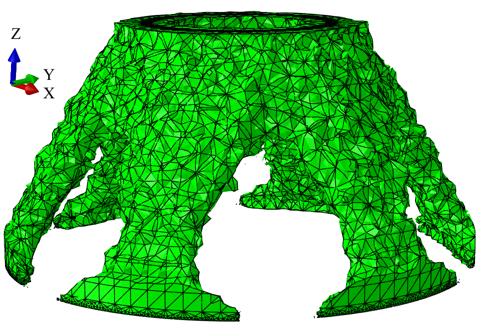

Figure 6.1: *Topology optimized short transition piece.*

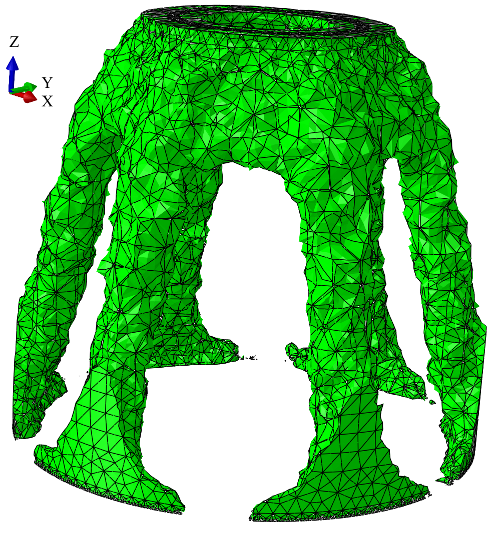

Figure 6.2: *Topology optimized high transition piece.*

Chapter 5 The design of a pedestrian footbridge is investigated using topology optimization. The investigation is performed in four steps: A 2D solution, a 3D solution in steel, a 3D solution in concrete and a solution where the structures eigenfrequency is constrained. The resulting topologies are shown in Figure 6.3 to 6.6.

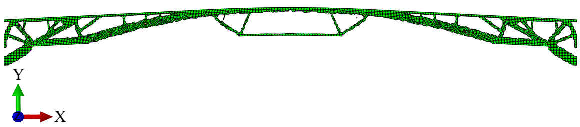

Figure 6.3: *Topology of 2D solution in steel.*

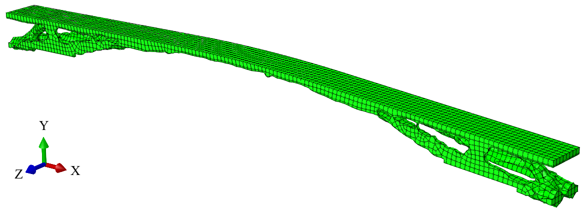

Figure 6.4: *Topology of 3D solution in steel.*

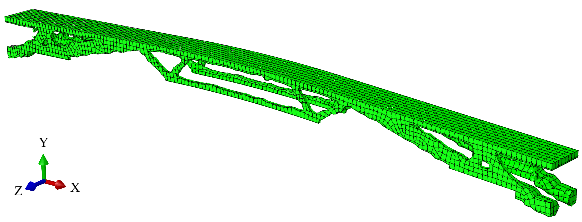

Figure 6.5: *Topology of 3D solution in concrete.*

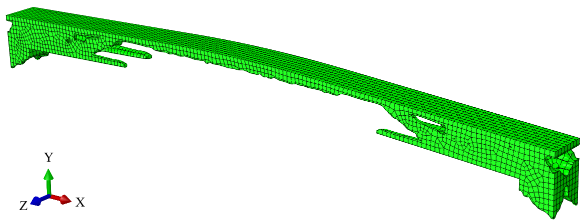

Figure 6.6: *Topology of 3D solution with eigenfrequency constrain.*

The first investigation is a 2D model. The influence of boundary conditions and slope of the pedestrian deck are investigated with topology optimization. The final compliances are compared and a model where both sides of the bridge are pinned in both vertical and horizontal directions has the lowest compliance and is used for further investigation. The influence of the slope of the pedestrian deck is investigated and it is found that a solution with the maximal allowable slope of 1:20 gives the lowest compliance.

In the second and third topology optimization of the pedestrian footbridge are a 3D model of the design domain optimized using topology optimization. A volume fraction of 20 % gives the final topologies showed in Figure 6.4 and 6.5. It is found that the difference material parameters and the use of geometric non-linearity give different resulting topologyies.

In the fourth topology optimization a eigenfrequency constrain is applied to the optimization task. It is desired to move the structures eigenfrequency above a critical interval for frequencies created from pedestrians. A critical interval is defined for both vertical and lateral movement. The topology with a eigenfrequenct constrain is showed in Figure 6.6. It is found that a volume fraction of 30 % is necessary to satisfy the eigenfrequency constrain. The final compliance is lower when the frequency constrain is added. This is due to relocation of material to satisfy the eigenfrequency constrain which gives a less stiff structure.

The investigation with topology optimization provides a good initial design for the further design process. With the use of topology optimization it is possible to investigate the influence of different parameters and make a well-founded chose of the topology of the structure.

6.2 Overall Conclusions

The use of topology optimization in civil engineering has been investigated and the main conclusions are summarized in the following points.

- Topology optimization methods in commercial programs are successfully used to preform SIMP optimization. SIMP optimization with compliance as object and volume as an constrain is compared and it is found that using both Abaqua CAE and Altair Optistruct it is possible to preform optimized topology. The final topology is similar for the two programs.
- Topology optimization can be used to optimize civil engineering structures. The complex nature of most civil engineering structures in shape, load patterns and material makes it important to simplify the model and use appropriated constrains to obtain a feasible final topology.
- Complex load patterns acting on the part of the structure that is optimized are not possible to model correct. Instead it is necessary to simplify the load and move it to a frozen zone of the structure. The structure can after a topology optimization be optimized using shape optimization where the loads can be applied more correctly. In general topology optimization is more powerful on structures where the dominating load is not acting inside the design domain and where the main loads size and direction are not depended of the structures shape and size.
- It is possible to account for load acting in multiple directions. A symmetry constrain can be applied to the structure to ensure that the structure can withstand load from several directions. This is done for the transition piece with a rotation constrain around the middle axis. If a vertical load was applied to the pedestrian bridge a symmetry plane through the middle of the bridge could be used to ensure that the bridge could obtain the load from both sides of the bridge.
- A frequency constrain can successfully be used together with a SIMP optimization. This is done for the pedestrian footbridge. The interpretation of the topology of the optimization can be used as a base for the design or to evaluate other possibilities for securing the bridge against oscillations.
- The resulting topology is dependent of the definition of the design task. Therefore it is imported to use appropriate constrains to define the optimization task.

- Topology optimization is a powerful design tool. In the initial face of the design of a civil engineering structure topology optimization can successfully be used to determine the overall topology. The investigations of two civil engineering structures show that topology optimization cannot make it out for the entire design process. After the topology optimization is finished it is necessary to preform additional designing of the structure. Nevertheless with the use of topology optimization it is possible to obtain an effective and high preforming topology for a civil engineering structure. The use of topology optimization can lead to an unconventional and unexpected design that else would not have been taken into consideration.

6.3 Further Work

With the new tools in commercial programs topology optimization has become more easily accessible to use in civil engineering. In this thesis topology optimization has been performed on two different civil engineering structures with success. A number of simplifications and assumptions have been made to make this possible. There is still many areas of topology optimization there can be investigate to make the optimization more effective and give better results.

This thesis has mainly focused on using topology optimization to maximise the stiffness of a structure while being constrained by a volume constrain. Other constrains have been added to different optimization tasks. There are other approaches for finding an optimal topology e.g. minimising weight with a stress constraints. A further investigation of the use of different optimization task set-up and the influence on the final topology is needed to determine the best approach when using a penalty method as SIMP.

Topology optimization using SIMP method can only be used on isotropic material. An implementation of the homogenization method in a commercial program could be used to model composite material. The use of the homogenization method could also be used to determine the properties of the a composite material as well as the topology of the structure of composite materials.

Reinforced concrete consists of both concrete and steel reinforcement. In this thesis the combined material is simplified to act as a combined isotropic material. This can be used as an approximation to find a topology for further design. An area for further work would be to model both materials combined for a optimization. Combined optimizations of steel and concrete are proposed but the methods have so far not been used for large scale civil engineering structures.(Amir and Bogomolny, 2010) (Surit and Wethyavivorn, 2011)

A drawback for topology optimization is still computer capacity. The increased availability of computer capacity has made it possible to perform more and more complex finite element modelling.

Large civil engineering structures with a high level of detail demand a high number of degrees of freedoms. Topology optimization is an iterative process and the FEM model will have to be calculated many times in a optimization. Further optimization of the solving algorithms and more computer capacity will make topology optimization an even more attractive design tool.

Bibliography

Abaqus, **2012**. Abaqus. *Abaqus Analysis User's Manual*. N/A, Version 6.11. Simulia, 2012.

Amir and Bogomolny, **2010**. Oded Amir and Michael Bogomolny. *Topology Optimization for Conceptual Design of Reinforced Concrete Structures*. World Congress on Structural and Multidisciplinary Optimization, 9, 2010.

Bendsøe, **1988**. Martin Philip Bendsøe. *Generating Optimal Topologies in Structural Design Using a Homogenization Method*. Computer Methods in Applied Mechanics and Engineering, 71, 1988.

Bendsøe, **1989**. M.P. Bendsøe. *Optimal shape design as a material distribution problem*. Structural Optimization, 1, 1989.

Bendsøe and Sigmund, **2003**. M.P. Bendsøe and O. Sigmund. *Topology Optimization - Theory, Method and Applications*. ISBN: 3-540-42992-1, 2nd. edition. Springer-Verlag, 2003.

Chan, **1960**. A. S. L. Chan. *The Design of Michell Optimum Structure*. Ministry of Aviation, Reports and Memoranda No. 33o3, 1960.

Dallard, Fitzpatrick, Flint, Bourva, Low, Smith, and Willford, **2001**. P. Dallard, A. J. Fitzpatrick, A. Flint, S. Le Bourva, A. Low, R. M. Ridsdill Smith, and M. Willford. *The London Millennium Footbridge*. The Structural Engineer, 79, 2001.

Heinemeyer, Butz, Keil, Schlaich, Goldack, Trometer, Lukic, Chabrolin, Lemaire, Martin, Cunha, and Caetano, **2009**. Christoph Heinemeyer, Christiane Butz, Andreas Keil, Mike Schlaich, Arndt Goldack, Stefan Trometer, Mladen Lukic, Bruno Chabrolin, Arnaud Lemaire, Pierre-Olivier Martin, Álvaro Cunha, and Elsa Caetano. *Design of lightweight Footbridges for Human Vibrations*. ISBN: 987-92-79-13387-9, 1. edition. European Commission, 2009.

Huang and Xie, **2010**. X. Huang and Y.M. Xie. *Topology Optimization of Continuum Structures - Methods and applications*. ISBN: 978-0-470-74653-0, 1st. edition. John Wiley and Sons, Ltd, 2010.

Jensen, **2008**. Bjerne Chr. Jensen. *Beton-konstriktioner efter DS/EN 1992-1-1*. ISBN: 978-87-571-2668-6, 1. edition. Nyt teknins Forlag, 2008.

Krog, Tucker, and Rollema, **2002**. Lars Krog, Alastair Tucker, and Gerrit Rollema. *Application of Topology, Sizing and Shape Optimization Method to Optimal Design of Aircraft Components*. 2002.

Liang, **2005**. Qing Qang Liang. *Performance-based Optimization of Structures - Theory and applications*. ISBN: 0-415-33594-9, 1st. edition. Spon Press, 2005.

Nezhentseva, Andersen, Ibsen, and Sørensen, **2010**. A. Nezhentseva, L. Andersen, L.B. Ibsen, and E.V. Sørensen. *Material Composition of Bucket Foundation Transition Pieces for Offshore Wind Turbines*. Proceedings of the Tenth International Conference on Computational Structures Technology, Paper 109, 2010.

Nezhentseva, Andersen, Ibsen, and Sørensen, 2011. A. Nezhentseva, L. Andersen, L.B. Ibsen, and E.V. Sørensen. *Performance-Based Design Optimization of a Transition Piece for Bucket Foundations for Offshore Wind Turbines.* Proceedings of the Thirteenth International Conference on Civil, Structural and Environmental Engineering Computing, 2011.

Ohmori, 2008. Hiroshi Ohmori. *Computational Morphogenesis - Its Current State and Possibilityof the Future.* IASS-IACM2008, Cornell University, 2008.

Schmidt, 2010. H. Schmidt. *Strategy for Optimal Configuration Design of Existing Structures by Topology and Shape Optimization Tools.* International Journal of Aerospace and Mechanical Engineering, 4, 2010.

Sigmund, 2001. O. Sigmund. *A 99 line topology optimization code written in Matlab.* Structural and Multidisciplinary Optimization, 21, 2001.

Surit and Wethyavivorn, 2011. Siradech Surit and Benjapon Wethyavivorn. *Topology Optimization of Reinforced Concrete Beams by a Spread-over Reinforcement Model With Fixed Grid Mesh.* Songklanakarin Journal of Science and Technology, 33, 2011.

www.qatarconvention.com, 2012. www.qatarconvention.com. *Quatar National Convention Centre.* URL: `http://www.qatarconvention.com/`, 2012.

Xie and Steven, 1997. Y.M. Xie and G.P. Steven. *Evolutionary Structural Optimization.* ISBN: 3-540-76153-5, 1st. edition. Springer-Verlag, 1997.

Xie, Zuo, Huang, Tang, Zhao, and Felicetti, 2011. Y.M. Xie, Z.H. Zuo, X. Huang, J.W. Tang, B. Zhao, and P. Felicetti. *Computational Morphogenesis - Its Current State and Possibilityof the Future.* ALGODE TOKYO 2011, 2011.

Part V

Appendices

2nd Topology Optimization of Transition Piece

Figure A1.1 to A1.4 shows the optimized structures of the short transition piece shown. Figure A1.5 to A1.8 shows the optimized structures of the high transition piece shown. There are applied a rotation constrain between 45° to 120°.

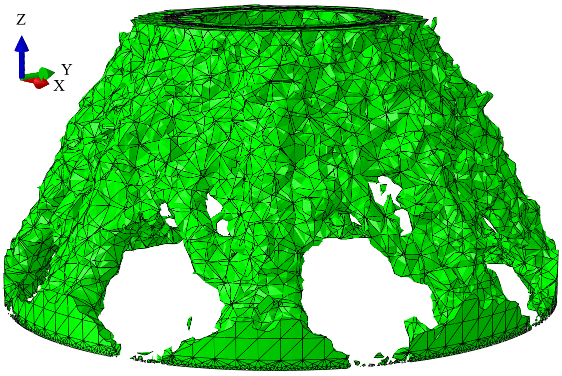

Figure A1.1: *Short Transition Piece topology optimized with a 45° rotation constrain.*

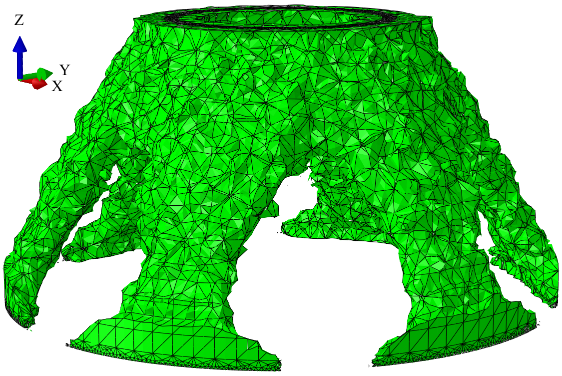

Figure A1.2: *Short Transition Piece topology optimized with a 60° rotation constrain.*

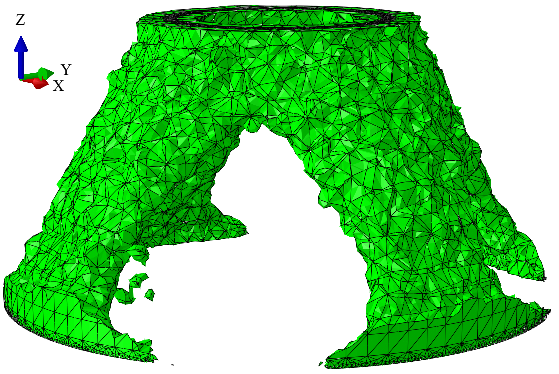

Figure A1.3: *Short Transition Piece topology optimized with a 90° rotation constrain.*

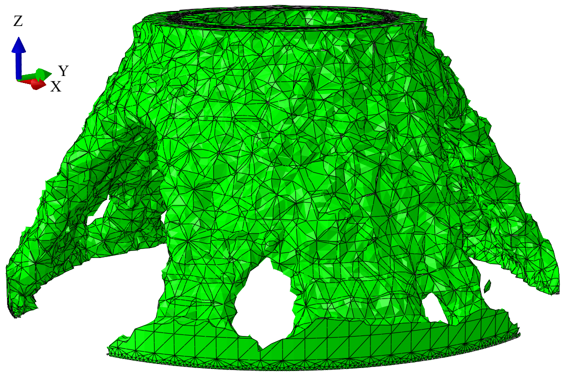

Figure A1.4: *Short Transition Piece topology optimized with a 120° rotation constrain.*

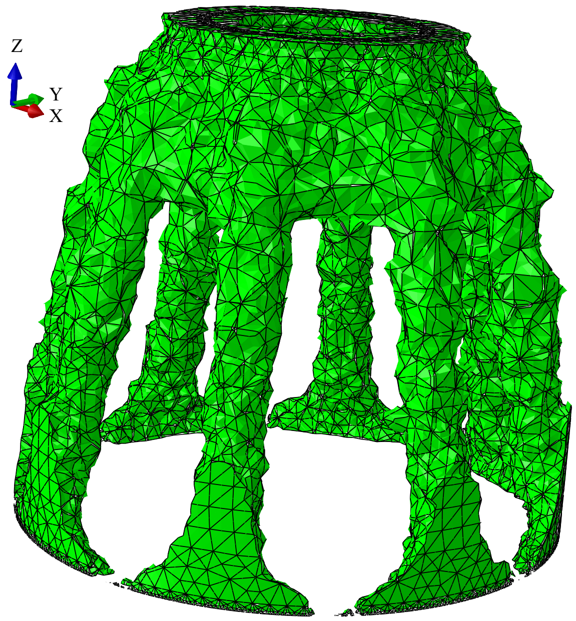

Figure A1.5: *High Transition Piece topology optimized with a 45° rotation constrain.*

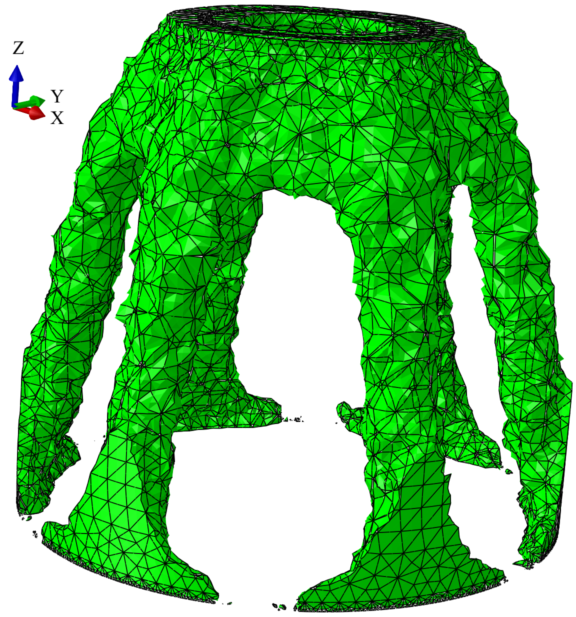

Figure A1.6: *High Transition Piece topology optimized with a 60° rotation constrain.*

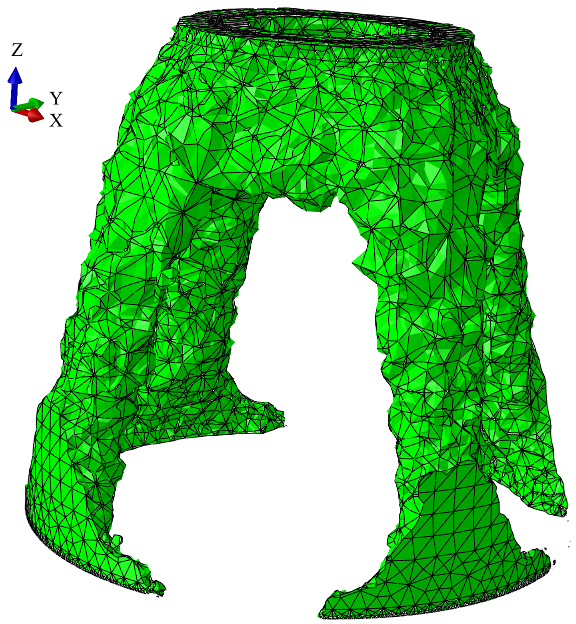

Figure A1.7: *High Transition Piece topology optimized with a 90° rotation constrain.*

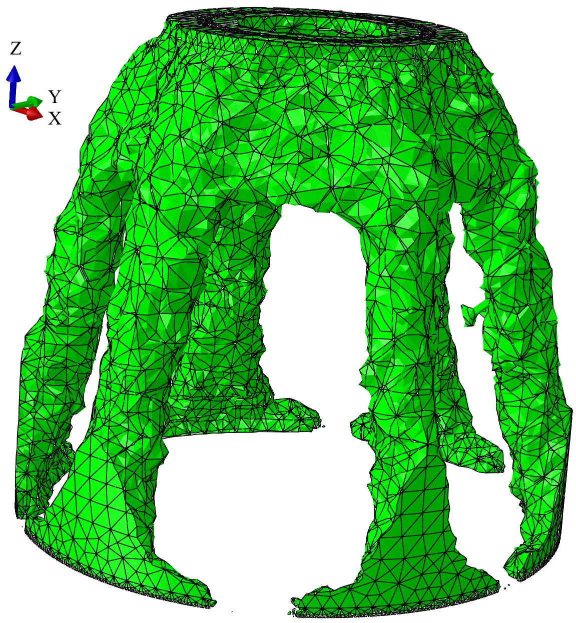

Figure A1.8: *High Transition Piece topology optimized with a 120° rotation constrain.*

3rd Topology Optimization of Transition Piece

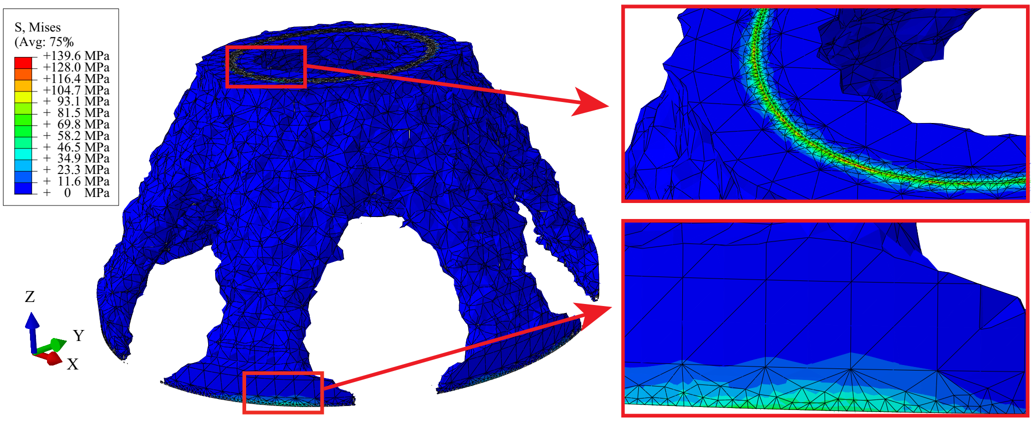

Figure A2.1: *Distribution of Von Mises stresses in the short transition piece.*

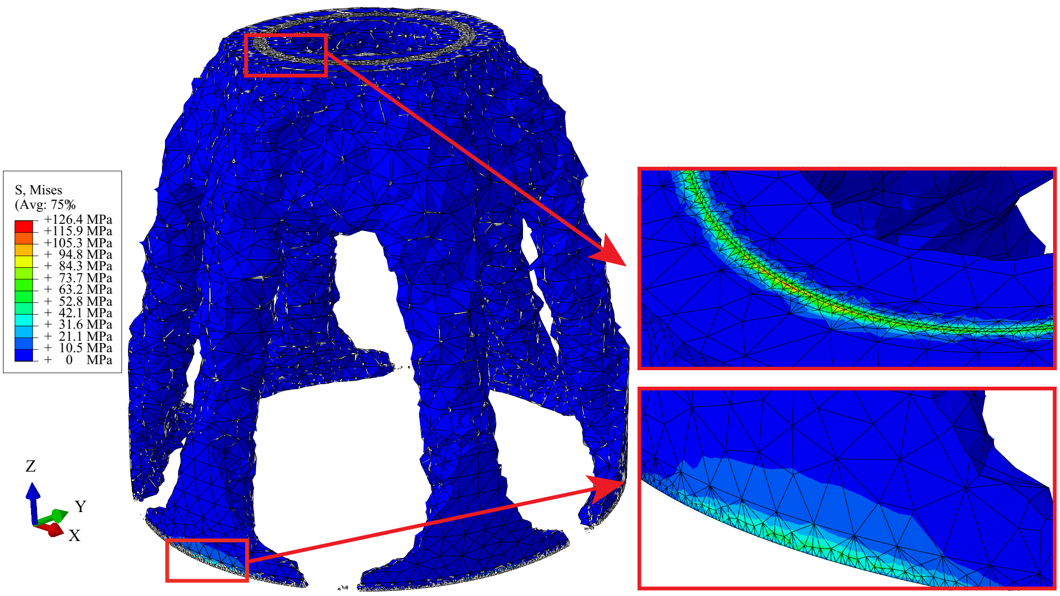

Figure A2.2: *Distribution of Von Mises stresses in the high transition piece.*

Appendices **A3**

1st Topology Optimization of Pedestrian Footbridge

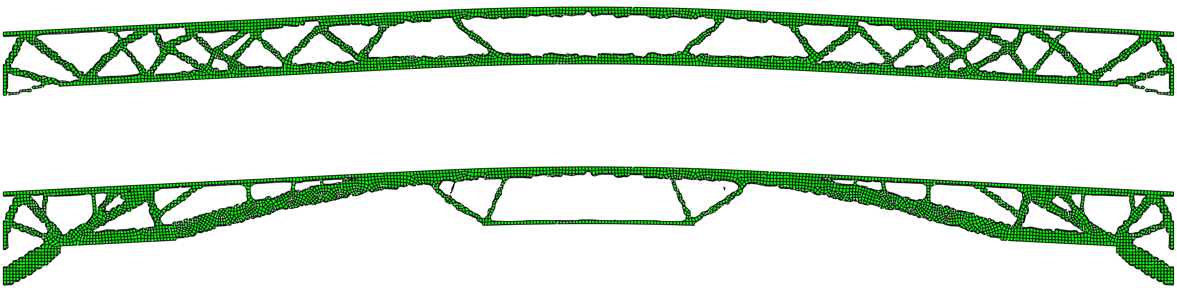

Figure A3.1: *Topology of model 1 pedestrian footbridge. Top: Bridge is pinned in both sides of the bridge. Bottom: Bridge is fixed in both sides.*

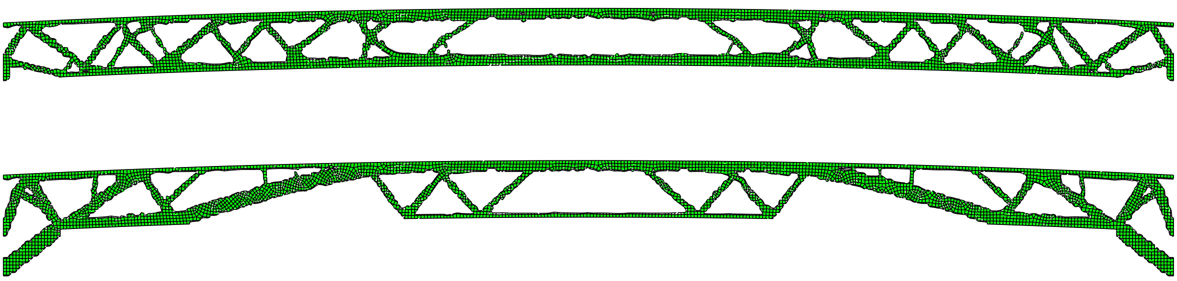

Figure A3.2: *Topology of model 2 pedestrian footbridge. Top: Bridge is pinned in both sides of the bridge. Bottom: Bridge is fixed in both sides.*

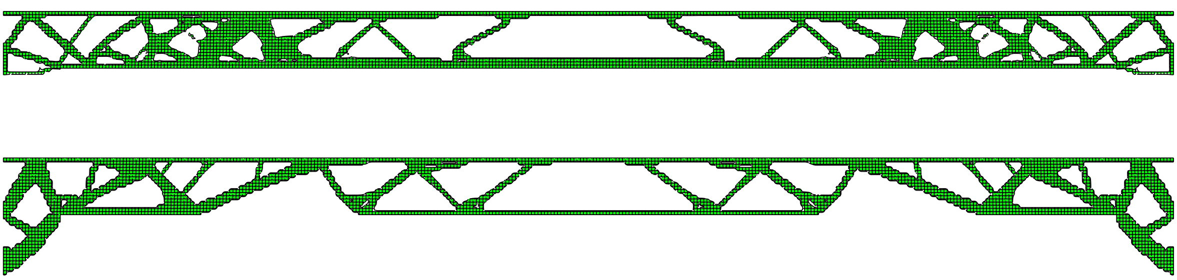

Figure A3.3: *Topology of model 2 pedestrian footbridge. Top: Bridge is pinned in both sides of the bridge. Bottom: Bridge is fixed in both sides.*

2nd Topology Optimization of Pedestrian Footbridge

Topology Optimized Footbridge With Different Volume Fractions

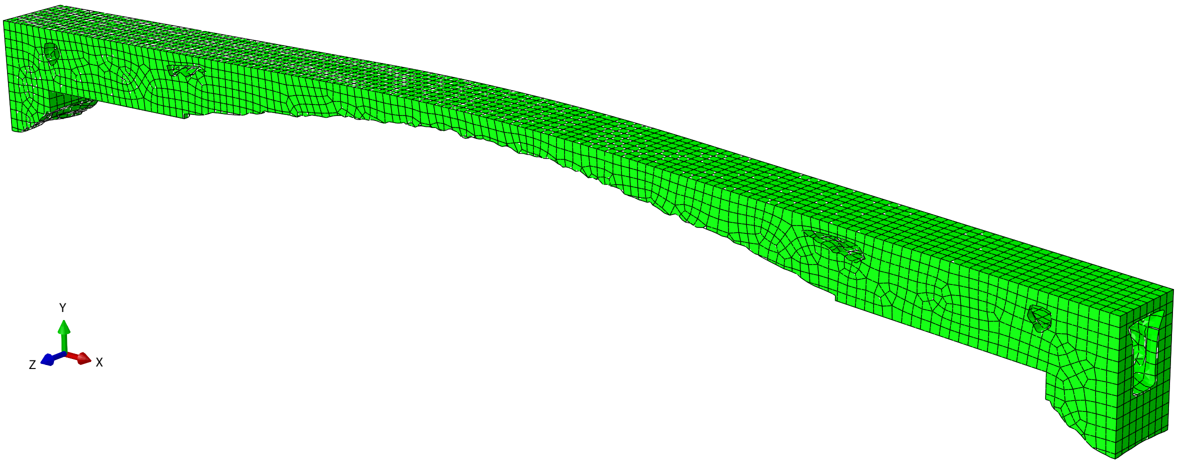

Figure A4.1: *Topology optimized footbridge with a volume fraction of 50 %.*

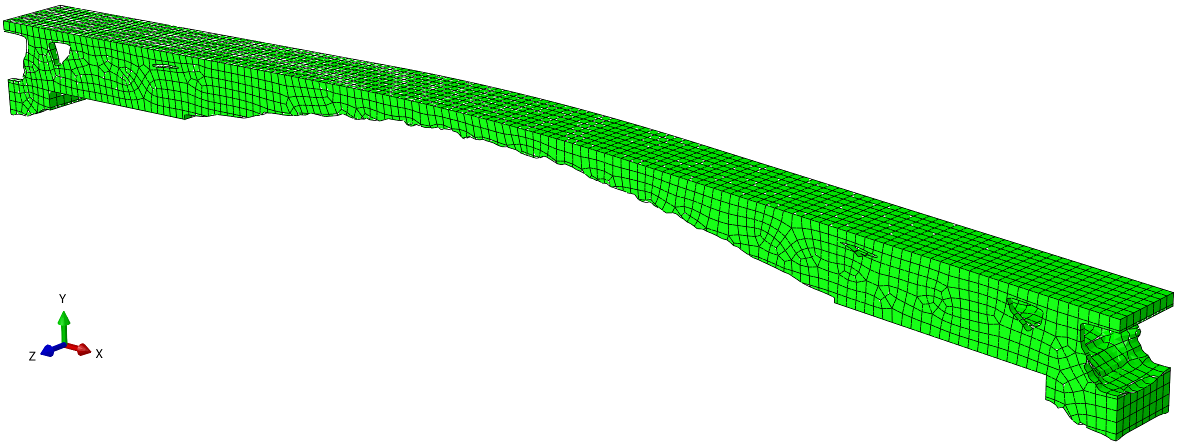

Figure A4.2: *Topology optimized footbridge with a volume fraction of 40 %.*

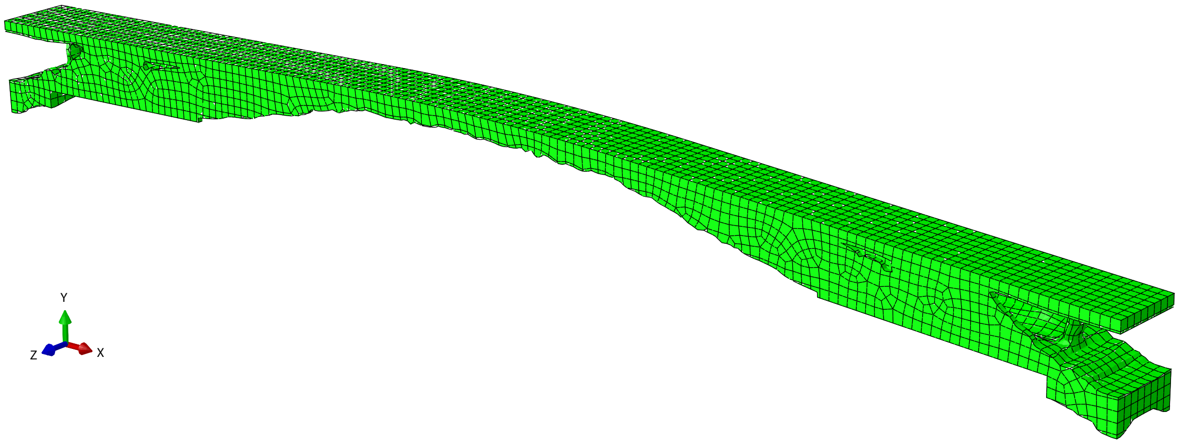

Figure A4.3: *Topology optimized footbridge with a volume fraction of 30 %.*

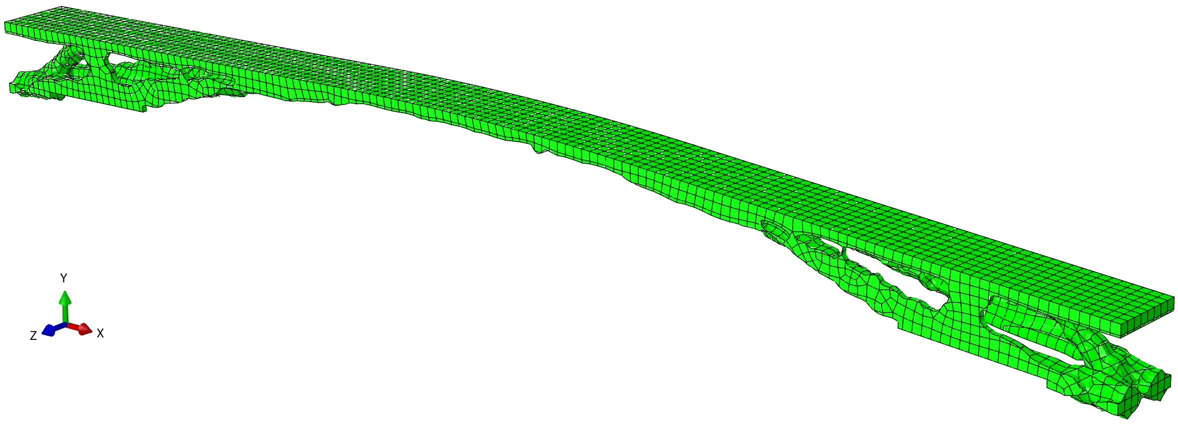

Figure A4.4: *Topology optimized footbridge with a volume fraction of 20 %.*

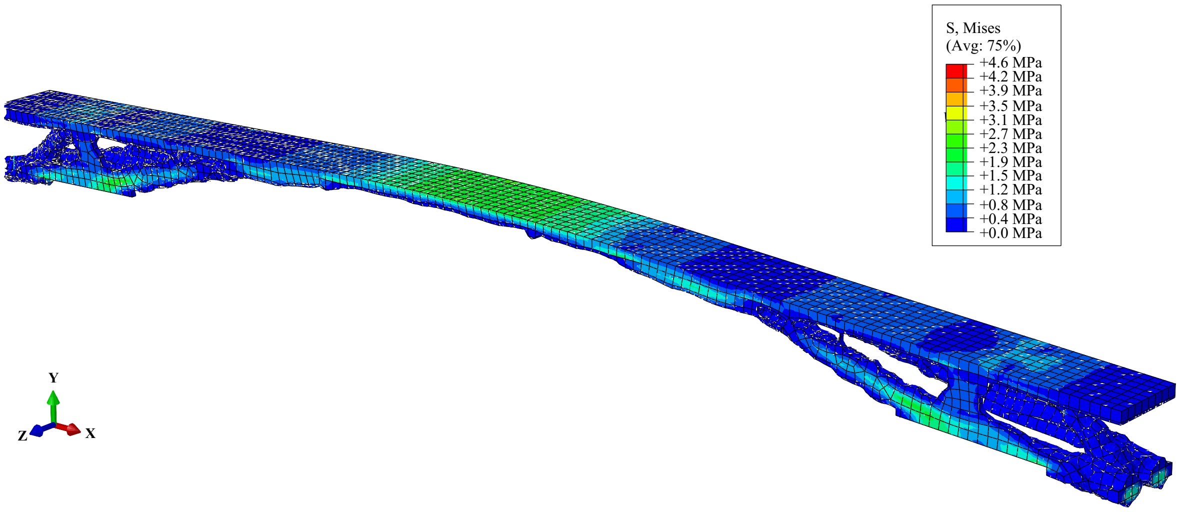

Figure A4.5: *Distribution of von Mises stresses in pedestrian bridge of steel.*

3nd Topology Optimization of Pedestrian Footbridge.

Topology Optimized Footbridge With Concrete Material

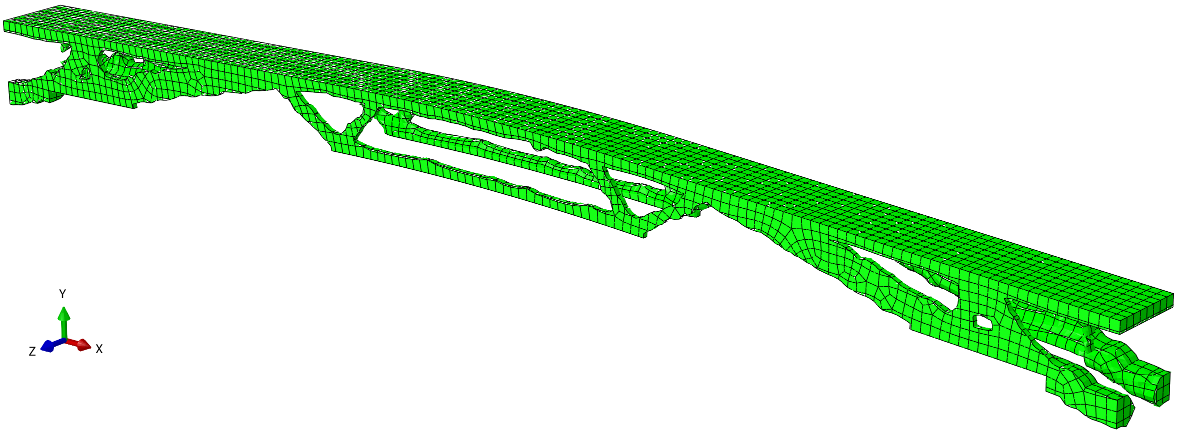

Figure A5.1: *Topology optimized footbridge with concrete as the material and a volume fraction of 20 %. Geometric non-linearity is taken into account in the finite element analysis.*

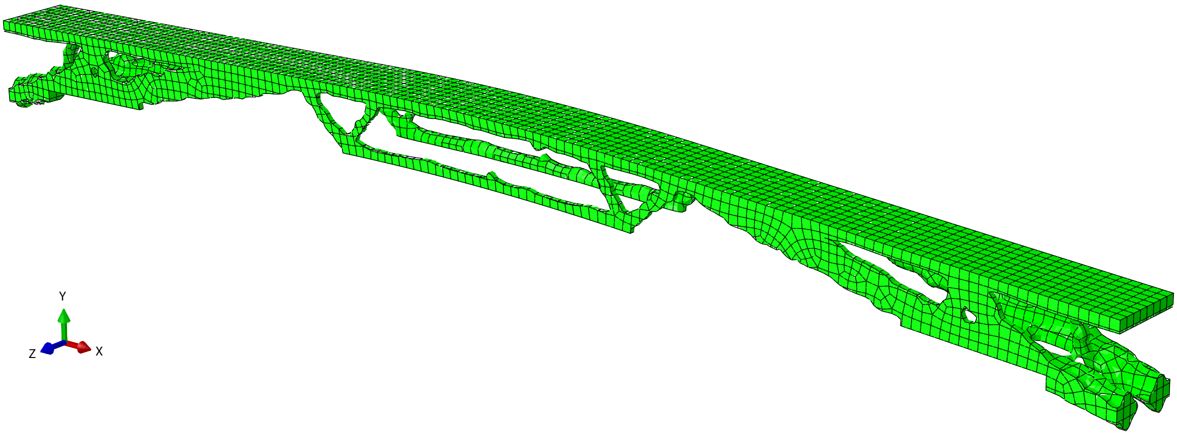

Figure A5.2: *Topology optimized footbridge with concrete as the material and a volume fraction of 20 %. Geometric non-linearity is not taken into account in the finite element analysis.*

4th Topology Optimization of Pedestrian Footbridge.

Mode Shape and Eigenfrequency Analysis

Figure A6.1 to A6.9 shows mode shapes for the first nine modes from a frequency analysis of the design domain. A table of data from the test are shown i Table A6.1.

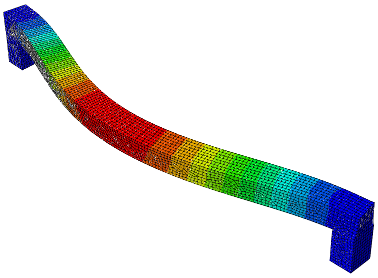

Figure A6.1: *1^{st} mode shape.*

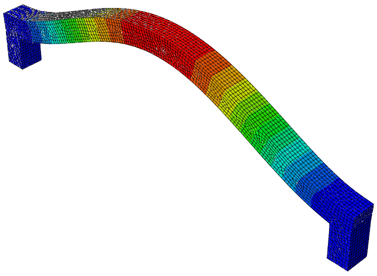

Figure A6.2: *2^{nd} mode shape.*

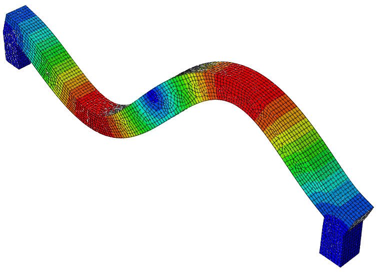

Figure A6.3: *3^{rd} mode shape.*

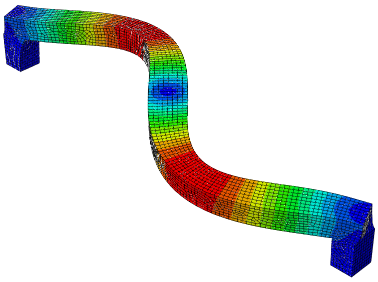

Figure A6.4: *4^{th} mode shape.*

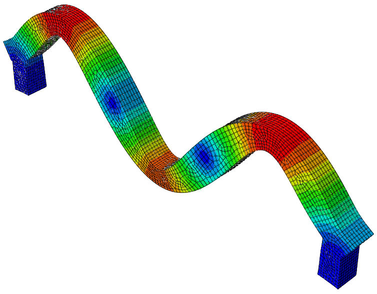

Figure A6.5: *5^{th} mode shape.*

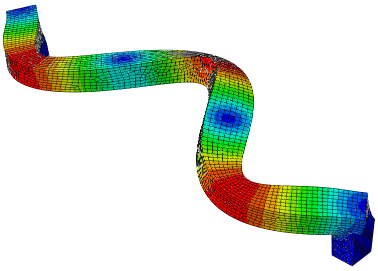

Figure A6.6: *6^{th} mode shape.*

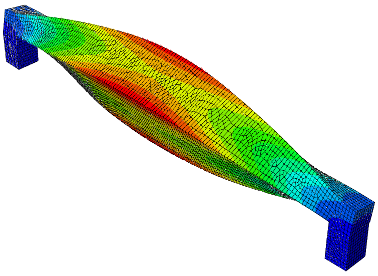

Figure A6.7: *7th mode shape.*

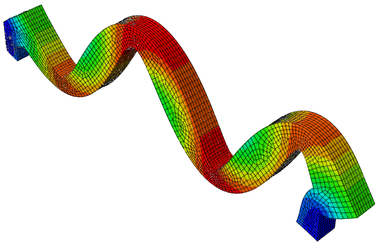

Figure A6.8: *8th mode shape.*

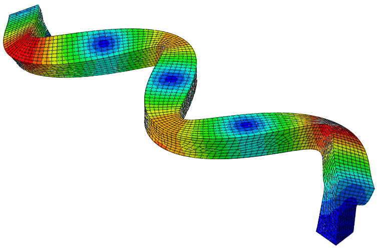

Figure A6.9: *9nd mode shape.*

Table A6.1: *Mode shape and Eigenfrequency information for design domain.*

Mode No.	Eigenfrequency [Hz]	Number of half waves	Description of mode shape
1	3.31	1	Lateral effects
2	3.73	1	Vertical effects
3	8.23	2	Vertical effects
4	9.03	2	Lateral effects
5	16.18	3	Vertical effects
6	17.25	3	Lateral + torsion effects
7	18.61	1	Torsion effects
8	22.69	4	Vertical effects
9	27.46	4	Lateral + torsion effects

Topologies with Eigenfrequency Constrain

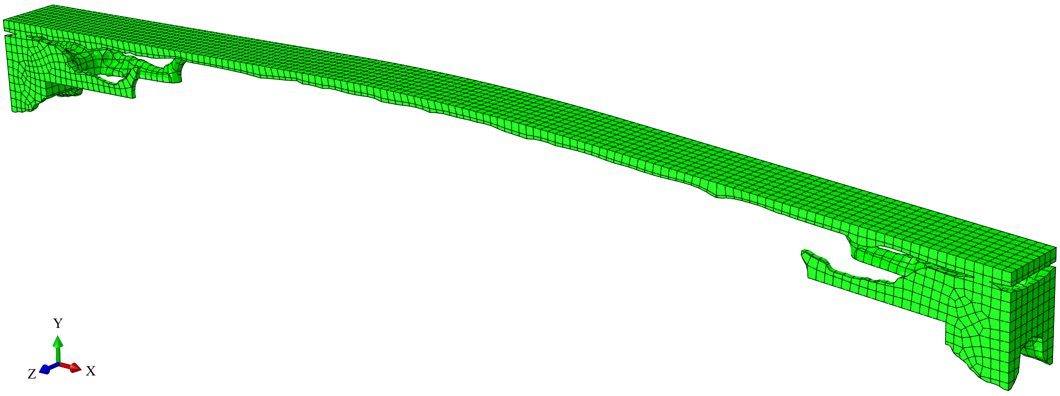

Figure A6.10: *Topology optimized pedestrian footbridge with eigenfrequency constrain and 20 % volume constrain.*

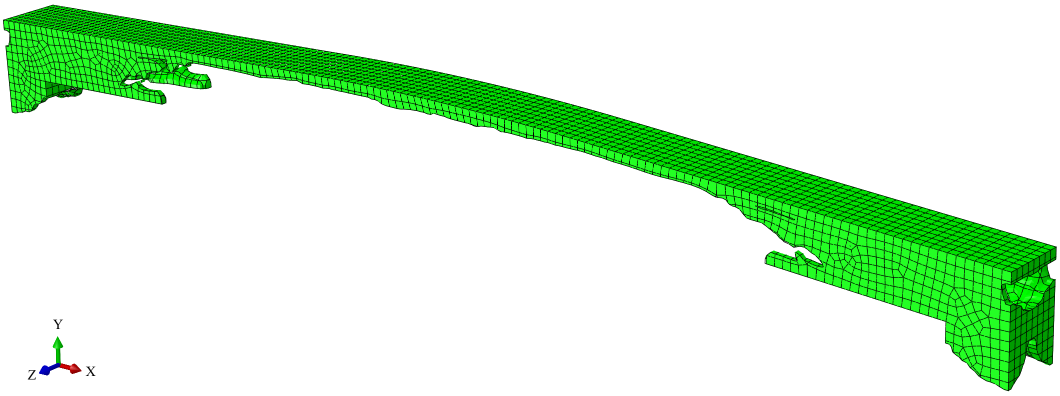

Figure A6.11: *Topology optimized pedestrian footbridge with eigenfrequency constrain and 25 % volume constrain.*

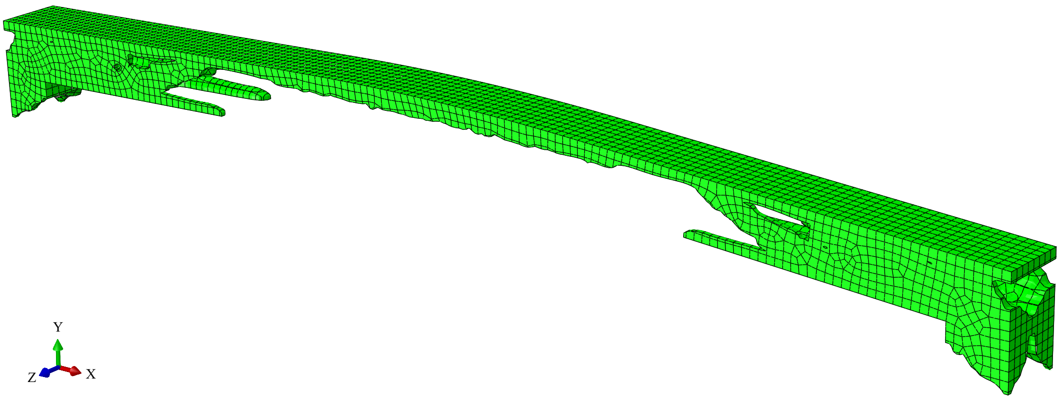

Figure A6.12: *Topology optimized pedestrian footbridge with eigenfrequency constrain and 30 % volume constrain.*

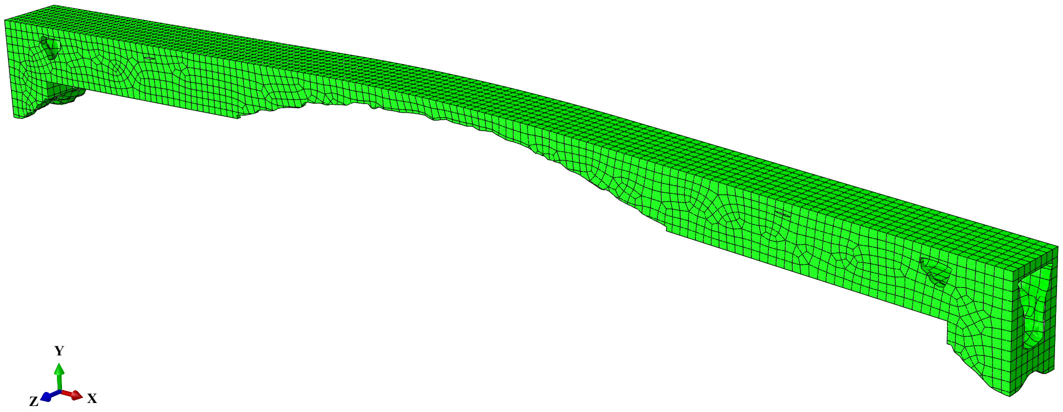

Figure A6.13: *Topology optimized pedestrian footbridge with eigenfrequency constrain and 40 % volume constrain.*

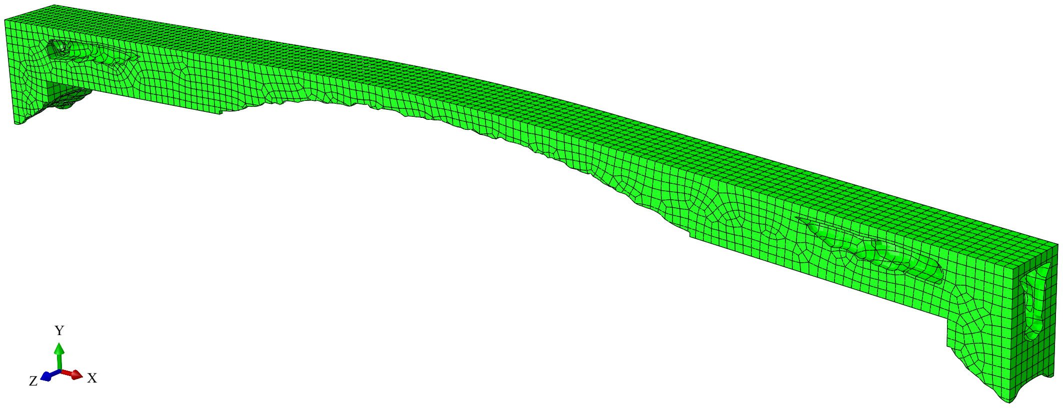

Figure A6.14: *Topology optimized pedestrian footbridge with eigenfrequency constrain and 50 % volume constrain.*

Compliance and Eigenfrequencies

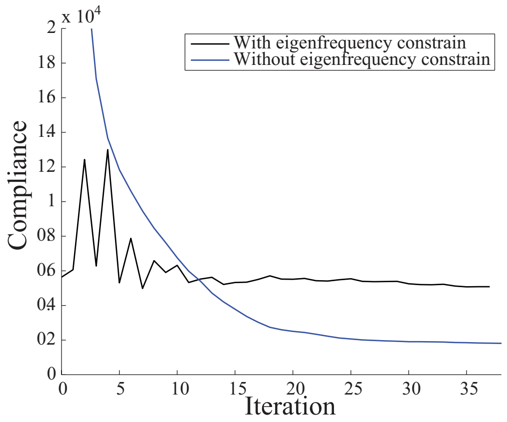

Figure A6.15: Compliance plotted with and without frequency constrain and 20 % volume fraction constrain.

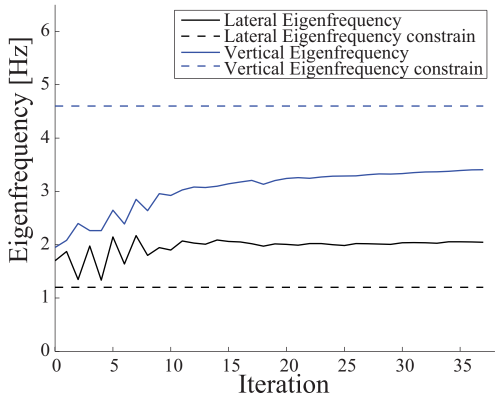

Figure A6.16: Lateral and vertical eigenfrequencys plotted with a 20 % volume fraction constrain.

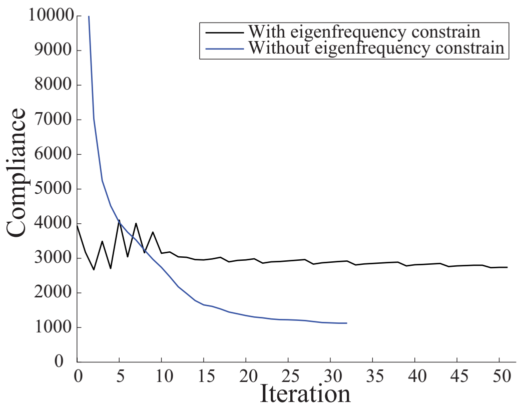

Figure A6.17: Compliance plotted with and without frequency constrain and 25 % volume fraction constrain.

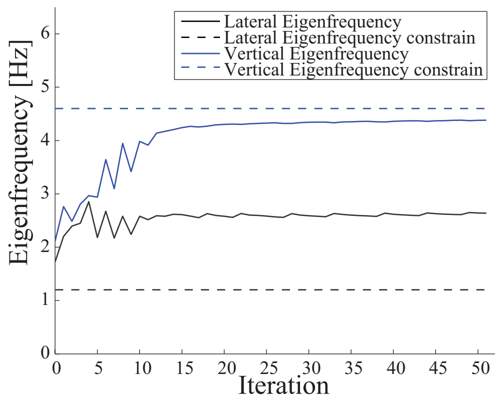

Figure A6.18: Lateral and vertical eigenfrequencys plotted with a 25 % volume fraction constrain.

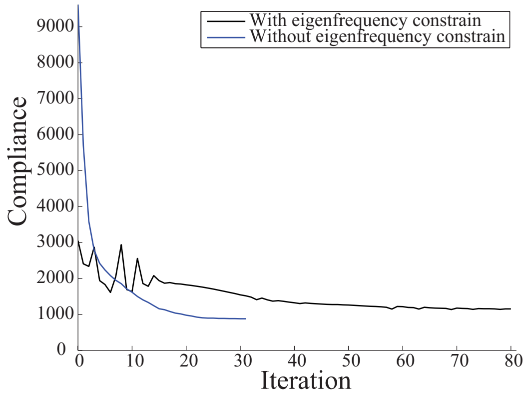

Figure A6.19: *Compliance plotted with and without frequency constrain and 30 % volume fraction constrain.*

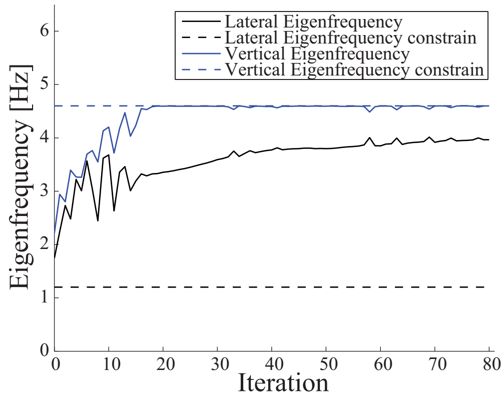

Figure A6.20: *Lateral and vertical eigenfrequencys plotted with a 30 % volume fraction constrain.*

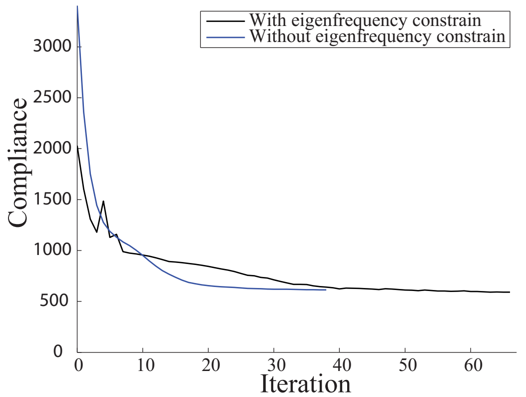

Figure A6.21: *Compliance plotted with and without frequency constrain and 40 % volume fraction constrain.*

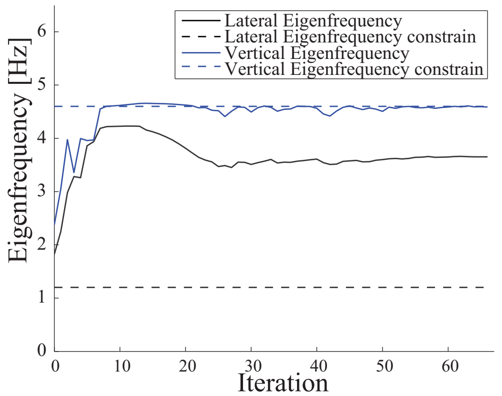

Figure A6.22: *Lateral and vertical eigenfrequencys plotted with a 40 % volume fraction constrain.*

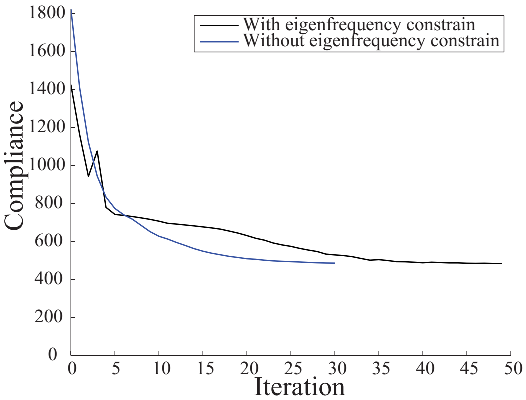

Figure A6.23: *Compliance plotted with and without frequency constrain and 50 % volume fraction constrain.*

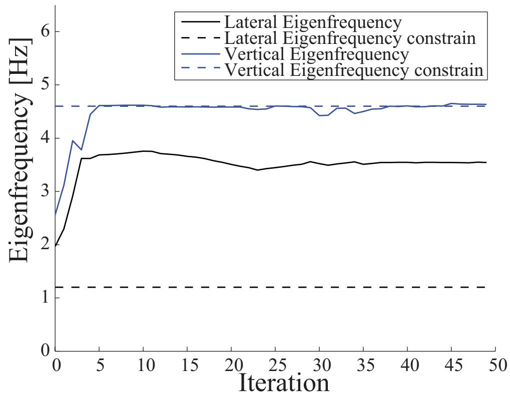

Figure A6.24: *Lateral and vertical eigenfrequencys plotted with a 50 % volume fraction constrain.*